Life cycle environmental and techno-economic assessments of monocrystalline titanium dioxide nanorod-based perovskite solar cells

by

Harshadeep Kukkikatte Ramamurthy Rao

A thesis submitted in partial fulfillment of the requirements for the degree of

Master of Science

in

Engineering Management

Department of Mechanical Engineering

University of Alberta

Abstract

There is an increased interest in utilization of solar energy for power generation. A lot of research effort is being put to improve the efficiency of solar cells. Perovskite architectures that use titanium dioxide nanorods as electron transport layers have been proven to have enhanced efficiency. There is very limited information on life cycle environmental and economic assessments of these perovskite cells (PSC). In this thesis, a cradle-to-grave life cycle analysis is used to evaluate the environmental benefit in terms of energy payback time, greenhouse gas emissions, and the net energy ratio of this architecture. Unlike most studies that focus on the life cycle of the cell processing, this study extends the scope to include the balance of the system and also to evaluate the environmental effects of reusing important components such as fluorine-doped tin oxide glass and the gold layer, which appear to significantly impact energy consumption and associated greenhouse gas emissions (GHG). The energy payback time is calculated to be 0.97 years and the life cycle GHG emissions is 181.50g CO_2 eq./kWh of electricity produced for a solar system installed in a colder climate like Alberta, Canada. The net energy ratio is 3.10, indicating the system is a net energy generator. The assembly life cycle stage, comprising the panel production, balance of the system, and mounting of solar panels, generates the most GHG emissions while the contribution from the cell fabrication stage is second. The GHG emissions associated with raw material extraction and production (81%) dominate the on-site GHG emissions caused during cell fabrication and assembly. We observed that the embodied GHG emissions for fluorine-doped tin oxide glass and gold contribute just 4% of the total GHG emissions associated with the perovskite solar cell for a three-time reuse case. Aluminum used during panel production and mounting emits the highest GHG emissions among the materials used.

Furthermore, to commercialize this PV technology for electricity generation, they must be manufactured at economical costs and have low levelized cost of electricity that can compete with existing technologies. In this thesis, a pathway for production of TiO_2 nanorod-based perovskite solar modules is established and cost of manufacturing them is estimated. Material, utilities, and equipment requirements from the available laboratory data to a mass production capacity of up to 21.0 MW annually were estimated through development of scale factors based on first principle. Key parameters contributing to the manufacturing costs are identified, and the minimum sustainable price and levelized cost of electricity are calculated. The direct manufacturing cost of the reference PSC module is estimated at \$80.23/m^2 and \$0.73/W with a production capacity of 3.5 MWp. These costs decline to \$47.15/m^2 and \$0.43/W when estimated for an annual production capacity of 21 MWp due to economy of scale benefits. Material costs dominate the overall costs with fluorine doped tin oxide (FTO) glass being the most expensive material used for fabrication. The labour costs rank second but decrease drastically with increased production. The material costs and the capital cost on the equipment purchased are seen to have a scale factor of 0.81 and 0.78, respectively. The perovskite solar cell panels when installed at residential homes in Alberta, Canada are estimated to have a competitive levelized cost of electricity ranging from 7 to 17 cents per kWh. However, this parameter is found to be extremely sensitive to the module efficiency, lifetime, and the solar insolation at the location of installation.

Sensitivity and uncertainty analyses were performed for both life cycle assessment and techno-economic assessment studies to identify the key input parameters that have significant impacts on the outputs (energy payback time, greenhouse gas emissions, the net energy ratio, minimum sustainable price, and levelized cost of electricity) and to obtain a range of results (through a Monte Carlo simulation), respectively.

Preface

This thesis is an original contribution by Harshadeep Kukkikatte Ramamurthy Rao, under the supervision of Dr. Amit Kumar. Sections of chapters 2 and 3 are expected to be published as Kukkikatte Ramamurthy Rao H., Gemechu E., Thakur U., Shankar K., Kumar A., "Life cycle assessment of high-performance monocrystalline titanium dioxide nanorod-based perovskite solar cells", and Kukkikatte Ramamurthy Rao H., Gemechu E., Thakur U., Shankar K., Kumar A., "Techno-economic assessment of titanium dioxide nanorod-based perovskite solar cells: from lab-scale to large-scale manufacturing". My contributions to both the papers include formulation of the concepts, collection of data, development of the model and validation, and composition of the manuscript. Dr. Eskinder Gemechu contributed to model validation and manuscript edits. Dr. Ujwal Thakur and Dr. Karthik Shankar assisted this research by furnishing laboratory data and providing their valuable inputs throughout the research. Dr. A. Kumar was the supervisory author and was involved with concept formation, evaluation, assessment of results, and manuscript edits.

Acknowledgments

I, Harshadeep Kukkikatte Ramamurthy Rao, would like to express my sincere gratitude to Dr. Amit Kumar for his continuous support, insightful ideas and able guidance without which successful completion of this work would not have been possible.

The author would also like to acknowledge the University of Alberta's Future Energy Systems (FES)" research initiative, that made this work possible. I would like to further extend my thanks to Canada First Research Excellence Fund (CFREF) for partially funding this research.

I would like to extend my sincere thanks to Dr. Eskinder Gemechu, a postdoctoral fellow in the Department of Mechanical Engineering for reviewing the research model and papers, along with providing continuous support as needed. I am thankful to Dr. Karthik Shankar and Dr. Ujwal Thakur from the Department of Electrical and Computer Engineering for providing required laboratory data in a timely manner and their valuable inputs throughout this research. I am grateful to Astrid Blodgett for her editorial assistance.

I would like to acknowledge all my colleagues at the Sustainable Energy Research Lab for their useful advice and support. Lastly, I am ever grateful to my beloved family for their constant encouragement and motivation.

Table of Contents

List of Tables

List of Figures

List of Abbreviations

BOS	Balance of system
EPBT	Energy payback time
ETL	Electron transport layer
FAI	Formamidinium iodide
FTO	Fluorine doped tin oxide
GHG	Greenhouse gas
kWh	Kilowatt hours
LCA	Life cycle assessment
MSP	Minimum sustainable price
$MAPbI_3$	Methyl ammonium lead iodide
NER	Net energy ratio
PCE	Photo conversion efficiency
PR	Performance ratio
PSC	Perovskite solar cells
PV	Photovoltaic

TiO_2	Titanium dioxide
WACC	Weighted average cost of capital

Chapter 1: Introduction

1.1. Background

Over the last four decades, unprecedented economic growth and elevation in the standard of living have doubled global energy consumption [1]. Most of this energy is derived from fossil fuels such as coal, crude oil, and natural gas [2], presenting the world with two major problems. First, these fossil fuels are being used at a rate a significantly higher than their rate of deposition [3]. Second, the combustion of fossil fuels for energy leads to anthropogenic greenhouse gas (GHG) emissions that cause global warming [4]. For sustainable use of our energy sources, a balance between the economy and environment needs to be maintained; this is one of the critical challenges the world is facing today [5].

Renewable energy sources, i.e., hydro, geothermal, biomass, solar, and wind, are abundant and have comparatively lower environmental impacts than fossil fuel sources over their life cycle [6]. While their use may seem to significantly reduce the two problems mentioned above, there are several challenges we face in using these sources. For instance, hydro power requires a large initial investment, and its success is largely dependent on levels of precipitation [7]. Additionally, the establishment of reservoirs may displace land and wildlife habitat, causing ecological imbalance [7].

In the case of solar energy, cost and the land footprint are major barriers. The cost of solar energy is dictated by panel costs, cell efficiency, and battery system requirements to overcome the intermittency of sun's availability [7, 8]. However, on a positive note, the price of batteries used for energy storage has decreased significantly in the past few years [9]. The reduction in lithium

ion battery price in particular has exceeded expectations, and announcements on high-cycle stability have made their case strong and optimistic [9]. Between 2007 and 2014, battery cost estimates industry-wide fell by 8-14% [10-12]; the focus on areas in which to reduce costs has since shifted to panels and solar cell efficiency. First-generation crystalline silicon photovoltaic (PV) cells have efficiencies of around 25%; however, the problem is the scarcity of solar-grade silicon and associated costs in fabricating these PV cells [13, 14]. Nevertheless, crystalline silicon cells dominate the PV industry and had a market share of 93% in 2015 [15]. Though second-generation thin film PV cells have a smaller market share, they are relatively cheaper because they use fewer materials and low-cost processes [16, 17]. However, their photoconversion efficiencies have not been great for commercialization [18]. Therefore, inexpensive, abundant, and efficient materials are needed.

Perovskite solar cells (PSCs) are third-generation PV cells that have attracted considerable attention recently because of the potential of their low fabrication cost and technical advantages [19, 20]. Since PSCs are solution-processable via low-cost deposition techniques and characterized by their thin layers (up to 300 nm), reduced material and fabrication costs are expected [21, 22]. Furthermore, PSCs have a technical characteristic that causes almost all the photoexcited species to reach the charge collection electrodes, resulting in a superior performance [23]. The conventional PSC structure has a perovskite absorber between an electron transport and a hole transport layer as well as two electrodes on each end of the cell [24]. These layers are made from different materials using several processing techniques. Thakur et al. [25] showed that the efficiency of the PSCs can be increased by using monocrystalline TiO_2 nanorods as electron transport layers because of the reduced thermodynamic losses related to photons [26, 27]. With any new technology, it is important to carefully outline the economic, environmental and social

implications of the PSCs at their early stage of development [5]. Understanding their sustainability performances helps in the improvement of the technology while also highlighting its future potential [28].

Life cycle assessment (LCA) is a methodological framework that can be used to assess energy technologies both from environmental and socio-economic perspectives by considering their entire life cycle starting from raw material extraction to end of life [29, 30]. LCA is conducted based on the standards set by the International Organization for Standardization (ISO), ultimately assisting in identifying the GHG-intensive processes and providing valuable insights to policymakers and stakeholders [31, 32]. As per the guidelines and procedures provided by ISO, LCA has four phases: goal and scope definition, inventory analysis, impact assessment, and interpretation [31, 32]. The goal of an LCA sets the context of the study by clearly identifying the purpose, targeted audience, and the ways of communicating the results to the intended audience. The scope defines the system boundary of the study, the functional unit, time, location, and the procedures used [31, 32]. The inventory analysis involves compilation and calculation of material and energy requirements and the associate emissions at each stage of the product's life cycle. In the impact assessment, the results are translated to a number of environmental problems such as global warming, acidification, human health, depletion of resources, etc. The results are interpreted with an emphasis on the interest areas and conveyed to the audience in the final phase of the LCA. The outcomes of an LCA study are meant to help policymakers to frame policies around the recommendations made, favouring the commercialization of environmentally friendly energy technologies.

The environmental assessment needs to be integrated with the techno-economic assessment (TEA) to understand the cost implications of emerging energy technologies such as PSCs. As the name

suggests, TEA incorporates the technical and economic aspects of a technology to meaningfully evaluate its viability compared to alternative technologies that offer the same functions. Like LCA, TEA is a stepwise approach. It involves goal and scope definition and scenario assessment, system characterization, equipment sizing, cost estimation and profitability analysis, and results interpretation [33]. The overall focus of this thesis is to develop LCA and TEA frameworks to systematically quantify both the environmental sustainability and economic viability of a PSC-based energy system.

1.2. Literature review

A detailed literature review of LCA and TEA studies of perovskites was done as a part of this thesis to identify the key knowledge gaps. The LCAs conducted in the past have examined the various environmental impacts of changing the materials used and the fabricating processes adopted [24, 34-39]. For example, Espinosa et al. compared two deposition methods, spin-coating and evaporation, to conduct a cradle-to-gate LCA [35]. The processes were found to have excessive material losses, 90% for spin-coating and 70% for evaporation, highlighting a pressing need to replace them with other processes. Similarly, Celik et al. assessed processes that are suitable for mass production, such as spray and co-evaporation methods, to fabricate PSCs [24]. The authors found the energy requirements to be higher than those of commercialized solar technologies. The electrical energy used to fabricate the PSCs alone exceeded the overall energy consumption of other commercialized solar technologies. Gong et al. conducted an LCA of two perovskite architectures, one with titanium dioxide and the other with zinc oxide as electron transport layers, and Zhang et al. considered lead- and tin-based compounds in the absorber layer

[34, 38]. To summarize, most of the LCAs conducted have been attempts to identify the ideal combination of materials and processes having the least environmental impact.

Interestingly, most of these LCA studies were conducted from cradle-to-gate and did not evaluate the GHG emissions related to panel production and balance of the system (BOS) equipment, i.e., inverters, batteries, mountings, etc. In other words, material and energy data are included only as far as the fabrication of the cell; the studies cite the unavailability of perovskite-related data. Eventually, when this technology is commercialized, some equipment, such as the batteries, may be used in large quantities, and this will considerably increase environmental impacts and costs [40, 41]. Furthermore, some important materials used to fabricate the cell, for example, the gold layer or glass, have large environmental and economic impacts and need to be recycled or reused at the end of the PSC life. A cradle-to-grave study done at an early stage of technological development would assist policymakers. There is a scarcity of studies in this area. Therefore, in this thesis, a thorough material and energy consumption analysis was conducted from the cradle-to-grave life cycle stages of the PSC, including all the details relating to the BOS and reuse of some key materials.

With respect to cost estimation, there are very limited studies conducted on TEAs of PSC-based solar technology [28, 42-44]. The study by Cai et al. was the first and found the module cost to be much lower than that of other commercialized solar technologies [44]. This study assumed that perovskites can be printed like silicon and dye-sensitized cells. However, at the time of their research, there was no study to prove the feasibility of the printing. Chang et al. considered a more realistic PSC architecture based on earlier studies [28]. Their study found that the key contributors driving the manufacturing costs were the use of a gold or silver metallic layer and the expensive

hole transport layer, and so Song et al. considered a different but rare PSC architecture to estimate costs [42]. Their study used inorganic metal oxides as hole and electron transport layers. All the studies concluded that with an increase in module efficiency and lifetime, PSCs can compete with commercialized technologies. To reduce material costs, Chang et al. extended their research to replace glass with flexible substrates [43]. However, high temperature treatments can not be performed while fabricating the PSCs because of the low melting point of polymers [45]. The above-cited studies based their cost estimates on assumed production capacities of 100 MW [28, 44] and 200 MW [42]. However, since large-scale production of PSC panels is not a reality yet, these assumptions may lead to large uncertainty in the estimates. Further, given the current status of the technology, most of the data available to researchers is only from laboratories. There is very limited attention given to scaling up the material and energy consumption data from labs to large-scale production scenarios. This has a significant impact on the estimated costs, as most of the prior studies show that material costs play a deciding role in determining module costs. Given that Alberta, a province in Canada, has the highest solar insolation among the Canadian provinces, it would be interesting to see the impact of electricity generation from the PSC technology on the electricity costs and GHG grid intensity [46]. This study aims at addressing these gaps.

1.3. Research gaps

Based on the literature review conducted, the following research and knowledge gaps were identified.

- Even though the LCA studies conducted examine the environmental performances of several PSCs architectures and manufacturing processes, an architecture comprising

hydrothermally grown TiO_2 nanorods, used for a higher photoconversion efficiency, has not been explored.

- Though there are some LCA studies on PSCs, the environmental impacts relating to PSC panel production and BOS are excluded in most of these studies due to lack of data. There is still a need to conduct a comprehensive study covering all the components and life cycle phases of PSCs.
- Some key elements used to fabricate PSCs are rare and a few are detrimental to the economic or environmental performance of the PSC. Such materials need to be recycled and reused. There is very limited information available in the literature in this area.
- There is no robust framework in place to scale up laboratory data to large scale and so we cannot make cost estimates. Nor is there information on the scale factors of the cost components that contribute to overall cost. These factors help estimate the costs of PSCs with a greater level of accuracy, and a comprehensive study has not been done yet.
- Since PSC technology is at a low technology readiness level, its size and success depend on several factors, all of which elevate the level of uncertainty. Most studies have calculated the price of this technology based on large factory sizes similar to commercialized solar PV technologies. However, for decision making, we need to know the cost of electricity produced from this technology at different capacities in order to calculate sustainable costs and breakeven prices for a developer/investor. This is a gap in the literature.
- Previous studies have calculated the levelized cost of electricity (LCOE) and the minimum sustainable price for the PSCs; however, the real-life application of this technology and the additional costs involved have not been studied. This thesis attempts to answer the

question: “Can the PSC technology single-handedly meet the electricity needs of a residential consumer without additional economic burden?” Calculating the LCOE for residential application and comparing it with existing commercialized PV technologies can help in answering this question.

- There are very few LCA studies done in Canada on PSC technology, especially on how the Canadian electricity mix and available solar insolation would affect its performance. This is a major research goal of this thesis.

1.4. Research objectives

The overall aim of this study is to develop a framework to conduct an LCA and a TEA of TiO_2 nanorod-based PSC technology and explore its environmental sustainability and economic viability as a residential electricity-producing energy system.

The specific objectives of the thesis are to:

- Develop a bottom-up LCA framework to estimate PSC material and energy consumption, as well as the corresponding GHG emissions associated with the life cycle of PSCs;
- Systematically quantify the energy performance of the PSC technology and evaluate the energy payback time, net energy ratio, and the life cycle GHG emissions;
- Identify the key materials and processes of the PSCs that consume the most energy or emit the most GHGs and recommend alternatives to improve environmental performance;
- Reconstruct the production process flow based on the LCA results in order to accommodate low cost, high performance, scalable materials, and processes;

- Develop techno-economic models for estimation of cost of the large-scale production capacity of the PSC plant;
- Develop scale factors for PSC system components to estimate the individual cost of components and establish a relationship between the production capacity and the overall module costs;
- Calculate the cost-specific parameters of PV technologies – minimum sustainable price and LCOE, and
- Conduct a case study of a residential solar system with PSCs for installation in Canada.

1.5. Scope and limitations of the thesis

This research uses an LCA approach to evaluate the environmental performance of TiO_2 nanorod-based PSCs, including the material and energy consumption details from the raw material extraction stage to the end of life, where the degraded components are dismantled and discarded, while others are recycled and reused. The scope of this thesis includes a techno-economic assessment for estimation of cost based on the production pathway redesigned to include inputs from the LCA results.

This study has the following limitations:

- The focus of the study is confined to Alberta; the electricity mix, solar insolation values, and cost numbers considered are specific to this province in Canada. However, the framework can be applied to other jurisdictions by making minor changes to the input datasets.

- The production pathway includes the use of several materials and processes. Hence, all the results obtained in the thesis are specific to this set of materials and processes used. These materials and processes can be replaced with others, resulting in corresponding changes to the output. Similarly, some perovskite precursors can be replaced with environmentally friendly chemicals to improve PSC performance.
- The mass of materials and the energy consumption for panel production and BOS are assumed from studies on single Si PV cells only; there is no perovskite production data. Moreover, this study examines the slanted roof installation of perovskite solar panels only, as this is the most common way of installation.
- The PSC module cost was estimated based on an annual factory throughput of 3.5 MW_p. The results were extended to six other data points with a focus on every cost component up to 21 MW, and cost curves were developed for higher capacities. The scale factors were developed on the concept of economies of scale. However, the operations management philosophy explains the occurrence of diseconomies of scale after a certain point during production, which was not accounted for in this study.
- Given the short lifetime of PSC-based PV systems, costs were estimated for residential electricity generation only.

1.6. Organization of the thesis

This thesis is in paper format and is organized to have four chapters. Each chapter is independent and can be read separately. Some information might be repeated in different chapters. This chapter, the introduction, presents the overall background of the thesis. Chapters 2 and 3 will be submitted to journals for publication.

Chapter 2 presents a bottom-up approach to the LCA of TiO_2 nanorod-based PSCs. The goal and scope of the LCA, inventory-specific to the functional unit, and the method to calculate the key energy performance indicators are also discussed in this chapter. Key insights into the GHG emissions, net energy ratio, and energy payback time related to this technology are provided in the latter half.

Chapter 3 notes discusses the development of techno-economic assessment model. The important findings of the cost estimates through the TEA of PSCs are discussed in this chapter. This is an extension of chapter 2, as the PSC production pathway is redesigned based on the results from chapter 2. Further, the scale factors for individual cost components, cost curves to predict the price of PSCs, and the method to get to the LCOE are developed. Factors affecting the cost of PSC-based residential electricity generation are discussed in this chapter.

Chapter 4 presents the key results of this research, from the environmental and economic performance perspectives of PSCs. Recommendations for future work are also discussed.

Chapter 2: Life cycle assessment of high-performance monocrystalline titanium dioxide nanorod-based perovskite solar cells

2.1. Introduction

Climate change impacts caused by human activities are the major concern of the century. As a global effort to mitigate the risks and impacts of climate change, the Paris Agreement set a target of limiting the earth's average temperature rise to well below 2^{o}C above pre-industrial levels [47]. Such a target requires the transformation of the global energy system from fossil-based to renewable sources. Solar, along with wind energy, is a promising clean source that has significant role in decarbonizing the global energy system [48]. Photovoltaic (PV) technologies have shown remarkable development in the past decade due to breakthrough research in material advancement with improved energy conversion properties during this time [49-52]. The maximum power conversion efficiencies (PCE) of these solar modules are reported to be about 26.7% for single crystalline silicon, 21.9% for multi crystalline silicon, and 21% for cadmium telluride cells [13]. While these conversion efficiencies are promising, each solar cell type has its own set of challenges that researchers are attempting to address such as the scarcity of solar grade silicon, the cost of a crystalline silicon solar cell [14], and the high resistivity and work function of cadmium telluride (CdTe), which affects the carrier collection, semi-conductor, and metal junction [53]. Along with finding solutions to these problems, research on alternate materials can potentially provide better options. However, it is of utmost importance to evaluate the environmental benefits of alternative materials and emerging PV technologies.

Perovskite solar cells (PSCs) are one such promising new technology with the potential to enter the market in the near future. PSCs are seen as a highly competitive alternative to silicon and other solar cells [54]. PSCs have a perovskite absorber layer sandwiched between an electron and a hole transport layer as well as an electrode on both ends of the cell. Each layer is made from different materials [24]. While the silicon and thin film solar cells are typically around 300 μm and 2 μm thick, respectively, high efficiency PSCs can be as thin as 300 nm, thus reducing material cost [21]. Additionally, after an impressive increase in PCE from 10% in 2012 to ≤ 22.1% in early 2016, experts predict further efficiency improvements [55-57]. However, on the downside, the electron transport layer in PSCs is mostly mesoporous titanium dioxide (TiO_2). The mesoporous architecture is made of 20 nm-sized nanoparticles with grain boundaries that restrict the free flow of electrons, resulting in an unsatisfactory charge transfer. Furthermore, the mesoporous architecture does not support a random walk of electrons through the transport layer, thus hampering the photo conversion efficiency [58, 59].

Thakur et al., however, found that 17.6% efficiency PSCs, made of monocrystalline TiO_2 nanorods, can be built; these eliminate the shortcomings of mesoporous architecture [25]. The nano-structured electron transport layer also provides mechanical support to the perovskite absorber layer while reducing thermodynamic losses related to photons [26, 27]. As a result, these samples are capable of extracting electrons more efficiently from the absorber layer than mesoporous and monocrystalline structures. This is an indication that photo-generated electron-hole pairs are well separated in PSCs with TiO_2 nanorods before recombination [25].

With any new technology, it is important to analyse the materials and energy involved during production processes; this can be done through life cycle assessment (LCA) [29]. LCA is a

commonly used method to estimate the environmental impacts of a product system, throughout its life cycle [60]. Very limited LCA studies of perovskite solar modules have been conducted [24, 34-36]. These studies investigated the different materials for the various PSC layers and/or the different deposition methods during cell fabrication and their impacts on environment. Espinosa et al. compared two deposition methods, spin-coating and evaporation, for 1-year module lifetime PSCs with 15.4% and 11.5% efficiencies, respectively [35]. Both deposition methods have high material losses and hence warrant the consideration of alternative methods of deposition [35]. Celik et al. considered spray and co-evaporation methods for the fabrication of PSCs [24]; these methods are more amenable to large-scale manufacturing than spin-coating and dipping, which are currently used in laboratories. That study found that the electrical energy used in the fabrication of PSCs alone exceeded the energy consumed in all current commercialized solar technologies [24]. Gong et al. conducted an LCA of TiO_2 and ZnO module PSCs to calculate two sustainability indicators, energy payback time (EPBT) and carbon dioxide (CO_2) emission factor [34]. Zhang et al. conducted a comparative LCA of different lead- and tin-based PSCs [38]. The study found that methylammonium lead iodide and formamidinium lead iodide PSCs have higher environmental impacts than other technologies.

In the reviewed studies, when TiO_2 is used in the cell architecture as the electron transport layer, it is mostly compact/mesoporous TiO_2. However, two studies were conducted on TiO_2 nanorods as electron transport layers in PSCs, and low PCEs were found [61, 62]. Li et al. reported a PCE of 18.2% by changing the morphology of TiO_2 nanorods using organic acids in the growth solution of nanorods followed by a UV-ozone treatment to improve the TiO_2 nanorod /perovskite interface [63]. In the study by Thakur et al., the only surface treatment used was titanium tetra chloride, which is a common procedure for nano-structured TiO_2 [64-66]. This study aims at evaluating how

this simple yet effective fabrication technique improves the environmental performance of TiO_2 nanorod-based perovskite solar modules. To the best of the authors' knowledge, there is no LCA on this novel architecture. One study, by Zhang et al., performed a cradle-to-gate LCA of a liquid PSC technology with TiO_2 nanotube electrodes [37]. But the way in which TiO_2 nanotubes were prepared in that study is completely different from the preparation considered by Thakur et al. [25]. While Zhang et al.'s study used electrochemical anodization, Thakur et al. in their research, hydrothermally grew TiO_2 nanorods on the Fluorine doped tin oxide (FTO) glass substrate. The hydrothermal growth was further controlled by the concentration of titanium precursor, thus changing the morphology of the grown nanorods as needed, to minimize interfacial recombination, thereby increasing the efficiency [25]. TiO_2 nanotube anodization was found to have a large environmental impact and since that step is not used by Thakur et al., our study aimed to conduct an LCA with a nanoscale electron transport layer as the centre of attraction, as this area has not been explored enough so far.

The studies cited above considered the life cycle impacts only to the point of solar cell fabrication. Panel production and the balance of the system (BOS), comprising mounting systems, inverters, and other electric installations, were not included due to the lack of data on perovskites and to allow for ease of comparison between studies [39]. However, several LCA studies conducted on other types of solar cells found that the BOS has a considerable share in the overall environmental impact [40, 41]. Hence, keeping the BOS out of the system boundary can lead to an underestimation of the environmental impacts associated with a PSC. In this study, the life cycle greenhouse gas (GHG) emissions and energy requirements associated with panel production and the BOS are included to provide better insights into the overall environmental impacts of PSCs.

The primary aim of this paper is to evaluate the overall environmental performance of TiO_2 nanorod-based PSCs (fabricated through the simple process explained by Thakur et al.) in order to identify the major areas of improvement [25]. The specific objectives of this paper are to:

- Develop a bottom-up LCA framework to estimate the life cycle GHG footprint of PSCs to supply electricity produced from solar insolation;
- Compute the energy performance indicators of the PSC, namely the energy payback time (EPBT) and the net energy ratio (NER);
- Identify the key materials and processes of the PSC that consume the most energy or emit to the most GHGs;
- Conduct sensitivity and uncertainty analyses to determine the important parameters;
- Conduct a case study for a fossil-fuel intensive jurisdiction, Alberta, a western province of Canada.

2.2. Method

2.2.1. Goal and scope definition

The primary goal of this study is to apply life cycle assessment (LCA) as a methodological framework to evaluate the environmental benefits of TiO_2 nanorod-based PSCs. Since the function of this system is to generate electrical energy, the material and energy requirements and the associated environmental and energy performances over the life cycle of the product system are normalized to 1 kWh, which is the defined functional unit of the system. The results of this research are expected to help researchers in this field understand the technology's critical environmental concerns and develop alternatives for better performance. The information might also help policy

makers to frame long-term policies favouring the commercialization of environmentally friendly power generation systems.

Figure 2.1 shows the system boundary, which includes four life cycle stages: perovskite solar cell production, BOS and assembly, operation, and end-of-life. The emissions related to transportation are assumed to be marginal as most of the raw materials can be chemically synthesised locally. This assumption is widely accepted for organic PV systems [67]. Each life cycle stage is further discussed in detail below.

2.2.2. Perovskite solar cell production

The first life cycle (LC) stage is the extraction of the raw materials necessary to produce the precursors and components used in manufacturing PSCs. The mass of the materials needed per functional unit is detailed in Table 2.2. The required components and precursors are progressively deposited on the glass substrate to fabricate PSCs. PSC fabrication details are taken from Thakur et al.[25]. First, the FTO-coated glass substrates are cleaned by sonication in cleaning solvents for 30 minutes. A thin layer of TiO_2 is then deposited on the cleaned substrates, followed by calcination. Next, a TiO_2 nanorod array is hydrothermally grown on the substrates by adding an appropriate amount of titanium (IV) n-butoxide to a solution of hydrochloric acid, glacial acetic acid and water [25].

The resulting transparent array of nanorods is again rinsed in deionized water and dried. Next, the TiO_2 nanorod array is treated with 40 mM of titanium tetrachloride for 30 minutes at 70 °C and annealed at 500 °C for 30 minutes [25]. This post-treatment is necessary to increase the efficiency of the solar cells [64]. The perovskite layer is deposited on the electron transport layer, a perovskite

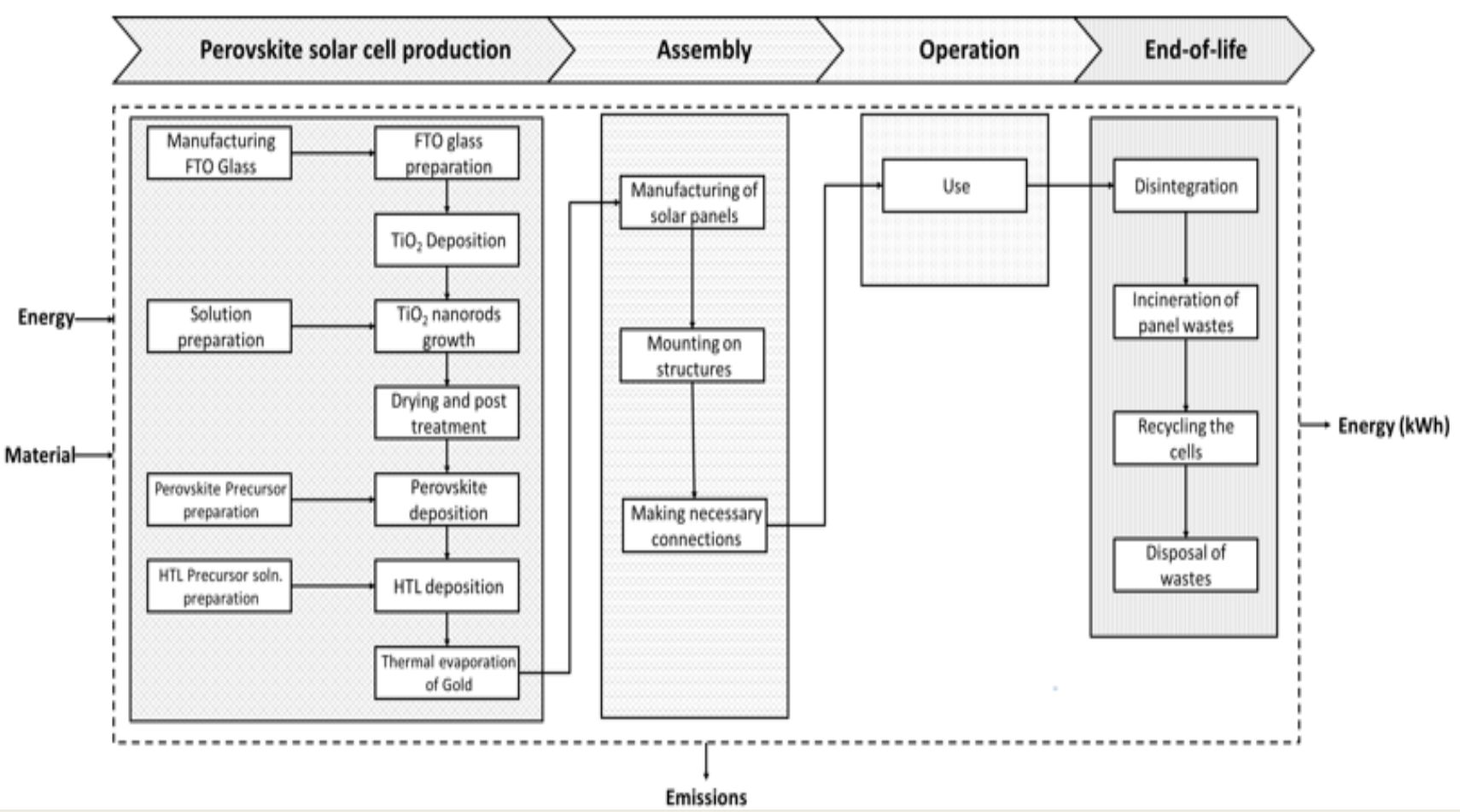

Figure 2. 1: System boundary of TiO_2 nanorod-based PSCs

precursor solution consisting of 1M formamidinium iodide (FAI), 1.1M lead iodide, 0.2M methylammonium bromide, and 0.22M lead bromide in a 4:1 mixture of dimethylformamide and dimethyl sulfoxide. A Spiro-OMeTAD hole transporting layer is deposited by spin-casting. The final stage is to thermally evaporate a 70nm thick gold layer, thus completing the fabrication of the cell [25].

Apart from accounting for the materials, the energy used for fabrication is included in this life cycle stage. Details are available in the energy inventory table (Table 2.3).

2.2.3. Balance of system (BOS) and assembly

This life cycle stage accounts for the materials and energy used for panel production and the BOS. The BOS typically includes the mounting system, inverters, junction box, and other components for making necessary connections. The panels are mounted in a pre-decided location and the necessary connections are made before the PSCs become operational. Due to the lack of data on PSCs, the material and energy requirements for the BOS were approximated from commercialized PV technology [68] based on the assumption, as in another study [69], that similar systems can be used for a PSC. The details of the calculations related to this phase are discussed in the inventory analysis section.

2.2.4. Operation

For PV technologies, since electricity is generated from solar energy, energy consumption and GHG emissions during operation are zero. Therefore, the use phase impacts are omitted even though this phase lies within the system boundary of the study [70].

2.2.5. End-of-life

The last stage is the end-of-life and accounts for the environmental impacts of separating the layers of panels, recycling, and the reuse of certain components as well as disposing the wastes. The dismantling and reuse of FTO glass and the gold layer are modelled as per the study by Binek et al. [71], and is explained later in this paper.

2.3. Inventory analysis

The inventory analysis involves the compilation and calculation of material and energy input requirements at each process in the life cycle of the product system. Tables 2.2 and 2.3 list the raw materials and energy necessary to generate 1 kWh of electricity from TiO_2 nanorod-based PSC architecture. The total lifetime electricity generation is calculated using Equation 1 [39] based on the assumptions and considerations mentioned in Table 2.1.

$$E_{out} = A \times PR \times I \times \eta \times LT \qquad \text{Equation (1)}$$

Table 2. 1: Inputs and assumptions - calculation of lifetime electricity generation

Parameter	Definition	Value	Comments/ Remarks
E_{out}	Total energy output from the PSC panel in kWh	1135.8 kWh	Electricity output through the lifecycle of the panel
A	Panel dimensions	1.635 m^2	Standard 60-cell rooftop panel
PR	Performance ratio	0.85	0.75 is used in Europe and 0.95 is used in the US [72]. The average of the two is chosen

Parameter	Definition	Value	Comments/ Remarks
I	Annual solar insolation	1513.5 kWh/m^2/yr	Based on the data from the Natural Resources Canada dataset [73]. The dataset provides monthly insolation data for every municipality across Canada.
η	Panel efficiency	18%	[25]
LT	Lifetime in years	3 years	[24]
Emission factor	GHG emissions caused during electricity production	0.6 kg CO_2 eq./kWh	Davis et al. [74]

There is ambiguity around the lifetime of perovskite solar cells because the technology is new. Lifetimes of one [35], two [34], and five years have been reported, similar to a commercial solar cell [37]. Until 2018, the longest lifetime reported for PSCs was around one year [75]. Since commercialized solar cells have longer lifetimes, perovskites cannot be commercialized with a very small lifespan. This study assumed a lifetime of 3 years, as Celik et al. did [24]. The difference is captured in the sensitivity and uncertainty analyses. The materials used to fabricate a PSC are based on detailed laboratory data from Thakur et al. [25]. The PSC sample used in this laboratory is 7.5 cm X 2.5 cm and all the data collected corresponds to this size. Relevant mass conversions were done to obtain the mass of input materials used for every 243.4 cm^2 (the standard cell size) of the PSC.

The energy required at each sub-step of PSC fabrication was estimated by considering the equipment's power rating, usage time, and use factor. The use factor for each equipment is calculated as explained by García-Valverde et al. [76]. The purpose of introducing the use factor is to ensure that only the energy relevant to the functional unit is included, as the equipment may not be used at its maximum capacity. In short, every parameter (speed, temperature, the volume at which the process occurs, etc.) is divided by the corresponding maximum capacity of the equipment and multiplied with each other to get the overall use factor for that particular process.

The mass of materials for panel production was calculated with data from Jungbluth et al. [68]. The panel production, BOS, and assembly data for single-Si photovoltaic panels were considered.

For the mounting system, to be in line with panel production, slanted roof construction is assumed. This is the most common way of installation [68].

Finally, the material inventory for the end-of-life were approximated from Binek et al. [71]. As explained in their work, the PSCs are immersed in chlorobenzene to categorically separate the hole transport layer and the gold layer. The gold layer is then filtered out, cleaned, and reused. The perovskite layer that remains on the FTO glass layer is converted back to lead iodide through brief immersion in double distilled water. Treatment with dimethylformamide subsequently dissolves lead iodide, leaving a reusable FTO glass substrate with a hydrothermally grown electron transport layer [71]. A three-time reuse case was adopted in this study; as observed by Binek et al., there is no considerable change in performance when PSCs are thrice recycled [71]. The emissions arising from the reused and recycled FTO glass and gold layer were considered.

Table 2. 2: Material inventory results per the functional unit (kWh)

Life cycle stage	Sub-step	Material	Mass, g	Remarks	Comments/ Remarks
Perovskite solar cell (PSC) fabrication	FTO glass preparation	FTO coated glass slides*	2.5E+0	Substrate	Materials used to fabricate PSCs are based on detailed laboratory data from Thakur et al. [25]. The PSC sample dimensions are 7.5 cm X 2.5 cm and all the data collected corresponds to this size. Relevant mass conversions were done to obtain the mass of input
		Acetone	2.0E+0	Cleaning solvent	
		Methanol	2.0E+0	Cleaning solvent	
		Deionized water	2.6E+0	Cleaning solvent	
	TiO_2 deposition	Titanium(IV) isopropoxide	2.2E-2	For the thin compact layer of TiO_2	
		1 M Hydrochloric acid	5.3E-3		
		Isopropanol	2.5E-1		
	TiO_2 nanorod growth	Hydrochloric acid (37%)	3.4E+0	Solution preparation for hydrothermal growth of TiO_2 nanorods on the glass substrate	
		Glacial acetic acid	3.0E+0		
		Deionized water	5.6E+0		
		Titanium (IV) n-butoxide	6.8E-1		
	Drying and post-treatment	Deionized water	5.1E-3	Rinsing the nanorod array	
		Flowing nitrogen	7.1E-2	Drying	
		Titanium tetra chloride	3.9E-1	Post-treatment	
	Perovskite deposition	Methylammonium bromide	1.0E-2	Preparation of the perovskite precursor solution	
		Formamidinium iodide	8.7E-2		
		Lead bromide	3.7E-2		
		Lead iodide	2.3E-1		
		Dimethylformamide	3.5E-1	4:1 mixture added to the solution	
		Dimethyl sulfoxide	1.0E-1		

Life cycle stage	Sub-step	Material	Mass, g	Remarks	Comments/ Remarks
		Chlorobenzene	2.5E-1	For rapid crystallization	materials used for producing 1 kWh of electricity from the PSC panels
	Hole transport layer deposition	Spiro-OMeOTAD	8.1E-3	Hole transport layer	
		Chlorobenzene	2.5E-1	Mixture for deposition of the hole transport layer. Approximately 200nm thick	
		4-tert-butylpyridine	3.0E-3		
		Acetonitrile	3.2E-3		
		Lithium bis trifluoromethanesulfonyl-imide	1.0E-3		
	Thermal evaporation of gold	Gold*	7.1E-4	Device completion	
Panel production, balance of the system and assembly [68]	Manufacturing of solar panels	Low-iron glass	1.5E+1	Panel top cover	Data from Jungbluth et al. [68]. The panel production, balance of the system, and
		Wire drawing, copper	1.6E-1	For wires	
		Aluminum alloy	3.8E+0	Panel edges	
		Ethyl vinyl acetate	1.4E+0	Front and rear cover for cells	
		Polyester	5.4E-1	Bottom cover	
		Polyvinyl fluoride	1.6E-1	Bottom cover	
		Acetone	1.9E-2	Cleaning fluid	

Life cycle stage	Sub-step	Material	Mass, g	Remarks	Comments/ Remarks
		Methanol	3.1E-3	Auxiliary material	assembly data for single-Si photovoltaic panels were considered. For the mounting system to be in line with panel production, slanted roof construction is assumed [68]. Relevant mass conversions were done to obtain the mass of input materials required, after calculating the panel area used to produce 1kWh of electricity.
		Propanol	1.2E-2	Soldering flux	
	Mounting on structures	Aluminum for mounting system	4.1E+0	For mounting	
		Steel	2.2E+0	For mounting	
		Corrugated board	1.9E-1	Correction factor of 1.54/m^2 used	
		Plastics (polyethylene)	2.0E-3		
		Section bar extrusion	4.4E-3		
		Polystyrene	1.0E-2		
	Inverters	Aluminum alloy	5.5E-1	Inverter capacity calculated as 280W per m^2 area from Jungbluth et al. [68] All the masses presented are converted to the functional unit. Minor electronic components excluded.	
		Copper	1.6E-3		
		Low alloyed steel	1.1E-1		
		Corrugated board box	7.1E-1		
		Capacitor, electrolytic	4.3E-2		
		Capacitor, film	5.8E-2		
		Capacitor, CMC	3.9E-3		
		Resistors	8.1E-4		
		Acrylonitrile ABS polymer	1.2E-1		
		Transformer	2.5E-1		
		Polycarbonate	5.5E-2		
		Polyethylene	1.1E-2		
		Polyvinyl chloride	1.6E-3		

Life cycle stage	Sub-step	Material	Mass, g	Remarks	Comments/ Remarks
End-of-life [71]	Disintegration	Chlorobenzene	3.5E+0	To separate the gold layer and the hole transport layer	Mass of materials required for the re-use of FTO glass and gold layer was approximated from a study by Binek et al. [71]
		Nitrogen stream	7.1E-2	Drying after peeling the hole transport layer	
		Deionized water	3.2E+0	To remove perovskites leaving behind lead iodide	
	Recycling the cells (cleaning)	Dimethylformamide	3.0E+0	To dissolve lead iodide	
		Dimethylformamide	3.5E-1	To clean the glass substrate	
*Reuse of materials considered as per the specifications in PAS 2050:2011 [77].					

Table 2. 3: Energy inventory results per the functional unit (kWh)

Life cycle stage	Sub-step	Process	Equipment	Energy consumption (kWh/ functional unit)	Comments/ Remarks
Perovskite solar cell fabrication	FTO glass preparation	Sonication	Aquasonic ultrasonic cleaner	5.64E-03	The energy required at each sub-step of PSC fabrication was estimated by considering the equipment's power rating, usage time, and use factor.
	TiO_2 deposition	Stirring	Thermo Scientific Cimarec	7.60E-05	
		Spin casting	KW-4A Spin Coater	6.78E-05	
		Calcination	Lindberg/Blue M™ 1100°C Tube furnaces	1.49E-02	
	TiO_2 nanorod growth	Hydrothermal growth	Thermo scientific oven Fisherbrand ™ 3511FSQ	4.50E-03	
	Drying and post-treatment	Titanium tetra chloride treatment	Thermo Scientific Cimarec	1.09E-03	

Life cycle stage	Sub-step	Process	Equipment	Energy consumption (kWh/ functional unit)	Comments/ Remarks
		Annealing	Lindberg/Blue M™ 1100°C Tube furnaces	1.65E-02	
	Perovskite deposition	Stirring	Thermo Scientific Cimarec	5.91E-05	
		Spin casting-stage 1	KW-4A Spin Coater	7.54E-06	
		Spin casting-stage 2	KW-4A Spin Coater	6.03E-05	
		Annealing	Lindberg/Blue M™ 1100°C/ tube furnaces	3.30E-03	
	Hole transport layer deposition	Spin casting	KW-4A Spin Coater	2.26E-05	
	Thermal deposition of gold	Thermal evaporation [34, 76]		4.76E-03	

Life cycle stage	Sub-step	Process	Equipment	Energy consumption (kWh/ functional unit)	Comments/ Remarks
Panel production, BOS and assembly	Manufacturing of solar panels	Lamination – electricity use		6.78E-03	[68]
		Lamination – heat use		2.16E-03	[68]
	Inverters	Electricity for production [68]		3.41E-03	Capacity of the inverter per m^2 is 280W. It is approximated for the functional unit.
End-of-life	Disintegration	Gold filtration [34]		1.34E-07	Pressure filter is assumed to filter the gold layer. 0.21 MJ electrical energy per kg of solid.

2.4. Energy and environmental impact estimate

The inventory data for each life cycle stage is translated into GHG emissions, EPBT, and NER. This section describes the approach used to estimate both the energy and environmental metrics.

2.4.1. Energy payback time and net energy ratio

The EPBT measures the time in years the system requires to recover the energy used to produce the module [37]. The materials used in module preparation, energy conversion efficiency of the cell, and location-related irradiation are the key factors that affect the EPBT of a solar system. The EPBT of the PSC system is calculated using Equation 2.

$$EPBT = \frac{\mathrm{E}_{tot}}{E_{out}/\gamma} \qquad \text{Equation (2)}$$

E_{tot} refers to the total embedded energy consumed in the entire life cycle of the PSC from raw material extraction to final disposal, recycle, or reuse, and is represented as megajoules of primary energy consumption per m^2. E_{out} , in MJ/m^2-year, is the annual energy production capacity of the PSC. γ is the average electrical to primary energy conversion; it was calculated to be 0.3 based on the electricity mix chosen.

For any system, the NER is used to compare the output energy generated by the system over the life cycle to its primary energy input [78]. The NER is expressed as:

$$NER = \frac{LCE_{out}}{LCE_{in}} \qquad \text{Equation (3)}$$

where LCE_{out} is the life cycle energy output in MJ/m^2 and LCE_{in} is the life cycle energy input in MJ/m^2.

2.4.2. The life cycle greenhouse gas emissions

The life cycle GHG emissions are calculated by summing the emissions associated with production of each of the raw material and energy used. The contributions from the different sources of energy used to generate electricity in Alberta change every year. Hence the GHG emissions associated with generating electricity (expressed as g CO_2 equivalent per kWh of electricity produced) will change. An emissions factor of 0.6 kg CO_2 eq/kWh was considered for the year 2019, taken from an extended study from Davis et al. [74]. This factor is bound to change over years with changes in the electricity mix and this change is therefore considered in sensitivity and uncertainty analyses.

2.5. Results and discussion

2.5.1. Greenhouse gas emissions footprint

The life cycle GHG emissions associated with PSC architecture were estimated to be 182 g CO_2 eq per kWh of electricity. Figure 2.2 shows the emissions breakdown by life cycle stages and Figure 2.3 the contribution by major processes. The emissions associated with material preparation and direct use of energy are presented separately.

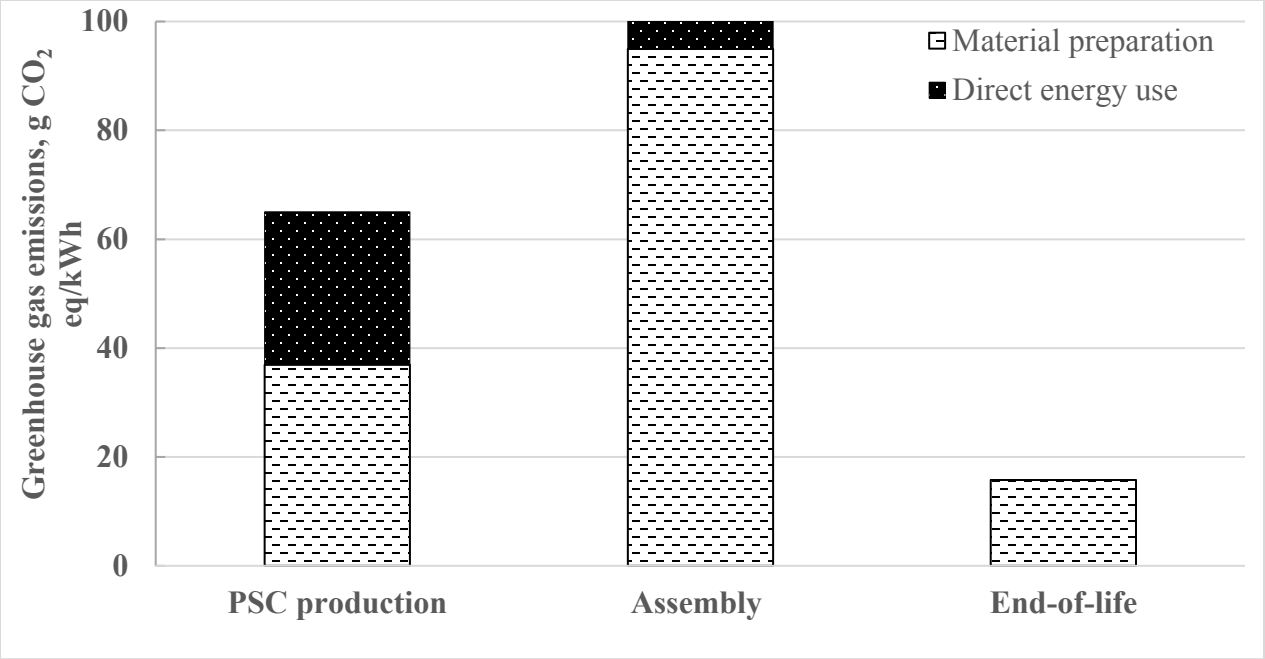

Figure 2. 2: GHG emissions distribution across key life cycle stages

Significant GHG emissions (56% of the total) associated with the BOS and assembly stage were found in this study. These GHG emissions are predominantly from raw material use. Module assembly, mounting, and inverters are the key contributors. These impacts were left out of most perovskite LCA studies as their system boundaries ended with cell fabrication. Further, the PSC production stage accounted for around 36% of GHG emissions. This stage involves several important material- and energy-intensive processes such as FTO glass preparation, TiO_2 deposition, perovskite deposition, drying and post-treatment. The perovskite deposition step accounts for the highest GHG emissions from this life cycle stage, mainly because of the use of chemicals such as formamidinium iodide and methylammonium bromide. The energy consumed and the GHG emissions associated with the production of formamidinium iodide are extremely high, though small amounts are used. Reusing these chemicals could reduce the GHG emissions associated with PSC production. High-temperature processing techniques such as calcination and

annealing used for TiO_2 deposition and post-treatment of the nanorods, respectively, contribute to more than half of the direct energy use. However, the possibility of ultrasonic spray-coating large-scale TiO_2 compact layer on the substrates has been illustrated by Zhou et al., who further perform calcination at a lower temperature of 135^{o}C [79]. Such a modification to the process flow can bring down the energy consumption and the GHG emissions for this PSC architecture. Therefore, the need to adopt low-temperature processes can be reiterated based on the results of this study. The GHG emissions related to the end-of-life stage are only 9%. At the end of life, panels are disintegrated, and the PSCs are immersed in chlorobenzene to separate the gold layer and the hole transport layer. The top layer perovskites are removed from the glass substrate through thorough rinsing with deionized water. Washing multiple times with dimethylformamide thereafter leaves behind the glass substrate and the hydrothermally grown TiO_2 electron transport layer, which is reused [71]. Apart from gold layer filtration, no process requires electrical or heat energy throughout the end-of-life recycling stage. Therefore, the GHG emissions related to this life cycle stage are predominantly due to the use of materials that require reuse.

Overall, 80% of the total life cycle GHG emissions are related to the material requirement at each stage of the life cycle. Therefore, choosing environmentally friendly materials is the key area than alternative fabrication processes for this PSC.

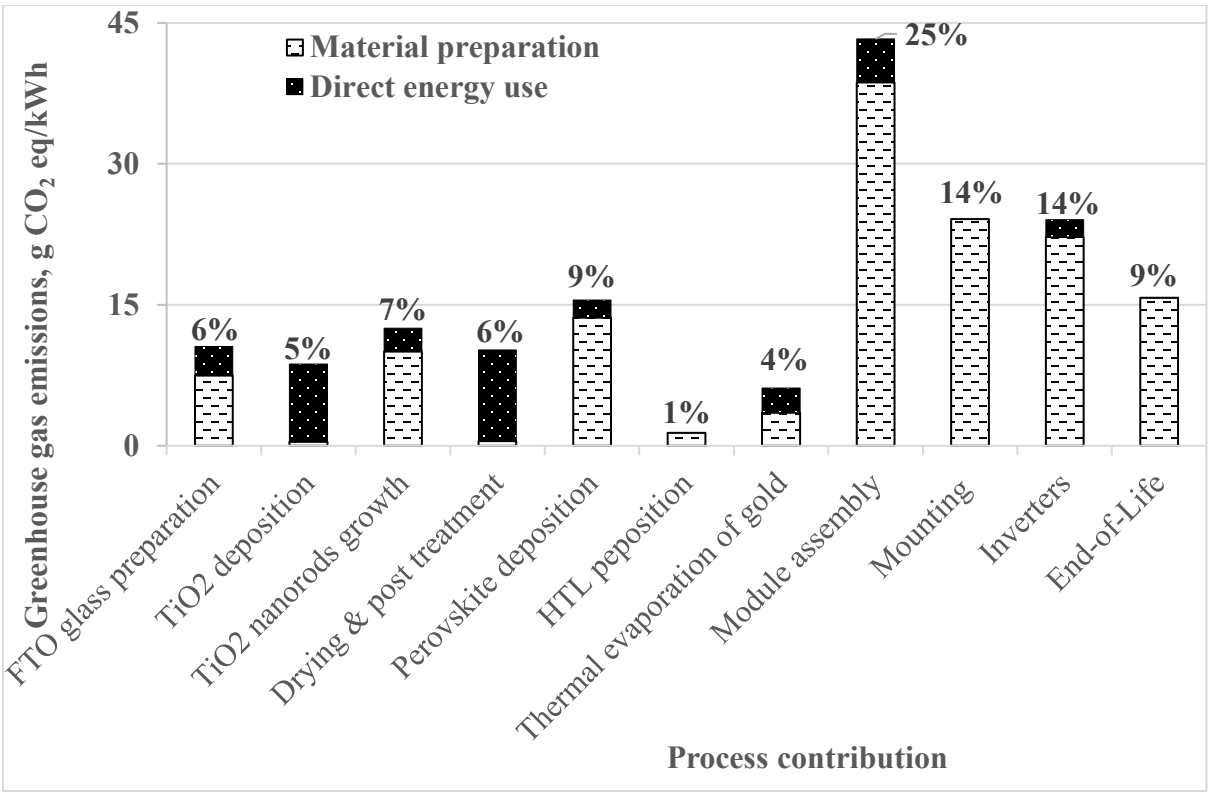

Figure 2. 3: Process contributions to GHG emissions for the PSC

Figure 2.4 presents the elemental contributions of materials towards life cycle GHG emissions. The aluminum frame used in panels and for the mounting system makes up about 30% of the total GHG emissions from material production. This is because industrial aluminum is obtained from bauxite ore through the Bayer and Hall Héroult processes, both of which are high-temperature processes [80]. Jungbluth et al. report that many producers use plastics and wood instead of aluminum in their mounting systems for economic and energy reasons [68]. Gong et al., however, showed FTO glass and gold to be the key contributors in similar architecture when the BOS is not considered in the system boundary [34]. This study found that FTO glass and gold together take up just 4% of the total GHG emissions related to material preparation, proving the benefits of recycling and reuse of key elements of the PSC. Similarly, the recycling and reuse of organic

solvents such as chlorobenzene, acetic acid, and dimethylformamide, if considered, may result in further reductions in energy consumption and carbon footprint for this PSC.

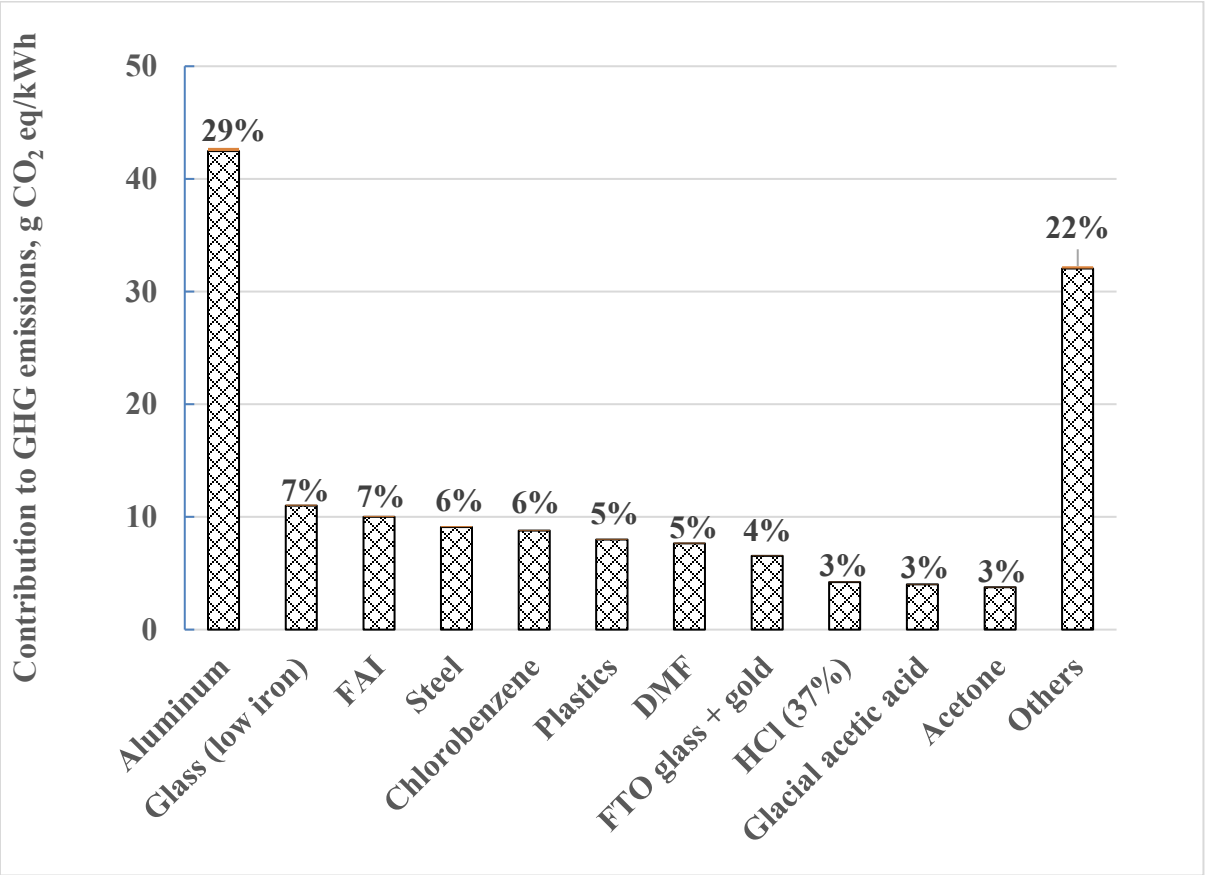

Figure 2. 4: Elemental contributions of materials to GHG emissions

4 mm thick low-iron glass is used in a higher quantity than any other material used for making panels, as it is the top cover [68]. Low-iron glass is preferred over conventional glass because of its high transmission rate and efficiency in trapping solar energy [81, 82]. However, silica sand, one of the main ingredients used in glass-making, naturally contains iron oxides that need to be retained in small quantities to prepare the best low-iron glass [83]. Consequently, more energy-intensive processes are involved such as rapid heating and cooling the glass to improve its strength, resulting in emissions from glass manufacturing [81]. The authors of this study modelled the

energy use and GHG emission factors for manufacturing formamidinium iodide and found that because of the high electricity use during the process, formamidinium iodide production contributes towards GHG emissions significantly. More information can be found in the supplementary information document.

A review by Peng et al., reports the GHG emissions per kWh of electricity associated with mono-silicon, multi-silicon, amorphous silicon, and cadmium telluride solar cells to be less than 50g CO_2 eq. [70]. Even for the dye-sensitized solar cells, the GHG emissions are not expected to exceed 120g CO_2 eq. Importantly, the reported values are lower than those calculated for this PSC mainly because of the lifetime of the cells. Since silicon solar panels have a lifespan of 25-30 years, a significant decrease in associated GHG emissions is observed by Peng et al. [70]. PSCs can compete with other established or new solar PV technologies when their lifetime increases.

2.5.2. Energy payback time and net energy ratio

The EPBT was calculated using Equation 2. The parameters and the values used are explained in section 2.4. The PSC system considered in this study takes about 0.97 years to pay back the energy that was consumed throughout its life cycle.

EPBT studies conducted in the past for perovskite technology reported a wide range of values. One study considered the cradle-to-gate energy requirement of three perovskite structures and found EPBTs of 1.05 and 1.54 years [24], close to the value obtained in this study. However, excluding panel production, the BOS and end-of-life phases would lower the EPBT to 0.35 years, which is close to the value found in the study by Gong et al. [34]. Moreover, the EPBT calculated would be 1.05 years, if the FTO glass and gold layer are not reused.

The NER calculated from Equation 3 is 3.08, which indicates that the energy produced by the PSC system is more than three times the primary energy consumed through its life cycle. Since energy production largely depends on the efficiency and lifetime of the solar PV panels, these two parameters dictate the energy generation capacity of the PSC throughout the entire life cycle. As the PV industry thrives to reach higher efficiency and lifetimes, higher NERs can be expected in the near future.

2.5.3. Uncertainty and sensitivity analysis

Sensitivity analysis was conducted to identify the parameters to which the output is sensitive. The Morris statistical method was used to perform this analysis. This method is suitable when the number of inputs is high (as in this case) in order to identify the parameters that have greater impact on the output and need deeper analysis. Additionally, to address the uncertainty of some inputs on the results, a Monte Carlo simulation was used.

Uniform distributions were used for all the inputs with maximum and minimum values. There are two ways errors can enter when inputs are considered. First, the considered material and energy use may not be accurate. Second, the primary energy consumption for manufacturing these raw materials and their GHG emission factors might be incorrect. In both cases, an uncertainty range of ±20% was used to discern the impact of these errors. Apart from that, a few other key input parameters that govern the EPBT, NER, and GHG emissions associated with this PSC such as insolation have had values reported based on the location of the study, architecture of the PSC, and other assumptions. The uncertainty ranges for these parameters are shown in Table 2.4.

Table 2. 4: Uncertainty ranges for input parameters per functional unit (kWh)

Parameters	Unit	Uncertainty range
Insolation	MJ/m^2/year	3941 - 8047
Efficiency of the cell	%	14 - 22
Performance ratio	-	0.75 - 0.95
Lifetime	years	2 - 5
Panel efficiency	%	14 - 22

The lifetime of PSCs is uncertain at this moment; we assumed 2 to 5 years. The performance ratio is usually considered 0.75 in Europe and 0.95 in the US [72]. These values are used in setting the input range. The highest efficiency recorded for halide-based perovskite solar cells is 22% [25] and was used in the simulation. In addition, the insolation is lowest when the panels are horizontal (tilt = 0^o) at 3941 MJ/m^2-year and the maximum solar energy can be exploited when two-axis solar tracking is used [73]. This Alberta-specific insolation data was used to set the range. The sensitivity results are presented in Figures 2.5 and 2.6.

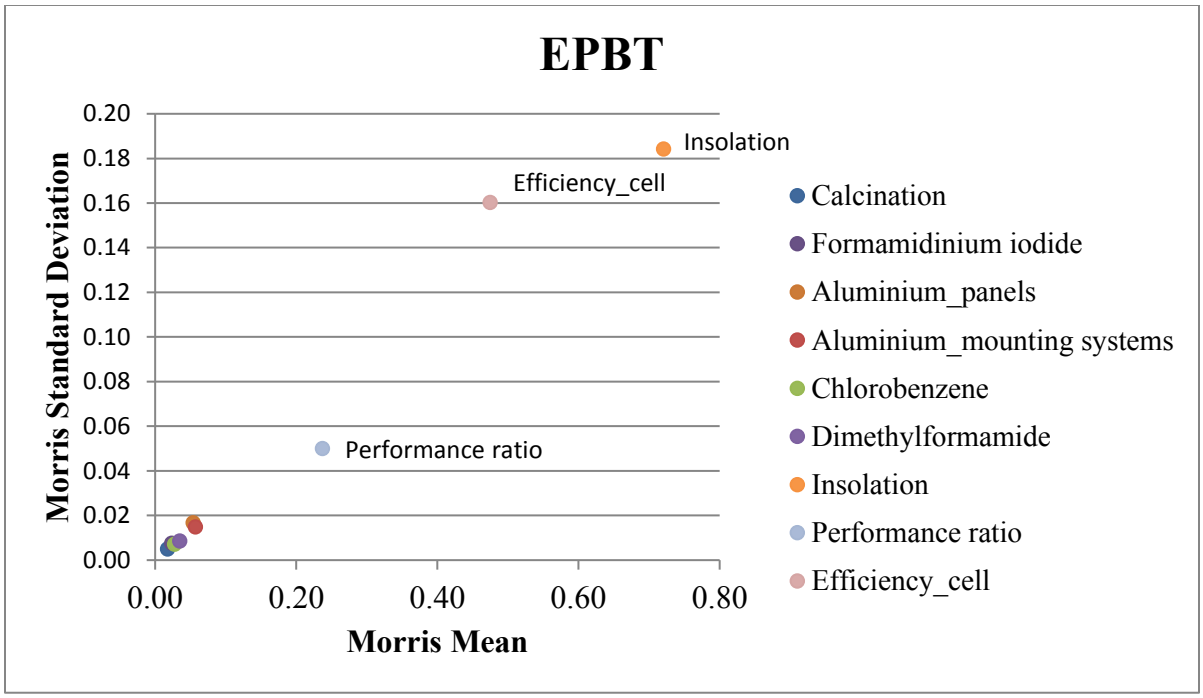

Figure 2. 5: Sensitivity analysis showing the effect of inputs on the EPBT of the PSC

Figures 2.5 and 2.6 show the sensitivity analysis results as Morris mean and standard deviations for the EPBT and GHG emissions, respectively. The Morris mean typically indicates the average change in the output as the input fluctuates from the minimum to maximum values. However, the Morris standard deviation represents the extent of variation in the output for every change of the input. The parameters in the right top corner are highly sensitive.

The EPBT result appears to be highly sensitive to solar insolation, the efficiency of the cells, and performance ratio. Changes in material and energy consumed during each life cycle stage have less impact on the overall EPBT result. For the GHG emissions, the lifetime of the cells is the most sensitive parameter. With every extension in the life of the PSC, the life cycle electricity production increases, thus decreasing the amount of GHG emissions per kWh electricity produced during its lifetime. A wider range can be considered in future, when this technology is developed

further and we can present a scenario comparable with silicon solar cells that have longer lifetimes. Clearly, the environmental impacts of the PSCs would exponentially decrease should their lifetimes increase. Nevertheless, panel efficiency and PR are also sensitive inputs that can considerably change the GHG emissions associated with a PSC. The NER is also sensitive to the lifetime, insolation, and efficiency of the PSC.

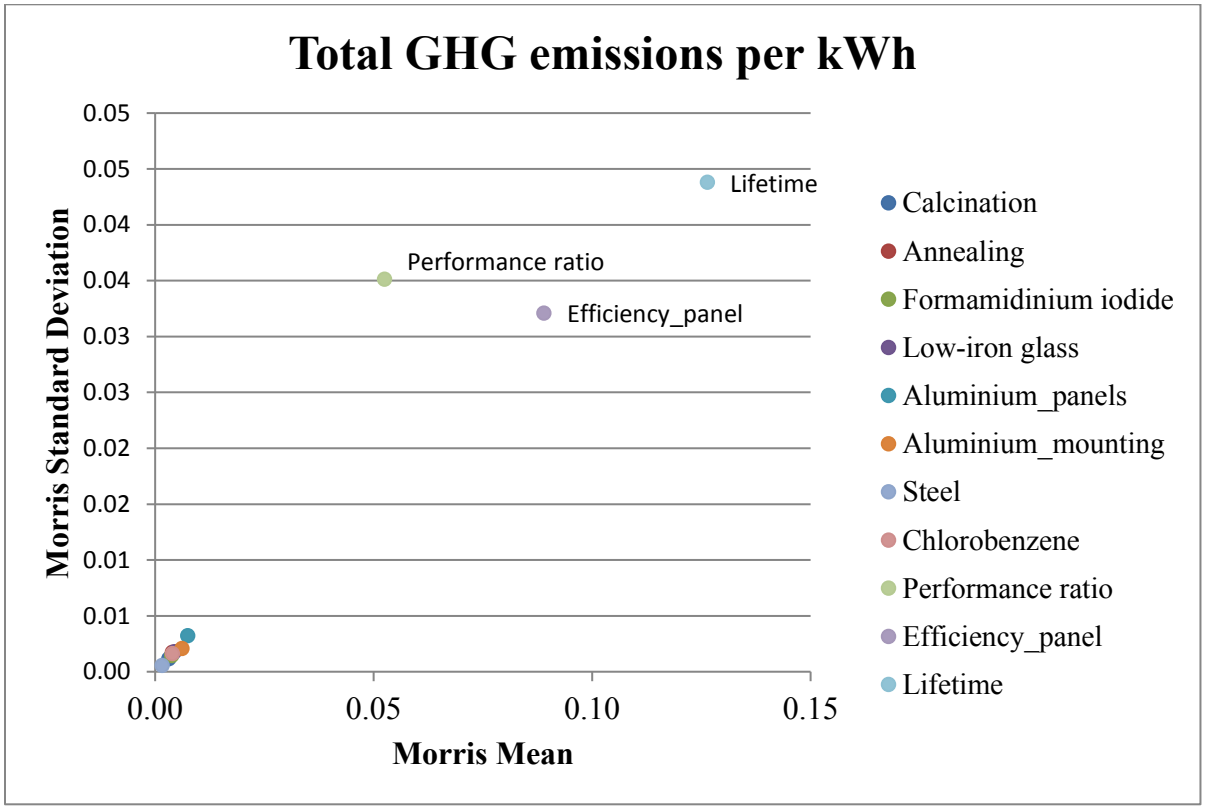

Figure 2. 6: Sensitivity analysis showing the effect of inputs on the GHG emissions associated with the PSC

The RUST model developed by Dilullo et al. was used to conduct the Monte Carlo simulation for uncertainty [84]. A uniform distribution of the inputs with specified minimum and maximum values were selected. A random sample was selected from the conservative distribution of inputs and iterated 5,000 times to obtain the final distribution.

The results of the uncertainty analysis are shown in the Figure 2.7. The mean EPBT was 0.9 years with a range of 0.5-1.9 years. This result is stable compared to the results of GHG emissions, where the uncertainty was observed to be very high. An extremely low GHG emission value of 85g/kWh was obtained with a lifetime of 5 years and a panel efficiency of 21%. These are the targets to be set for the near future. With every increase in the lifetime of the PSC, the associated GHG emissions decrease quickly, with the PSCs gaining an upper hand over other commercialized solar cells.

From the uncertainty results, at a 70% confidence level the GHG emissions/kWh of electricity produced would be less than 200g CO_2 eq/kWh. The EPBT of the PSC is not expected to exceed 1 year at a 50% confidence level. When the top 2 sensitive contributors to EPBT, solar insolation and PR, are considered at their minimum and maximum values with other parameters allowed to change within their respective ranges, the EPBT mean shifts from 0.876 to 1.3 years. Similarly, when the lifetime of the PSC is kept constant at its minimum 2 years while the other parameters are changed, the mean GHG/kWh of electricity can be as high as 300 g CO_2 eq. When the lifetime is fixed at 5 years, the mean value of GHG emissions was found to be 122 g CO_2 eq. This clearly explains the sensitivity of this output to the lifetime.

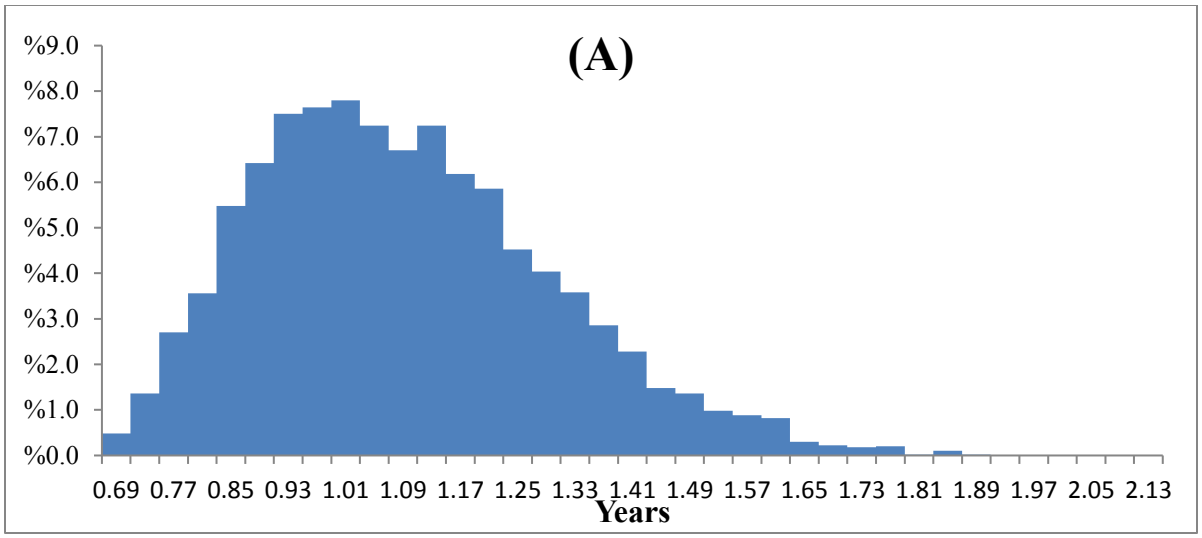
(A)
%9.0
%8.0
%7.0
%6.0
%5.0
%4.0
%3.0
%2.0
%1.0
%0.0
0.69 0.77 0.85 0.93 1.01 1.09 1.17 1.25 1.33 1.41 1.49 1.57 1.65 1.73 1.81 1.89 1.97 2.05 2.13
Years

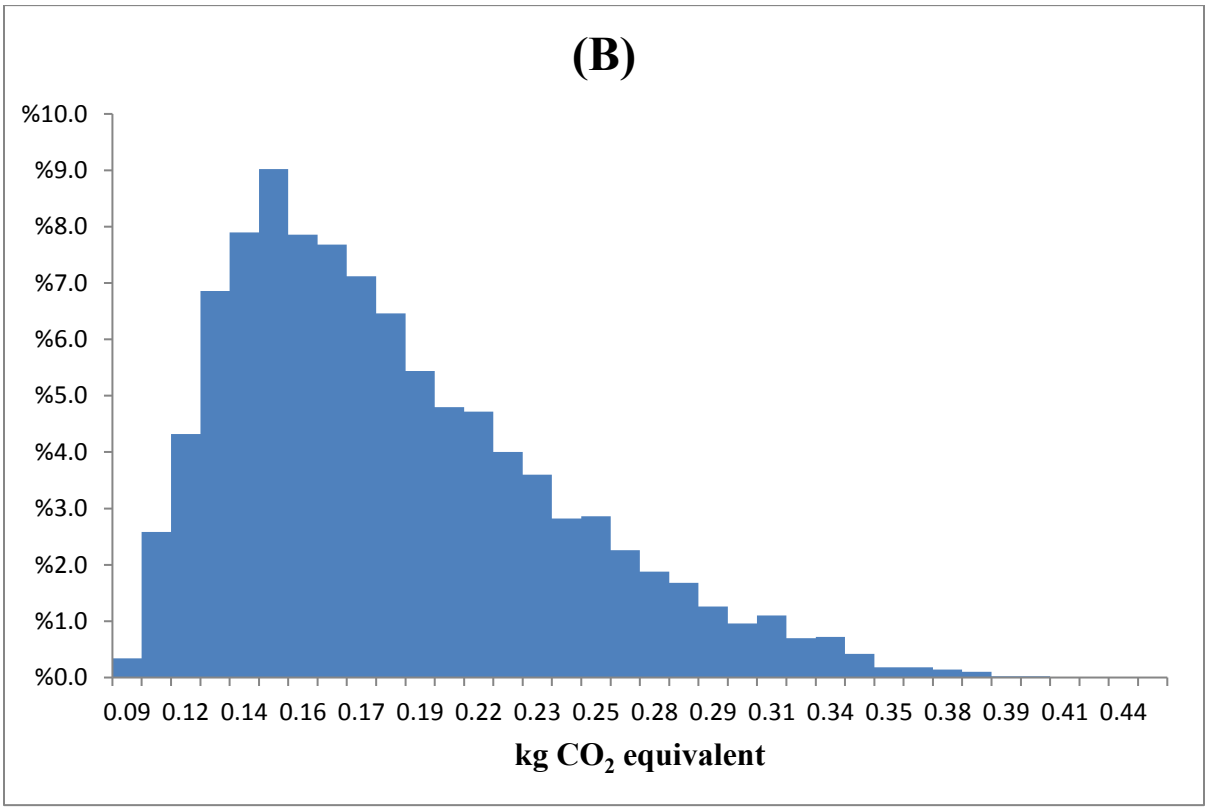
(B)
%10.0
%9.0
%8.0
%7.0
%6.0
%5.0
%4.0
%3.0
%2.0
%1.0
%0.0
0.09 0.12 0.14 0.16 0.17 0.19 0.22 0.23 0.25 0.28 0.29 0.31 0.34 0.35 0.38 0.39 0.41 0.44
kg CO_2 equivalent

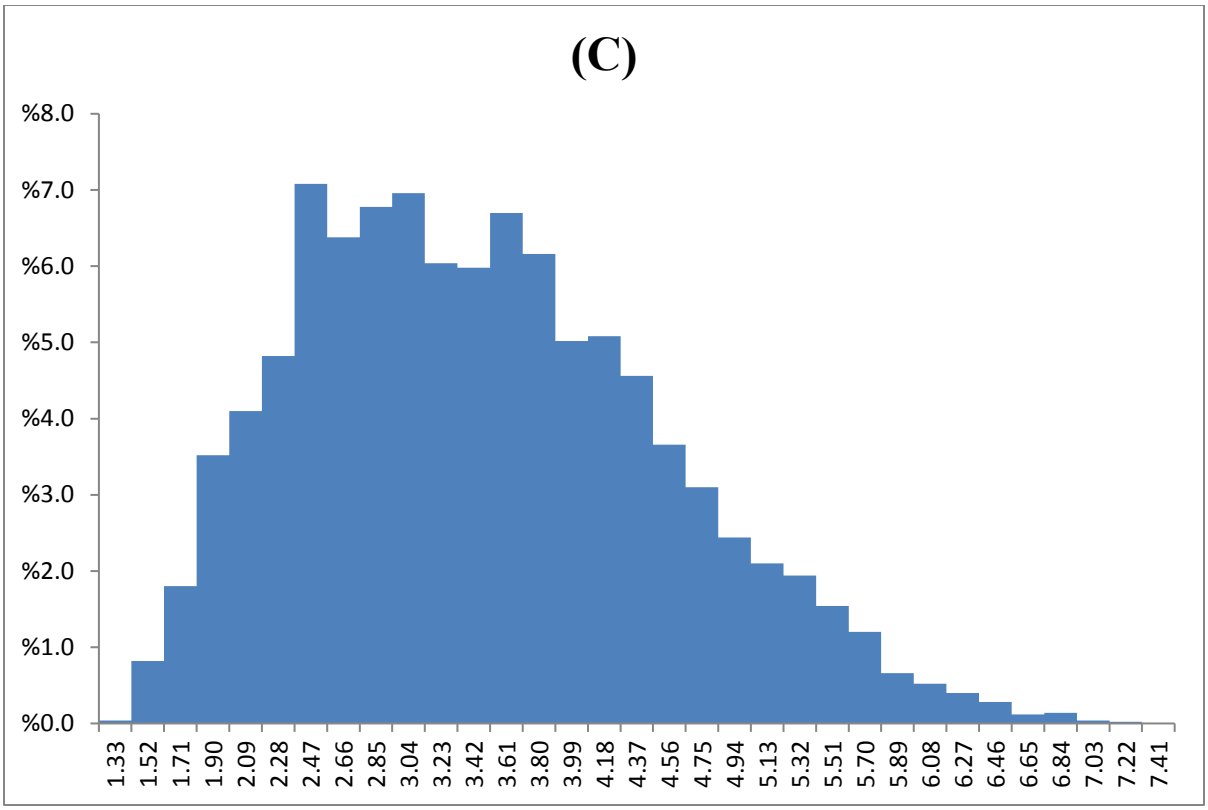

Figure 2. 7: Distribution curves for (A) EPBT, (B) GHG emissions per kWh of electricity produced, and (C) NER for the PSC based on uncertainty results.

2.6. Conclusions

Reducing the climate change impacts caused by human activities requires a collective effort to transform the global energy system from fossil-based to renewable energy sources. Since its conception, solar technology has shown remarkable advancement. Perovskite solar cells (PSCs) are among the promising future solar technologies as they provide high photoconversion efficiency. Moreover, the perovskite architectures that use titanium dioxide nanorods as electron transport layers are proven to have high photoconversion efficiency. Because it is a new technology, there are few studies that extensively examine the environmental performance of its

material and energy requirements based on their full life cycle stages. The main purpose of the paper was to systematically assess the life cycle environmental performance of TiO_2 nanorod-based PSCs. A bottom-up life cycle assessment was used to estimate the greenhouse gas footprint, energy payback time, and net energy ratio with an emphasis on the unique architecture and scope extended to include the balance of the system and end-of-life. This was important in order to compare PSC technology with established systems. It is estimated that the greenhouse gas emissions per kWh would be 182g CO_2 equivalent, which is higher than that for many established solar technologies. The energy payback time is about a year with the net energy ratio proving this architecture to be a net energy generator. These results indicate that PSC technology can be a competitive alternative in the near future if higher efficiency and lifetimes are achieved.

The greenhouse gas emissions of the PSC are largely due to the use of aluminium and two high-temperature processes, calcination and annealing. With the recycling and reuse of FTO glass and the gold layer, the energy payback time and greenhouse gas emissions fall significantly. The panel production, balance of the system, and assembly phases of the PSC, excluded in most life cycle assessment studies, contribute to about 56% of the total emissions. Replacing aluminum metal with alternatives in this phase can greatly improve the environmental performance.

Sensitivity and uncertainty analyses were performed to identify the parameters that have significant influence on the outputs and to provide a range of results, respectively. The results suggest that the large fluctuations in the greenhouse gas emissions are due to the ambiguity surrounding the lifetime of the PSC. Until the exact lifetime is known, this uncertainty will remain.

Chapter 3: Techno-economic assessment of titanium dioxide nanorod-based perovskite solar cells: from lab-scale to large-scale manufacturing

3.1. Introduction

The decline in costs associated with photovoltaic (PV) manufacturing has led to a growth in its deployment rate globally [85, 86]. Since the 1970s, PV module costs have come down by about 20% with every doubling of the cumulative production capacity [87]. The reduction in costs can be attributed to research and development efforts, learning curves in the PV industry, and economies of scale benefits due to increased scale [88-90]. Yet the cost of electricity production from solar energy has remained higher than conventional fossil fuel sources [91, 92]. For better market penetration, PV technologies must have the combined advantage of high efficiency, high stability, and low cost [93] while being available for large-scale implementation. Three generations of solar cells have been identified so far, but only the first two are currently available in mass production. First-generation crystalline silicon cells dominated the market with a 93% share in 2015, followed by second-generation thin film technologies that include cadmium telluride, amorphous silicon, and few other technologies [15]. To avoid the common drawbacks in first-generation solar cells, such as higher material and energy costs, the latter was developed by depositing thin layers of PV materials using low-cost processes [16, 17]. However, the photoconversion efficiency of these devices has not worked well for large-scale commercialization yet without incentives [18].

Third-generation solar cells, such as polymer: fullerene, hybrid polymer, perovskite solar cells (PSCs), are solution-processable technologies with a foreseeable future in large-scale electricity production [94]. PSCs in particular have gained attention recently, following an impressive increase in photoconversion efficiency (PCE) from 10% in 2012 to 22% four years later, with experts predicting enhanced PCEs in the years to come [55-57]. Nevertheless, to achieve a low levelized cost of electricity (LCOE) comparable with conventional sources, PSCs need to have low cost and long-term stability along with their very high efficiencies. To that end, it is important to understand the costs associated with manufacturing PSC panels at their early stage, as it would assist in identifying critical areas and highlight the technology's potential once barriers are eliminated [28]. However, for technologies at a low technology readiness level (TRL), there are significant challenges in conducting techno-economic assessments. Unlike commercial scale energy technologies, information related to equipment use or energy and mass balances may not be readily available [95]. With limited information, process modelling is a difficult task. For technologies such as PSCs, scaling-up the laboratory data to estimate selling price is a challenge. Methods to deal with these challenges must be developed [95].

Only a few studies have conducted techno-economic assessments of PSCs [28, 42-44]. Cai et al. considered fully printable perovskite structures, assuming large modules to be fabricated using series-connected small-area PSCs [44]. Most cost components in these studies, including the capital cost, were taken from other commercial studies related to silicon and dye-sensitized solar cells which is not robust and fully justified. Currently, with technological advances, it is more relevant to conduct a detailed, perovskite-specific study. The cost analysis in Cai et al.'s study, however, did not include some balance of system (BOS) components [44]. Chang et al. considered laboratory-proven serially connectable modules but used gold and silver in the architecture [28].

This selection led to an increase in module costs. Because low cost is a major driver for the commercialization of PSCs, the technology's potential is in low cost materials and production processes. Though both Cai et al. [44] and Chang et al. [28] focussed on perovskites deposited on glass substrates, the latter extended their study to include flexible substrates using roll-to-roll processes to further examine the impact on the costs in another study [43]. Song et al. conducted a techno-economic assessment with a low cost, high throughput, and high efficiency PSC design [42]. The study used a rare architecture with nickel (II) oxide (NiO) and zinc oxide (ZnO) acting as hole and electron transport layers (ETL), respectively. However, the material use and cost components were primarily extracted from published sources, expert opinions, and online trading websites [42]. This approach led to a vast approximation of data and increased uncertainty. Furthermore, at this stage, information available from the literature for perovskites is mostly at the lab scale. A framework to scale all the cost components (material use, capital, and labour costs) to large-scale manufacturing is still a significant knowledge gap for low TRL technologies. Both Cai et al. and Chang et al. assumed an annual factory throughput of 100 MW [28, 44], while Song et al. considered 200 MW [28, 42, 44]. Although several PV companies claim to be close to commercializing PSCs, third-generation solar cells are not on the mass-production lines yet [96]. Therefore, annual production capacities of 100 MW and 200 MW may not be feasible in the near future.

To fill the knowledge and literature gaps mentioned above, in this paper we developed a bottom-up data-intensive techno-economic model to estimate the PSC module cost and the minimum sustainable price (MSP) for a smaller yet feasible annual production capacity of 3.5 MW. This approach allows the equipment costs to be accounted for with certainty based on the equipment available in the marketplace.

The specific objectives of this research paper are to:

- Identify a pathway for manufacturing PSCs with low-cost materials and scalable processes for mass production;
- Develop a techno-economic model to evaluate the economic feasibility of TiO_2 nanorod-based PSC technology with a base case annual production capacity of 3.5 MW;
- Develop scale factors to estimate the cost components contributing to the overall module cost and establish the relationship between the production capacity and the overall module costs;
- Calculate the cost performance indicators of PSC technology: the minimum sustainable price (MSP) ($/W) and the LCOE ($/kWh);
- Design the components of a self-reliant residential PSC system for installation in Canada; and,
- Conduct sensitivity and uncertainty analyzes to determine the impact of various parameters on the overall cost of the PSC system.

3.2. Method

Figure 3.1 shows the six-stage framework of this study. The goal and scope definition stage includes specifying the problem leading to this research, identifying the key systems considered in the assessment and establishing the system boundary of the study. The PSC process design stage includes the identification of all the unit processes involved (from the study by Thakur et al. [25]), highlighting the key processes impacting the overall performance of the PSCs, and determining the input and output of each process. The equipment sizing and scale-up stage includes the selection of equipment for every process, identification of the processes driving the output

production of the plant, and calculation of the overall capacity or the factory throughput. The calculation of the manufacturing costs, development of the scale factors for all the cost components contributing to the overall manufacturing costs, and the estimation of the MSP are completed in the next stage. In the system integration stage, the panels are integrated with the other components of a residential PV system. The levelized cost of electricity (LCOE) is calculated in the final stage of the framework.

3.2.1. Goal and scope definition

The primary goals of this study were to develop a bottom-up data-intensive techno-economic model of a TiO_2 nanorod-based PSC system and to calculate the two key cost performance indicators, MSP and LCOE. Other important objectives include developing scale factors for the cost components and determining the economic feasibility of this technology for electricity generation for residential sector in Canada. Scale factors are the parameters which help in determining the cost at different sizes of the system. The target audience for this study are the decision makers including industry and government. The results of this study would help in understanding the economic potential and limitations of PSC-based PV systems. Additionally, the insights from this study are expected to help policy makers frame long-term policies that support the commercialization of environmentally friendly and economically feasible PV technologies.

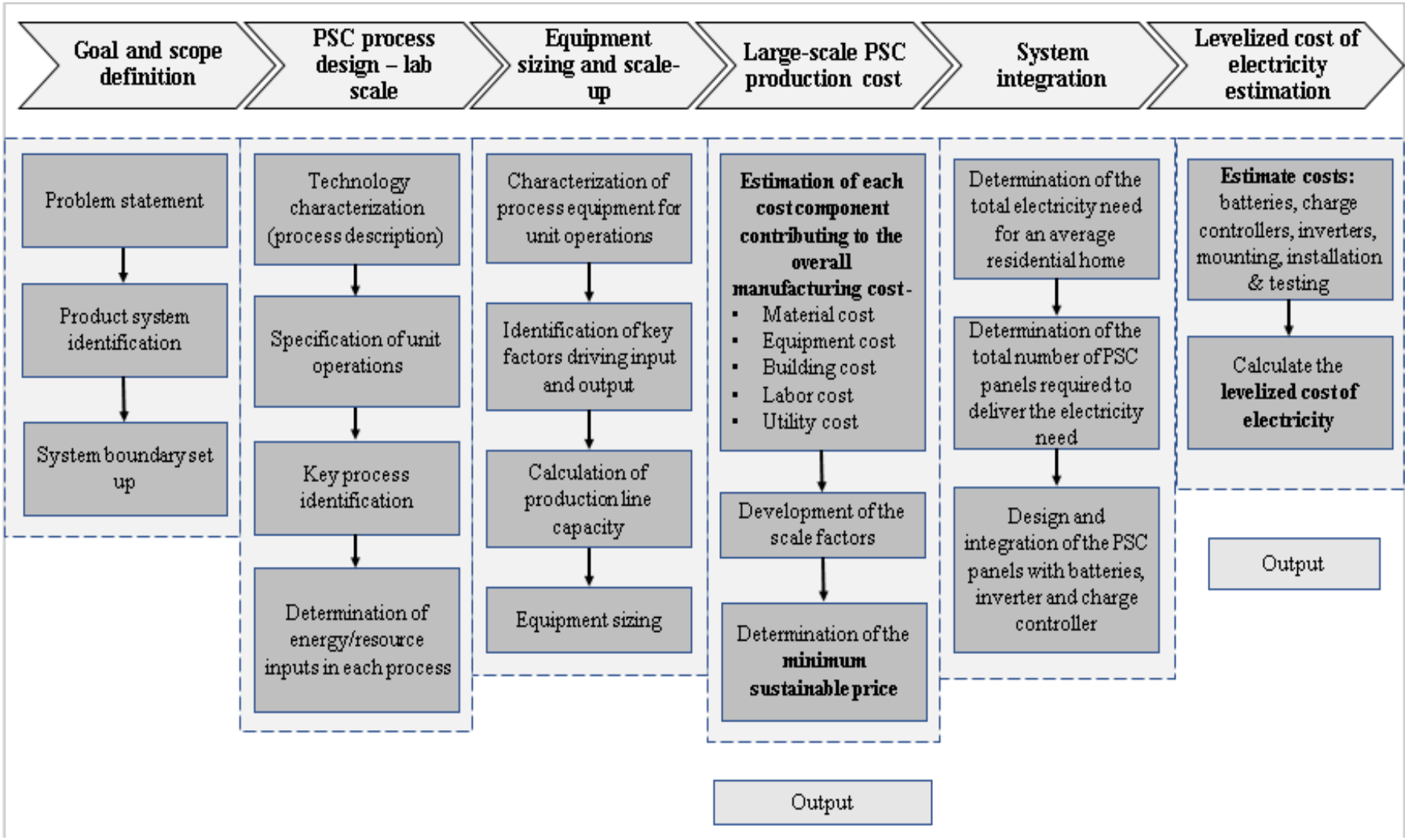

Figure 3. 1: Framework for the Perovskite solar cell (PSC) techno-economic assessment

3.2.2. PSC process design: lab scale

The standard size of commercialized solar panels available in the market is 165 cm by 100 cm, with several solar PV cells of 156 mm by 156 mm [97, 98]. However, as for other thin-film PV technologies, large-area PSCs cannot be fabricated on the glass substrates because of parasitic resistance losses in the conducting electrodes [99]. Therefore, in this study, each module was assumed to be made up of 100 monolithically integrated small-area PSCs of 2.5 cm by 2.5 cm, based on the laboratory scale study by Thakur et al. [25]. The module size was assumed to be 900 cm^2, which is currently the largest reported size [100]. Thakur et al. used monocrystalline titanium dioxide (TiO_2) nanorods as the electron transport layer (ETL) to reduce the thermodynamic losses associated with the photons, thus achieving greater photoconversion efficiency [26, 27]. However, to ensure cost optimization with efficiency, some minor modifications were made to the pathway presented by Thakur et al. Expensive materials and unscalable laboratory processes were replaced with cheaper materials and processes used for mass production. For example, a hole transport layer-free architecture and the replacement of the gold metal layer with aluminum were considered to reduce material costs. Laboratory processes such as spin-casting and thermal deposition were substituted, because these could not be scaled for mass-production [101]. Spin-casting is a typical process with low material use and increased difficulty with larger substrate sizes [102]; therefore, we replaced spin-casting of the compact TiO_2 on the glass substrates and the perovskites on the ETL with ultrasonic spray-coating and screen-printing, respectively, while estimating the module cost. The possibility of ultrasonic spray-coating large-scale TiO_2 compact layers on the substrates has been explored by Zhou et al. [79]. After the compact TiO_2 layer was deposited, the authors performed calcination at a low temperature of 135^oC [79]. Thakur et al. proposed the use of spiro-OMeTAD as the hole transport layer [25]. Two earlier studies found that methyl ammonium lead

iodide ($MAPbI_3$) perovskite can act both as a light harvester and a hole conductor [103, 104]. Therefore, in the cost estimation, we excluded the hole transport layer deposition step, thus lowering material costs and processing expenses. Song et al. demonstrated that gold deposition by thermal evaporation can be substituted by magnetron sputtering of aluminum [42]. This modification was done because gold is extremely expensive, even in very small quantities [28]. On the other hand, aluminum is abundantly available, has high electrical conductivity and costs less. However, a few studies suggest that using aluminum results in incompetent PSC efficiency, due to its low work function [105-107]. In the quest for high work function metals, sensitivity and uncertainty analysis was conducted by replacing aluminum with nickel, which has a work function close to that of gold [108]. The input considerations for substituting nickel with aluminum is provided in table B1 (appendix B). Figure 3.2 shows the flow diagram of the processes in manufacturing a solar PSC module.

3.2.3. Equipment sizing and scale-up

PSC module fabrication involves the successive deposition of several layers on the glass; most of the processes are interdependent, as shown in Figure 3.2. Therefore, the longest process of the production line drives the output, in this case, the calcination process with the substrates calcined at 135^{o}C for one hour. We chose a medium-sized furnace for this step and calculated the output per hour. Annual production volume was estimated to be approximately 3.5 MW_p based on the total working hours per year. Other equipment was selected thereafter to satisfy the output requirement of the longest step (calcination). Initially, as a base case, the authors considered a PSC module mass production plant of this capacity situated in Canada, starting operation in 2023. A post-analysis for higher production capacities is also included. Ultimately, the produced modules

were evaluated for installation at residential locations, satisfying electricity needs in Alberta, Canada. The details of the selected equipment are in Table 3.2. Other assumptions supporting this study are included in Table 3.1.

Table 3. 1: Important assumptions of the study

Parameter	Value	Assumption / Reference
Area of the PV modules	900 cm^2	Has 100 monolithically integrated small area cells
Module efficiency	11%	This is based on the cell efficiency and the geometric fill factor
Nominal power output	9.9W	1000 X 0.09 X 0.11 = 9.9W per panel
Manufacturer location	Canada	For residential use in Alberta, Canada
Equipment and building depreciation	10, 15 years	Generic assumption
Plant operation	3 shifts per day; 8 hours each; 2 functional shifts from 8AM to 12AM	One maintenance shift with minimum number of workers. 350 working days each year.
Plant capacity/ production line	3.5 MW_p	The slowest process of the line, calcination, can be performed in 9 batches each day. Based on the sizing of the furnace chosen for

		calcination, the output per batch is 112 modules/batch. Total output per day is 1008 modules. Annual production capacity of the plant 3.5 MW
Currency	USD	A conversion factor of 0.7 used for CAD to USD
SG&A	15%	Of the total revenue
Capital and building expenses	2-year investment profile	The capital expense was spread across the years 2020 and 2021. The equipment capital costs were accounted for in 2021 and 2022. Production begins in 2023.
WACC Yearly inflation rate	14% 2.25%	PV manufacturer average; in line with the study by Song et al. [42]

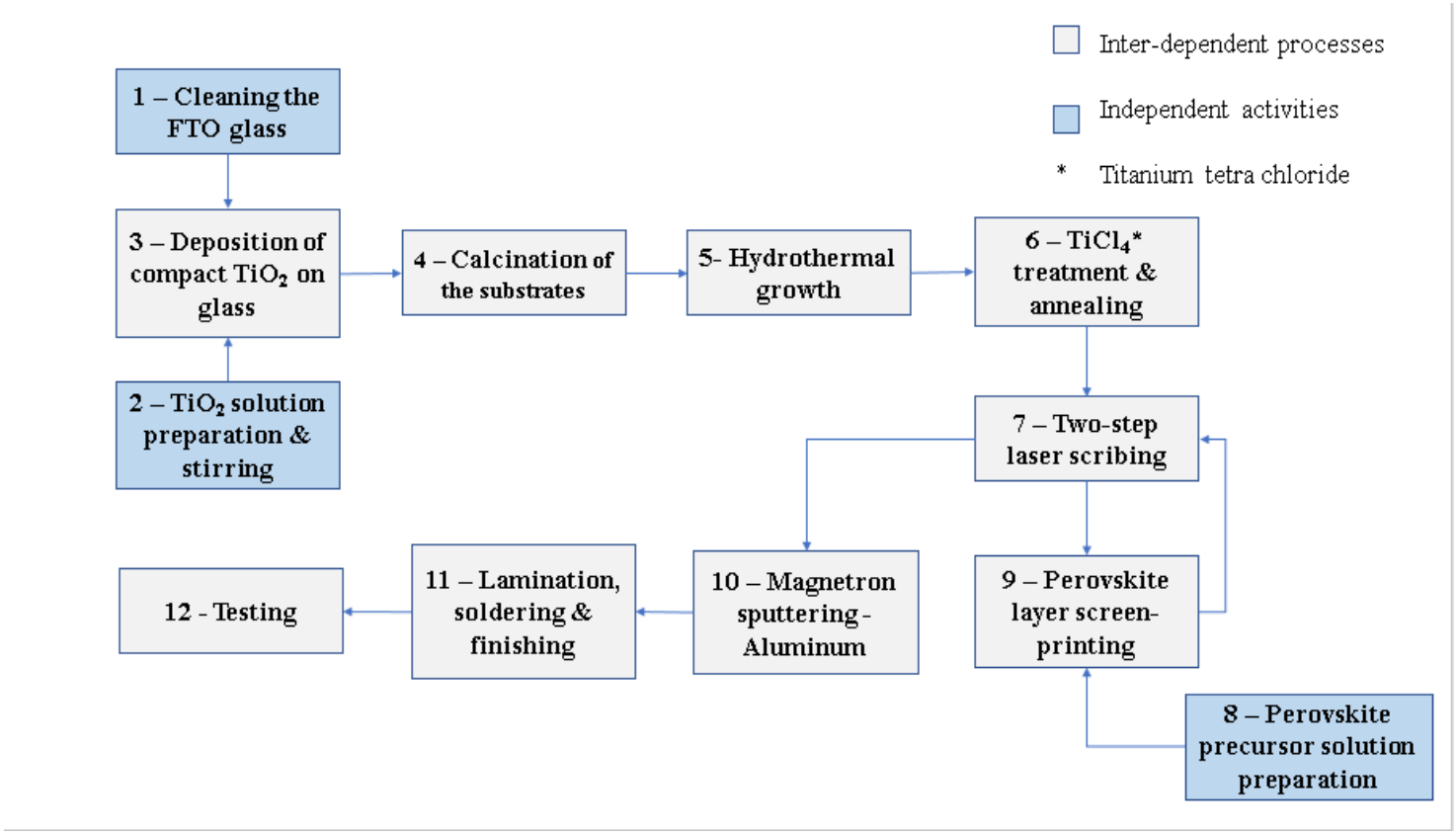

Figure 3. 2: PSC panel manufacturing process diagram

3.2.4. Large-scale PSC production cost estimation

We calculated the overall manufacturing cost of the perovskite modules for a production capacity of 3.5 MW per year based on the annual material costs, utility costs, labour costs, depreciation of the machines and the building, and the maintenance cost. Figure 3.3 is an overview of the techno-economic assessment framework used to determine the module manufacturing cost and the MSP calculation.

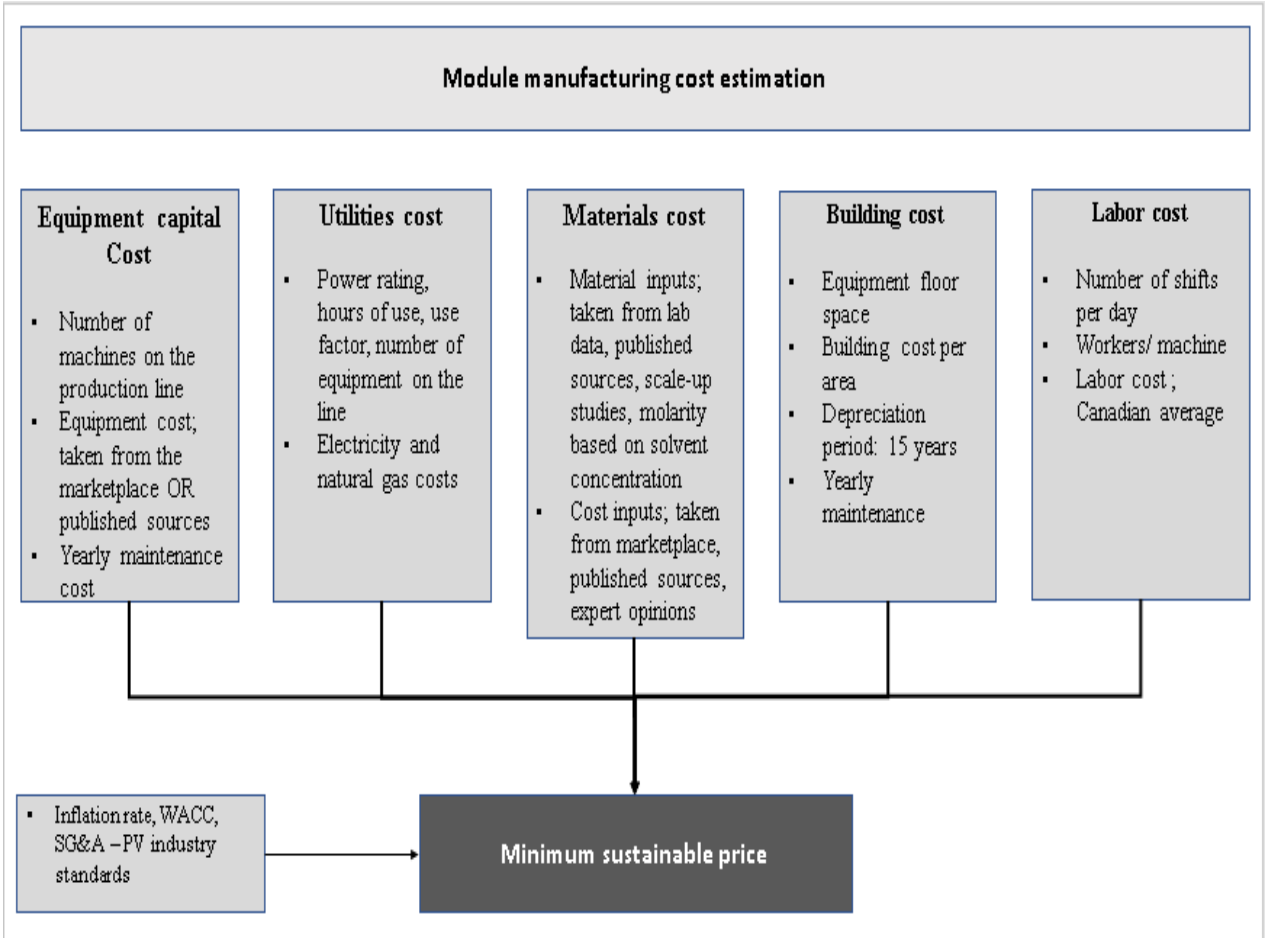

Figure 3. 3: Module manufacturing cost and minimum sustainable price calculation

Following equipment selection, we obtained costs from literature, development of models, and manufacturers. A linear depreciation of the machines over 10 years was assumed, similar to Chang et al.'s assumptions [28], as most of the equipment needs replacing after 10 years. The utility cost was calculated using the power rating of the machines, estimated hours of use, the use factor, and the number of each piece of equipment on each production line. The purpose of introducing the use factor is to ensure correct calculations when a machine is not running at maximum capacity. More details on these calculations are given by Garcia-Valverde et al. [76]. The average Canadian electricity and natural gas costs for commercial business are \$0.09/kWh and \$0.016/ MJ, respectively [109]. Other related details are provided in Table 3.2.

The material consumption was estimated based on the data generated by Thakur et al. [25]. Scaling up this data for mass production was done following the framework developed by Piccinno et al. [110]. All the major reactants were scaled up linearly; however, a 20% relative reduction in the solvent used was considered based on general expert opinion, as stated by Piccinno et al. Furthermore, the concentration of some chemicals that form the perovskite layer, i.e., methyl ammonium bromide and lead iodide, was estimated based on the revised solvent volumes and their corresponding molarity in the solution. The material costs were obtained from online literature, developed models and manufacturers, with an emphasis on bulk purchasing. All the material consumption details are provided in Table 3.3.

The building costs were estimated by calculating the total area requirement (which considers the physical dimensions of each piece of equipment and common areas such as office space, storage area, and washrooms) and a depreciation period of 15 years with an annual maintenance expense of 10% of the building depreciation. All the assumptions related to this calculation are as per the

PV industry standards and have been used by Chang et al. [28]. In addition, labour costs were estimated based on the degree of automation of each machine and the manual labour requirement per shift, together with the salaries for full-time technical staff, including research and development engineers. The basis for calculating labour costs for a 3.5 MW annual capacity is available in Tables 3.4 and 3.5 below. The building dimensions are calculated by multiplying the floor space of the individual equipment with the floor space ratio of 3 [28]. Details available in Table 3.6.

Table 3. 2: Input data and assumptions for equipment

Process No.	Equipment used	Number of each equipment used	Footprint	Power rating (W)	Total cost (US $)	Equipment use (min/m^2)	Comments/Reference
1	Ultrasonic cleaner	2	200 x 100 x 100 cm^3	7200	11200	30	Skymen Ultrasonic Cleaner [111].
2	Stirrer	1	32.5 x 21.5 x 12 cm^3	590	136.00	480	Maximum rotations per minute (rpm) of the stirrer is 1800; however, a use factor is considered as stirring is done at 180 rpm [111].
3	Ultrasonic coating system	1	120 x 110 x 160 cm^3	2100	25000	5.5	Ultrasonic Automatic Spray Coater [111].
4	Walk-in furnace 1	1	434 x 238 x 330 cm^3	72000	150000	60	Can be used to simultaneously accommodate 112 modules [112], [42].
5	Walk-in furnace 2	1	434 x 238 x 330 cm^3	72000	150000	40	[112], [42].
6	Furnace 3	1	434 x 238 x 330 cm^3	72000	200000	60	Slightly different than the other two furnaces as annealing has a higher

Process No.	Equipment used	Number of each equipment used	Footprint	Power rating (W)	Total cost (US $)	Equipment use (min/m^2)	Comments/Reference
							temperature requirement. Cost is slightly higher due to the change in the make [112], [42].
7	Laser system	1	252 x 321 x 123 cm^3	19600	169000	2.66	SP2000 laser machine [113].
8	Tank	1	49.5 x 38.2 cm^2	1040	378	120	Digital large stirrer [111].
9	Screen printer	1	358 x 230 x 160 cm^3	9000	50000	1.32	Used to screen-print perovskites on the modules [114], [42].
10	Magnetron sputtering system	1	500 x 250 cm^2	80000	155000	20	[111], [42].
11	Solar laminator	1	230 x 230 cm^2		15000		Utility costs estimated based on electric and heat energy use reported by Jungbluth et al. [68] [111].
12	Testing table	1	250 x 100 cm^2	500	12500	1.5	Selective testing of batch production [42].

Table 3. 3: Input data and assumptions on material consumption for the reference module

Activity no.	Material	Amount/ m^2	Unit	Cost ($/unit)	Comment/Reference
1. Cleaning FTO glass	FTO-coated glass	1.00	m^2	15.7	Cost inflated from Chang et al. [28].
	Acetone	0.41	Lt.	2.52	Bulk purchase as per price given in Sigma Aldrich website [115].
	Methanol	0.32	kg	0.483	20% relative reduction during scale up [110]. Cost estimated from literature [111].
	Deionized water	0.41	Lt.	0.012	Cost estimated from Chang et al. [28].
2. TiO_2 solution preparation	Titanium iso propoxide	0.02	kg	10	Linear scale-up of reactants [110]. Cost from literature [111].
	1M HCL	0.004	Lt.	7.5	Bulk purchasing.
	Isopropanol	0.04	Lt.	11.67	Cost estimated from Sigma Aldrich [116].
5. Hydrothermal growth of TiO_2 nanorods	HCl (37%)	0.37	Lt.	7.5	A facilitator of hydrothermal growth and not a reactant itself [117]. 20% relative solvent reduction considered from lab data.
	Glacial acetic acid	0.39	kg	0.8	Price from literature [111].
	Deionized water	0.74	Lt.	0.012	-

Activity no.	Material	Amount/ m^2	Unit	Cost ($/unit)	Comment/Reference
	Titanium (IV) n-butoxide	0.48	kg	3.85	Bulk purchase price from literature [111].
6. Titanium tetra chloride treatment	Titanium tetra chloride	0.086	kg	2.1	[111].
8. Perovskite solution preparation	Methyl ammonium bromide (MABr)	0.002	kg	688.5	Material consumption based on 0.2 M in solution.
	Formamidinium iodide (FAI)	0.02	kg	897	Cost curve developed from the available data points to estimate the price per kg.
	Lead bromide	0.01	kg	50	The mass of the chemical was estimated based on molar calculations and concentration in the solution. Price estimation from literature [111].
	Lead iodide	0.04	kg	20	Mass of the chemical was estimated based on molar calculations and concentration in the solution. Price estimation from literature [111].
	Dimethyl formamide	0.04	kg	3	Solvent scaling. Cost from literature [111].

Activity no.	Material	Amount/ m^2	Unit	Cost ($/unit)	Comment/Reference
	Dimethyl sulfoxide	0.01	kg	3.5	Solvent scaling. Bulk pricing from literature [111].
	Chlorobenzene	0.03	kg	30	Solvent scaling. Bulk pricing from literature [111].
10. Magnetron sputtering	Aluminum	3.4E-4	kg	2.5	Material consumption and cost estimate from Song et al. [42] and literature [111], respectively.
11. Lamination, soldering and finishing	Glass	1	m^2	1.3	Material use from Jungbluth et al. [68]. Bulk pricing considered from literature [111].
	Wire drawing, copper	0.11	kg	1.04	
	Aluminum	2.63	kg	2.5	
	Ethyl vinyl acetate	1.00	kg	2	
	Polyester	0.37	kg	2.08	
	Polyvenyl fluoride	0.11	kg	1.6	
	Acetone	0.02	Lt.	2.52	
	Methanol	0.002	kg	0.483	
	Propanol	0.01	Lt.	11.67	

Table 3. 4: Labour requirements on the production line

Activity	Equipment/ shift	Number of workers	Comments
Sonication of FTO glass	Ultrasonic cleaner	3	Continuous operation is necessary across all 3 shifts with a requirement of one person/shift. Cleaners have timers and do not need continuous attention.
TiO_2 solution preparation and stirring	Stirrer	0	Overnight stirring for 8 hours done during the non-production shift for the entire production day. Just starting the stirrer is the task to be carried out. Additional labor not needed irrespective of the capacity.
Deposition of compact TiO_2	Ultrasonic coating system	1	Includes filling the ink, making software adjustments, loading work pieces, clearing the spraying table. Needs attention. 1 person per machine all the time. Coating done only during the first production shift.
Calcination	Furnace 1	1	Manual tasks include loading the machine, setting temperature, and unloading after 1 hour. 1 person for 3 machines (as the away time is 1 hour).
HT growth + drying	Furnace 2	0.5	Load the solution, work pieces, set the temperature, and drying. 1 person for 2 machines.
$TiCl_4$ treatment + annealing	Furnace 3	1	Loading samples, annealing setup after 30 minutes. Removing samples and re-loading.
Perovskite precursor solution prep	Tank II / stirrer	0.5	Adding the chemicals and solvents. Setting temperature, timer, and rotations. Whatever the capacity, maximum 2 stirrer tanks needed.

Laser patterning	Laser system	1	Task has a slack time as the cycle time is shorter than the other processes. Though two stages of laser patterning operate at this station, about 20 minutes slack allows a slower work progress. One employee is enough to load, unload, and set the software.
Screen printing	Screen printer	1	Cycle time low. Frequent labour attention needed to load, unload, and lead other activities associated with this process. At least one labour necessary per machine always. Activity starts only in the second production shift.
Aluminum back contact - magnetron sputtering	Magnetron sputtering setup	2	2 employees for the machine always. Just 8 hours of sputtering each day to produce the required output.
Lamination, soldering, and finish-up	Solar laminator	1	Solar laminator functional after other processes are complete on at least one batch of panels. Therefore, functional only in the second manufacturing shift.
Cleaning staff	-	3	1 per shift
Testing	Testing table	2	1 employee/production shift

The total staff required is approximately 17 workers, and their wage rate is calculated at CAD $18 per hour [118].

Table 3. 5: Other employees of the manufacturing plant and their salaries

Designation	Workforce size	Yearly salary (CAD)	Comments
Floor manager	1	50,000	Since the job responsibilities are similar to those of a project coordinator, the CAD average salary of a project coordinator for the PV industry is used here [118]
Floor supervisor	2	100,000	Salary of a project coordinator considered
R & D	1	65,000	Salary matched with that of a research scientist [118]
Factory manager	1	69,000	Matched with the salary of an operations manager in the Canadian PV industry [118]

Table 3. 6: Equipment used and their floor dimensions

No.	Equipment	Floor space	Total Area (m^2)	Reference
1	Ultrasonic cleaner	200 x 100 cm	4	[111]
2	Stirrer	32.5 x 21.5 cm	0.07	[111]
3	Ultrasonic coating system	120 x 110 cm	1.32	[111]
4	Walk-in furnace I	434 x 238 cm	10.33	[112]
6	Walk-in furnace II	434 x 238 cm	10.33	[112]
7	Furnace III	434 x 238 cm	10.33	[112]
8	Tank	49.5 x 38.2 cm	0.19	[111]

No.	Equipment	Floor space	Total Area (m^2)	Reference
9	Laser system	252 x 321 cm	8.09	[113]
10	Screen printer	358 x 230 cm	8.23	[114]
11	Magnetron sputtering system	500 x 250 cm	12.5	[42]
12	Solar laminator	230 x 230 cm	5.29	[111]
13	Testing table	250 x 100 cm	2.5	[42]

Additional area, such as washrooms, dining rooms, office, and storage area are estimated. The building cost/m^2 is considered to be $376.6 [119].

Since 2001, increasing the production capacity in the PV industry has lowered the costs [120]. Establishing the cost vs capacity relationship is an important objective of this work. To understand the impact of production capacity on direct manufacturing costs, all the costs were further scaled up from the base case to 7, 10.5, 14, 17.5, and 21 MW_p production capacities. The capital cost was varied based on machine size and use. For example, to meet the annual production requirement of 3.5 MW_p, 2 ultrasonic cleaners, both running at 70%, need to be used on the production line. However, while this capacity was doubled to an annual production of 7 MW_p, only 3 such cleaners were used at 95%. Therefore, based on the change in the number of equipment used in the production line or the change in the equipment size to satisfy higher production capacities, the capital cost was modified accordingly. A change in the equipment use led to an increase or decrease in the cost of the utilities (electricity and natural gas). Similarly, as more machines were added or larger equipment was used, the factory size increased, thus changing the building costs. Material consumption and costs were estimated using the same technique used for scale-up from laboratory scale to 3.5 MW capacity. The module manufacturing cost was calculated for each

production capacity. Based on this, scale factors for all the cost components were developed. A cost curve was developed to reflect the economy of scale benefits through scale-up in production.

3.2.5. System integration

Based on the calculated MSP, we extended the study to design a stand-alone grid-independent PSC system that can self-sufficiently meet the electricity needs of an average residential home in Alberta, Canada. An average household in Canada consumes about 11 MWh of electricity each year [121]. To meet this requirement, we first identified the solar potential in Alberta, where the PSC solar system will be installed. Then, we calculated the area required to generate enough electricity to meet the household demand.

The capital cost of the PSC panels for a residential user would be the product of cost per area and the total required area of installation, calculated in the previous step. Along with the costs of a charge controller, battery, inverter, and overhead costs (installation), we estimated the overall capital cost of installing PSC powered electricity system.

3.2.6. Levelized cost of electricity estimation

Figure 3.4 has the details related to designing the PSC system for residential application in Alberta, Canada. Other important characteristics of the components used in the PSC system and their cost estimates are provided in Table 3.7. Table 3.8 lists the materials used for mounting the panels and their costs. The panel installation charges were estimated at $\$0.2/W_{DC}$, as mentioned by Song et al. [42].

Table 3. 7: Characteristics of the components of the PV system

System component	Characteristic	Value	Comments/Reference
Batteries	Battery voltage	12V	[111]
	Depth of discharge	80%	[122]
	Battery efficiency	85%	[123]
	Battery specification	120Ah	[111]
	Number of batteries	120	Details in supplementary document.
	Lifetime	10-11 years	[111]
	Days of autonomy	3 days	[124]
	Battery cost	$10/unit	[111]
Inverters	Inverter capacity (rated)	12.5 kW	Calculated based on a factor of safety of 25%.
	Input DC voltage	144V	String of 12 batteries in a group.
	Lifetime	10 years	[123]
	Inverter cost	$829	[111]
Charge controllers	Equipment	Home/commercial use: 144V solar charge controller with RS485/GPRS/WIFI	[111]
	Controller details	144V, 28kW PV power compatible	[111]
	Lifetime	5 years	[123]
	Cost	$1,000	[111]

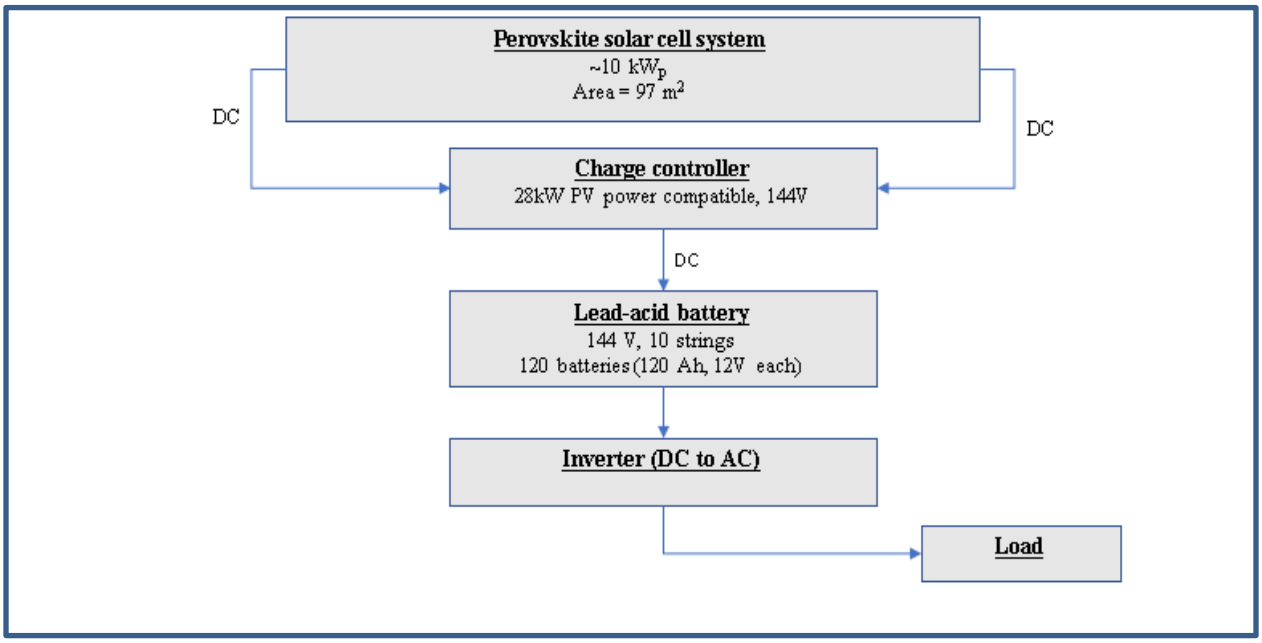

Figure 3. 4: PSC system for residential application

Table 3. 8: Material and cost estimate for mounting & installing PSC panels

Activity desc.	Material	Amount/ m^2	Unit	Cost ($/unit)	Comment/Reference
Mounting of panels	Aluminum	2.84	kg	2.5	Material consumption estimated from Jungbluth et al. [68], cost calculations from literature [111].
	Steel	1.5	kg	0.814	
	Corrugated board	0.133	kg	1.7	
	Section bar extrusion	3.025	kg	3	

A cash flow was developed with an 11- year analysis period to calculate the levelized cost of electricity, when the efficiency of the PSC system reaches 80% of its rated efficiency, as discussed earlier. An annual maintenance cost of 3% of the total project investment was assumed based on

data from Akbari et al. [125]. In general, the LCOE is the ratio of the total life cycle cost of the PV system to the total electricity generated during this period [126].

3.2.7. Sensitivity and uncertainty analysis

A sensitivity analysis was conducted to identify the important input parameters that the output is sensitive to. Morris's statistical method can be used to identify these key input parameters in a non-linear model, as illustrated by Campolongo et al. [127] This method is used when the number of inputs is very high (as in this case) and helps to pick out the few main cost inputs that likely have a significant impact on the output, thus needing a deeper analysis. Further, to address the uncertainty surrounding the cost inputs, a Monte Carlo simulation was conducted.

One of the key observations of this study is the reduction in cost with an increase in production capacity; therefore, we chose the large production capacity of 21 MW to get the benefit from the economies of scale, for which all the data points are estimated in the developed model, for the sensitivity and uncertainty analysis. The outputs, module manufacturing costs, and LCOE calculated at this capacity are \$0.43/W, \$47.15/m^2, and 11.4 ¢/kWh, respectively.

There are three reasons why sensitivity and uncertainty analyses were conducted in this study. First, some input cost numbers were estimated from published literature and have variations. Second, errors might be entered in the calculation of material and energy consumption for the fabrication of the PSC modules. Third, although assumptions were made logically based on available historical data, the inputs might be different from actual values in realistic scenarios. A conservative approach of using uniform distributions for all the inputs was selected. Apart from

the input parameters listed in Table 3.9, an uncertainty range of ± 25% was considered for every other input to investigate the impact of these errors.

Table 3. 9: Uncertainty range for input parameters

Parameters	Unit	Range	Comments
Insolation	$MJ/m^2/year$	3941 - 8047	Maximum and minimum insolation in Alberta, Canada [73].
Efficiency of the module	%	8.8-18	The highest efficiency is assumed to be the efficiency of the individual cells (18%) [25] and the lowest is 80% of the module efficiency as per standards.
Performance ratio	-	0.75-0.95	Location-specific. The US and Europe ranges considered in previous studies were chosen here [72].
Panel cost/area	$\$/m^2$	48-68	MSP range obtained from the uncertainty analysis of this study. Used as an input to calculate the LCOE.
Degradation rate of the panel	%/year	0.5-3	Range chosen from Song et al. [42].
Labour hourly rate	$/hour	16-22	[128].

The RUST model developed by Di Lullo et al. was used to conduct the Monte Carlo simulation for uncertainty analysis [129]. Uniform distribution with the same range of values for sensitive inputs was considered as listed in Table 3.9. However, for inputs with less uncertainty, a triangular distribution in a range with values closest to the chosen input value was selected. Random samples

were selected within the conservative distribution of the inputs and iterated 10,000 times to obtain the final uncertainty results.

3.3. Results and Discussion

This study aims to address three different aspects of PSCs: first, the PSC panel manufacturing cost estimate for a 3.5 MW_p pilot plant set up in Canada; second, the impact of economies of scale from increased production capacity on the manufacturing cost; third, the implications of extending the results to calculate the LCOE of PSC-powered electricity systems for use in residential homes in Alberta, Canada. Each point is discussed in detail in the following sections.

3.3.1. PSC module manufacturing cost

The estimated direct manufacturing costs of the reference PSC module were \$80.23/m^2 and \$0.73/W for the base case annual manufacturing capacity of 3.5 MW_p. As shown in Figure 3.5, the dominant cost categories are material costs and labour costs, which contribute 60% and 33%, respectively. The utility and the equipment and building depreciation costs together account for 7%. Performing calcination at a lower temperature has reduced energy consumption which in turn resulted in lower utility costs. Similarly, if the annealing of hydrothermally grown TiO_2 nanorods is performed at lower temperatures, the whole fabrication process can be completed below 200°C, further suppressing the module manufacturing costs. Normally, the equipment capital and building costs would surpass the labour costs; however, this is not the case. This is because, due to the small the production capacity, the equipment chosen is not expensive.

A detailed breakdown of the material cost is shown in Figure 3.6. Around 35% of the total material costs are due to the FTO glass substrate preparation. FTO glass itself costs about 32% of the total

material costs, while the solvents used to clean it (methanol and acetone) contribute the remaining 3%. The FTO glass accounts for about 90% of the total mass of the PSCs and is therefore needed in large quantities [37], which makes it the most expensive material used in manufacturing the PSCs through this pathway. The use of flexible substrates made of materials other than FTO glass has been gaining traction recently [130]. This also opens avenues to roll-to-roll manufacturing, easing large-scale production at lower costs [43]. However, on the downside, flexible polymer substrates cannot withstand higher temperatures because of their low melting points [45]. Next to FTO, the largest contribution associated with material costs is the perovskite precursor solution preparation stage. Most of the chemicals in the perovskite preparation stage are used in small quantities but are expensive. Bulk pricing is considered, where available. The top two contributors are formamidinium iodide and methyl ammonium bromide, followed by other chemicals that make the absorber. The materials used for the BOS come third. Aluminum, used for making frames to provide structural support to the solar panels, is a part of the BOS that contributes the most to its cost. Industrial aluminum is obtained from bauxite ore through the Bayer and Héroult processes, both of which are high-temperature processes [80]; therefore, aluminum is expensive. Ethyl vinyl acetate is used on both the front and rear ends of the PSCs and contributes to 17% of the total material costs from BOS while glass and polyester make up 11% and 13 %, respectively.

Our study found that the materials used for the ETL and the perovskite layer add up to about 40% of the total material costs, and the glass costs and BOS make up the rest. Use of cost curves to predict the costs of the chemicals (such as methyl ammonium bromide and formamidinium iodide) in this study is based on small-scale purchasing data points. Bulk-purchase pricing was not available for these chemicals. Therefore, we chose a range of cost values for them and examined

their impact on the manufacturing cost and LCOE while conducting uncertainty and sensitivity analyses.

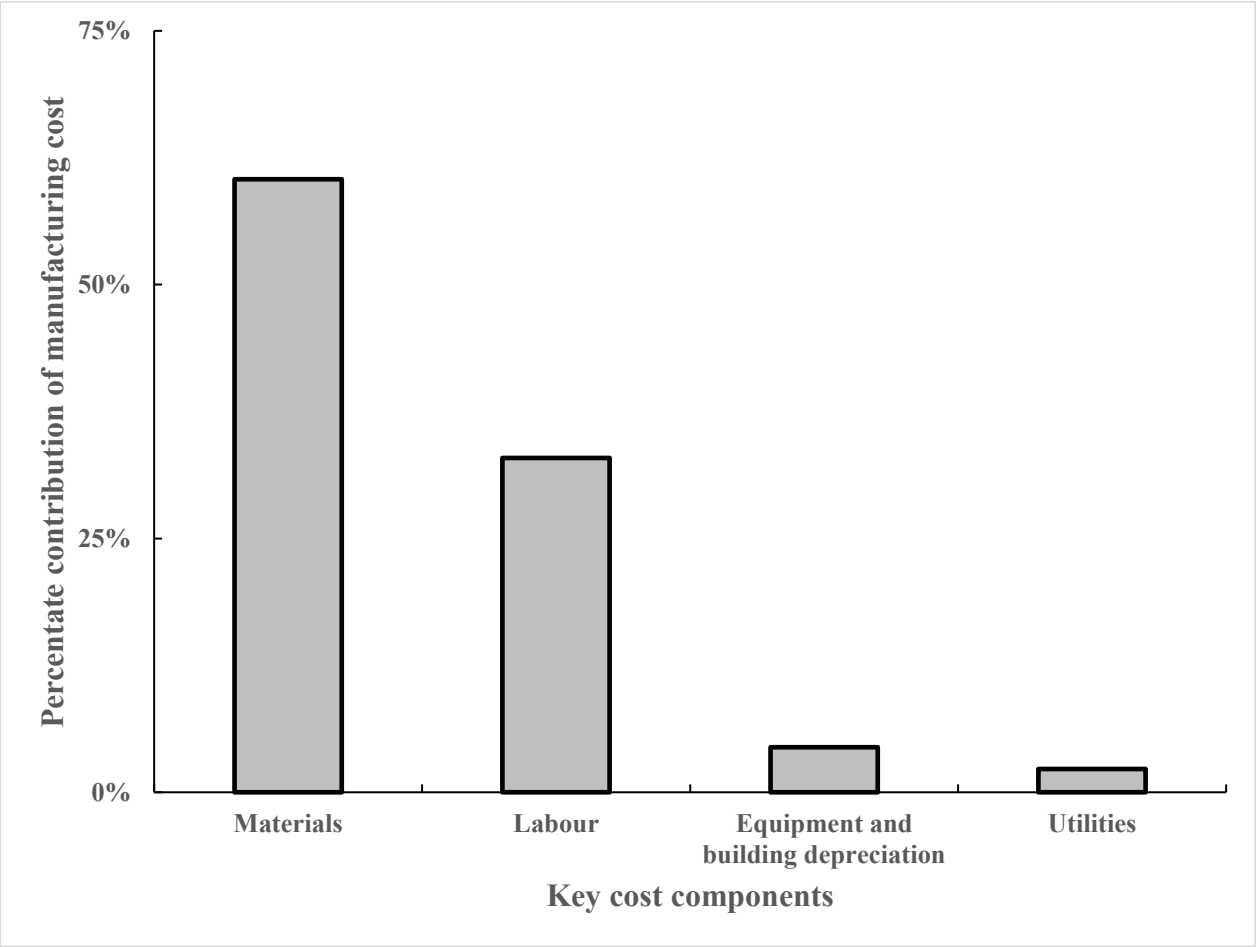

Figure 3. 5: Breakdown of the manufacturing cost of PSC modules

The manufacturing costs of cadmium telluride (CdTe) and wafer-based crystalline silicon modules were estimated to be \$86/m^2 and \$136/m^2, respectively [28, 131]. However, given that PSC modules are not widely commercialized, and the factory capacity is small, prices are expected to drop substantially with a higher technology readiness level and production capacity. Clearly, PSC modules hold an edge over the above-mentioned PV technologies.

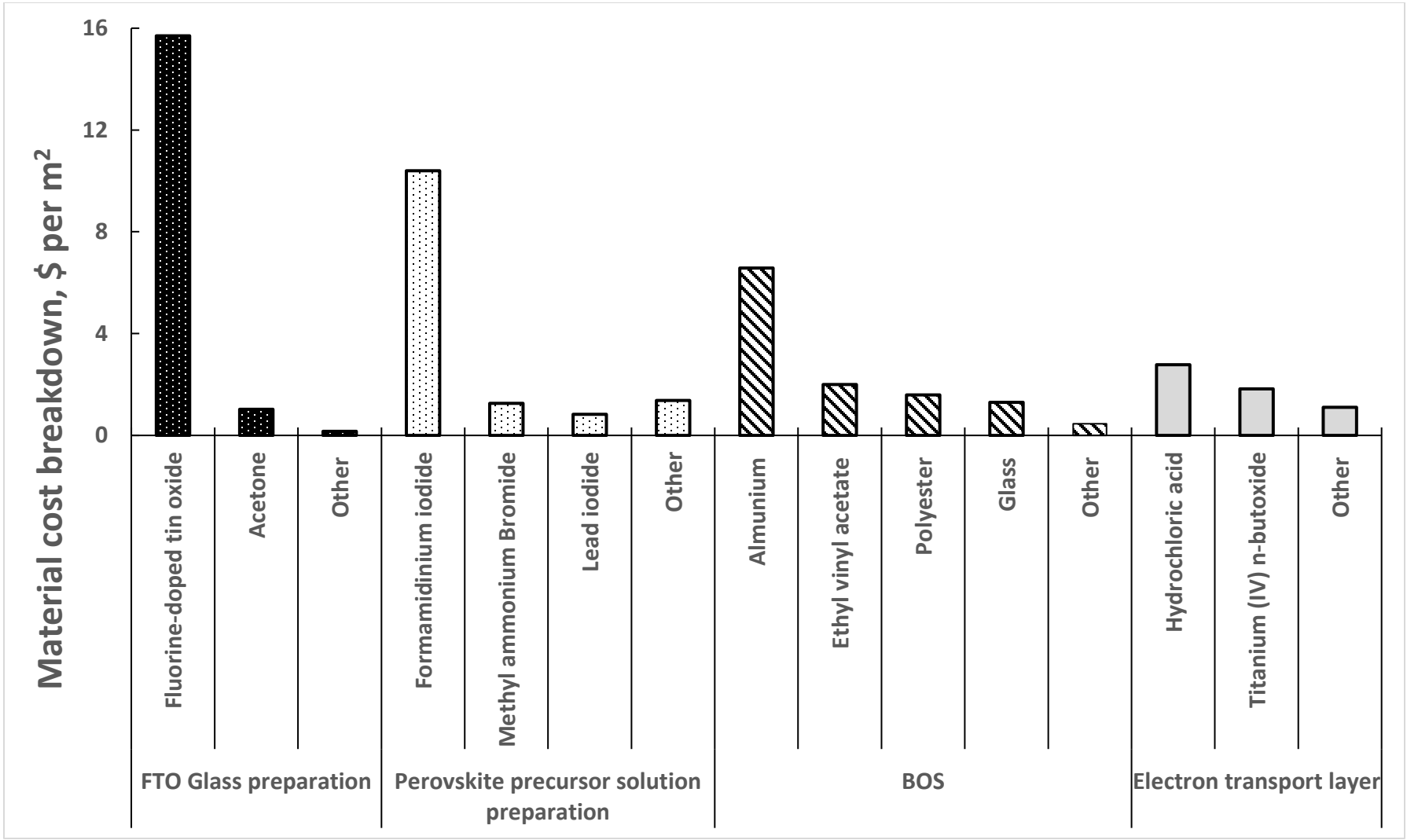

Figure 3. 6: Material cost breakdown

3.3.2. Development of the scale factor and cost-curves

Figure 3.7 shows the direct manufacturing costs per area of the PSC module at different capacities. The scale factor results indicate that with an increase in the production capacity, PSC module manufacturing costs per unit area decline. The largest capacity investigated was 21 MW; the manufacturing costs calculated were \$47.23/m^2 and \$0.43/W, a 41% decrease from a 3.5 MW capacity. At more than 90%, the material and labour costs continue to dominate the overall costs. Labour costs go down drastically when the capacity is doubled from 3.5 MW to 7 MW or higher. This is because a minimum number of workers is needed on the production line, irrespective of production capacity. However, employing double the number of workers may not be necessary, should the capacity double. Hence, the material costs take up a larger share of the overall costs in terms of percentage, though the material costs reduce considerably too. The estimated number of workers needed on the production line is between 17 and 33 when the capacity is increased from 3.5 MW to 21 MW. However, when the capacity is doubled from the base case, the increase in the number of workers is just 2. This causes a large reduction in the labour costs from 3.5 MW_p to 7 MW_p.

The utility costs remain linear throughout the analysis (about \$2/m^2). This is because with increased capacities, the number of machines on the production line or the available machine use increases proportionally, leading to a linear increase in the use of the utilities. Similarly, though most of the materials scale up linearly, a 20% reduction in the use of solvents and a corresponding decrease in the amount of certain chemicals (based on their molarity calculations in the solution) leads to a decrease in the material costs. A further decrease in overall manufacturing costs is

expected when production capacity is 100 MW or 200 MW, as they are governed largely by material costs.

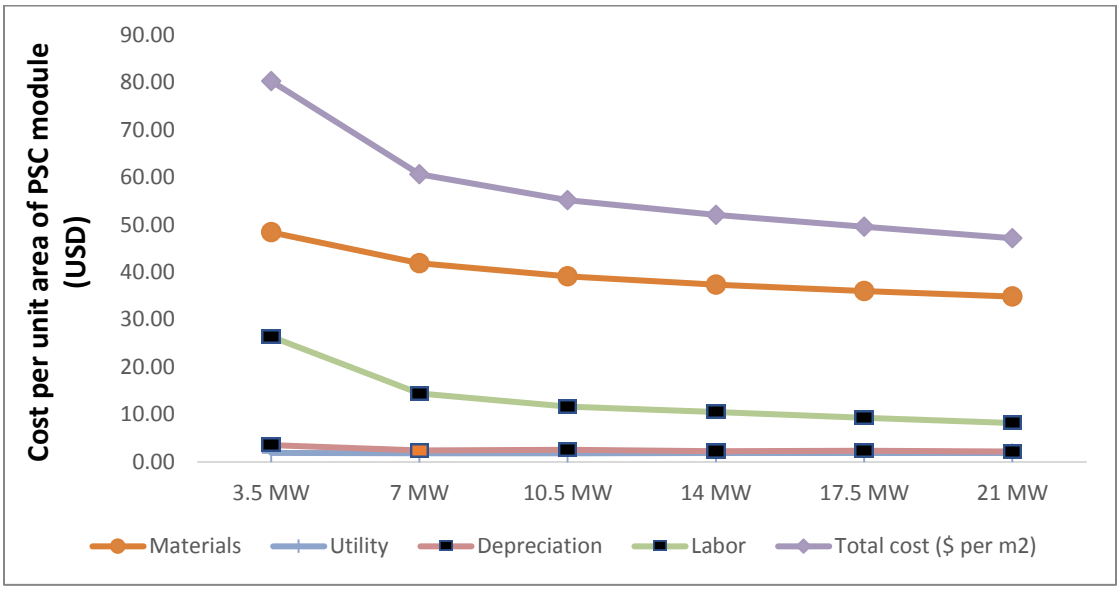

Figure 3. 7: Cost vs capacity for PSC module manufacturing cost ($/m^2)

As production capacity increases, the machine's use of the existing equipment also increases, or more such machines are added to the production line. Alternatively, some machines used for smaller production output may be replaced with larger ones to cater to increased demand. Because of these factors, the capital cost of the equipment does not scale up linearly and often economies of scale are seen until a particular production capacity beyond which an increase has no impact on the costs [132]. Consequently, the factory size changes, and with it the renting or building costs. In this study, we found that a six-fold increase in production capacity to 21 MW from the base case of 3.5 MW would only elevate the capital equipment costs by a factor of 4. Clearly, from Figure 3.8, a scaling factor of 0.78 can be used for capital equipment cost scaling. Likewise, a scaling factor of 0.81 may be used for material use cost scaling.

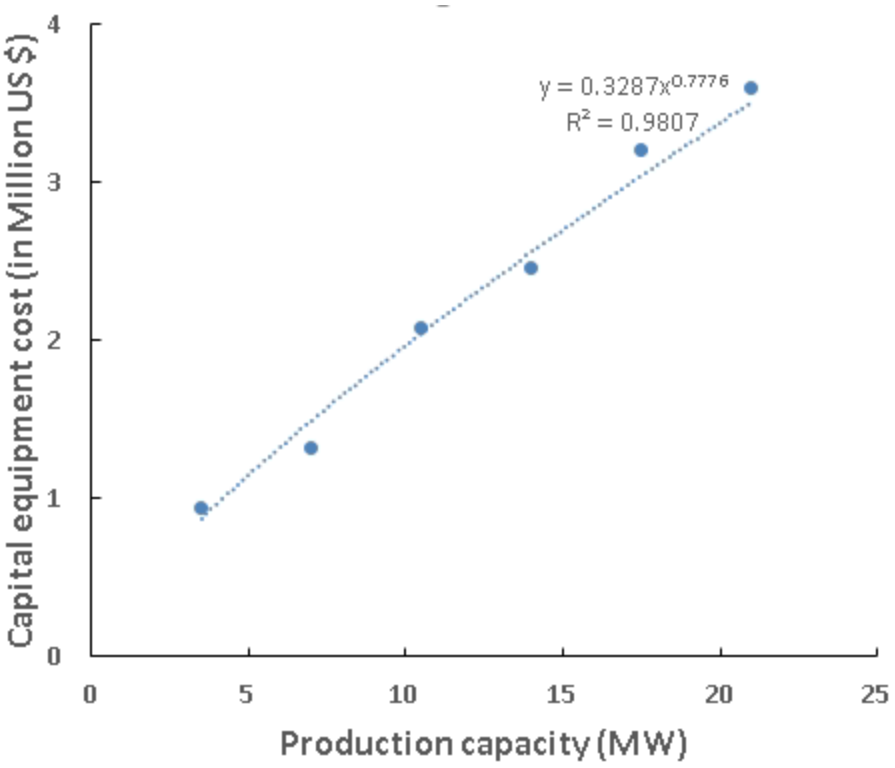

Figure 3. 8: Capital equipment cost and estimation of the scaling factor

3.3.3. Minimum sustainable price (MSP)

The MSP was calculated to be \$0.90/W at 3.5 MW and \$0.53/W at 21 MW annual production capacities for panels with 11% photoconversion efficiency. A power curve was also used to estimate the MSP in \$/W for a factory set-up with a capacity greater than 21 MW as depicted in Figure 3.9. The values are in good agreement with those reported in the literature for perovskite solar cells. For example, Chang et al.[28] and Song et al. [42] reported MSP values of \$0.57/W and \$0.41/W, respectively. The MSP values for established PV technologies are reported to be \$0.6/W for CdTe, \$0.67/W for copper indium gallium selenide (CIGS), and between \$0.64 and \$0.76/W for crystalline-silicon solar PV [131, 133-135]. The MSP value calculated at a 21 MW capacity in this study is competitive with that of other PV technologies, because of the lower

energy consumption costs and low-cost equipment used. The values reported by Chang et al. [28] and Song et al. [42] are for factory capacities of 100 MW and 200 MW, respectively. Using the power curves, we found the MSP values to be between \$0.2/W and \$0.3/W for large capacities. If government incentives are provided, perovskites can be competitive to commercially available technologies for electricity generation. However, the modelling assumptions can greatly impact the calculated MSP [136]. Therefore, we conducted an uncertainty analysis by varying the inputs to obtain a range of MSP values.

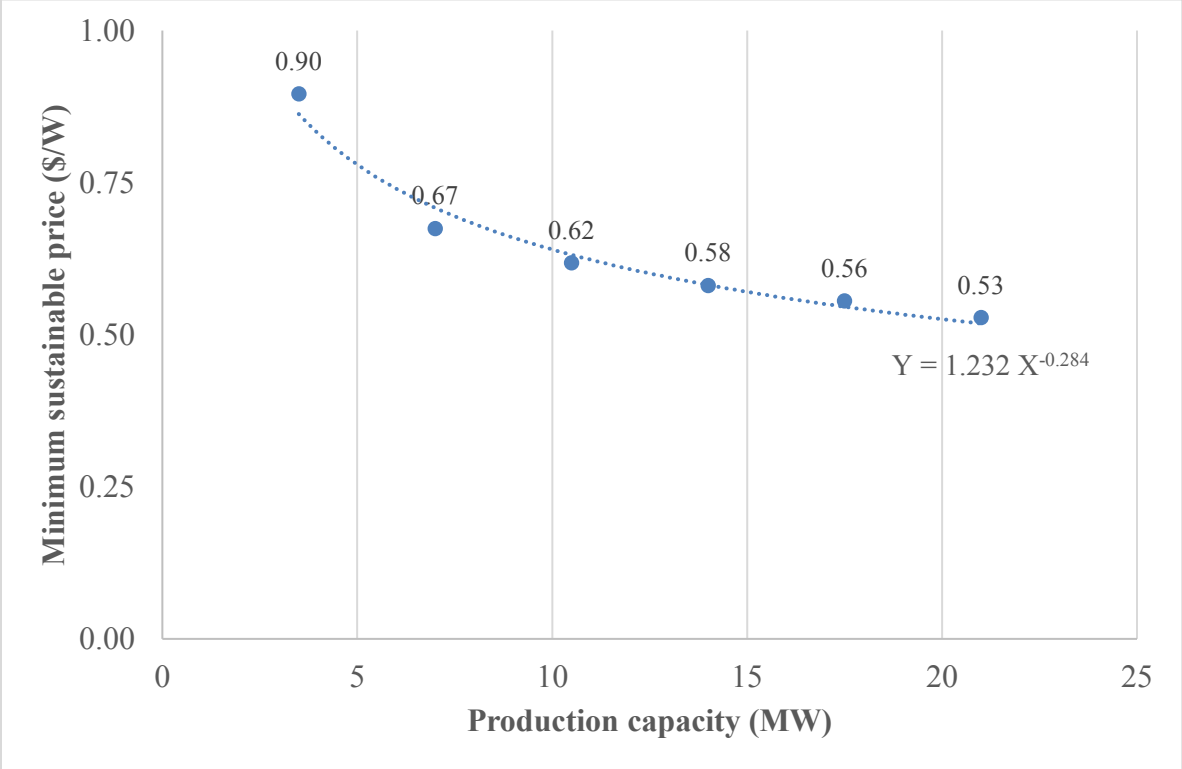

Figure 3. 9: Minimum sustainable price (MSP) for the PSC modules

3.3.4. Levelized cost of electricity (LCOE)

The LCOE was found to be between 11.4 and 14.8 ¢/kWh. The initial investment cost for a residential user in Alberta includes the costs associated with the PSC panels, batteries, inverter, charge controller, mounting, and installation. These costs were estimated as explained in sections 3.2.5 and 3.2.6. The PSC module cost was calculated by considering the MSP and PSC solar system rating of each house and is between $5655.21 and $9592.96, depending on the supplier's plant capacity.

In addition to the initial capital cost, the yearly maintenance costs and the charge controller replacement at the end of its lifetime were included. However, in this analysis, the advantage to the customer of not paying the electricity bills each year as a result of PSC system installation is considered as a yearly revenue. Under this consideration, the breakeven electricity cost is calculated to be $0.23/kWh. The average subsidized electricity price in Canada is $0.174/kWh [137]. Therefore, government subsidies would be helpful to promote PSC electricity generation systems in homes in Canada.

3.3.5. Sensitivity and uncertainty analyses

The important inputs impacting the module manufacturing costs and LCOE are shown in Figure 3.10. The Morris mean presents the variation of the output as the inputs sway from their minimum to maximum values. Morris's standard deviation is the extent to which the output deviates for every change in the input. Parameters in the top right corner of the figure are considered extremely sensitive.

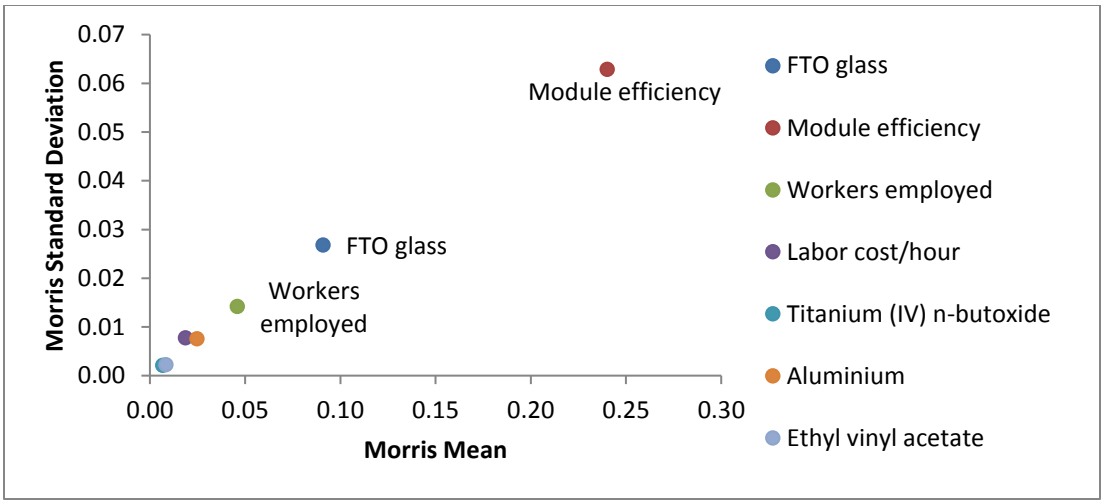
Morris Standard Deviation
0.07
0.06
0.05
0.04
0.03
0.02
0.01
0.00
0.00
0.05
0.10
0.15
0.20
0.25
0.30
Morris Mean
Module efficiency
FTO glass
Workers employed
FTO glass
Module efficiency
Workers employed
Labor cost/hour
Titanium (IV) n-butoxide
Aluminium
Ethyl vinyl acetate

a)

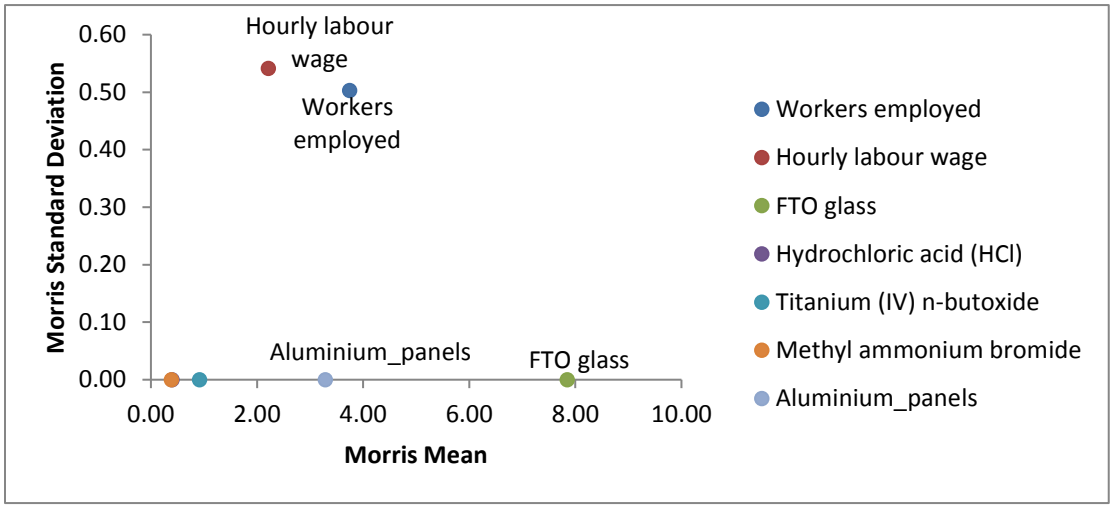
Morris Standard Deviation
0.60
0.50
0.40
0.30
0.20
0.10
0.00
0.00
2.00
4.00
6.00
8.00
10.00
Morris Mean
Hourly labour wage
Workers employed
Aluminium_panels
FTO glass
Workers employed
Hourly labour wage
FTO glass
Hydrochloric acid (HCl)
Titanium (IV) n-butoxide
Methyl ammonium bromide
Aluminium_panels

b)

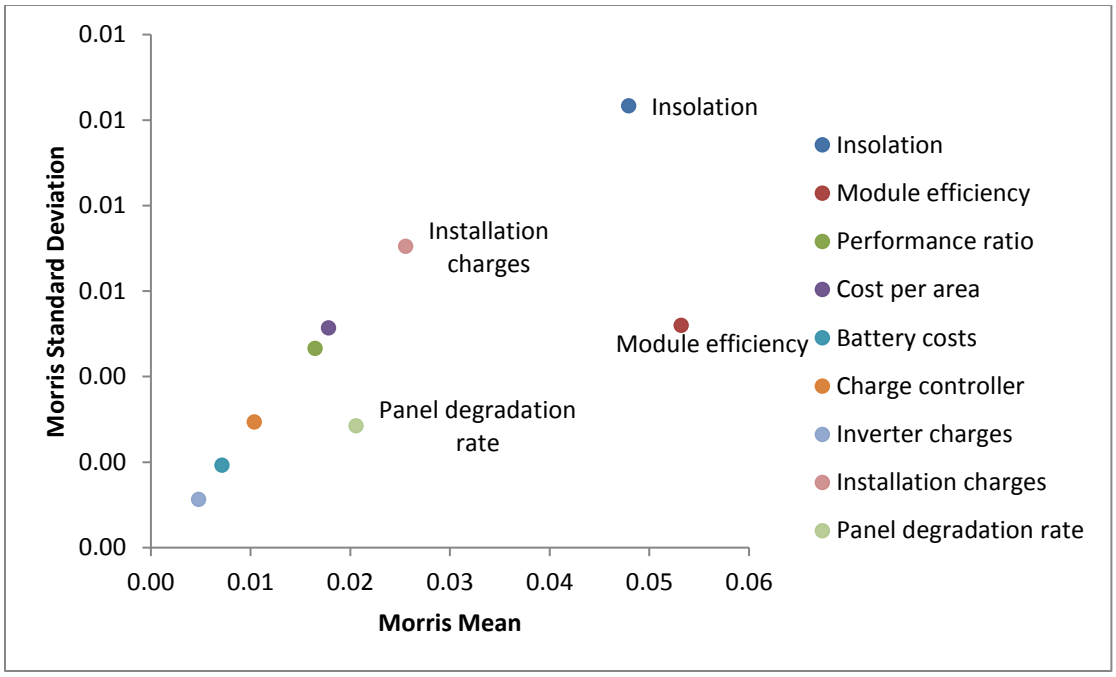

c)

Figure 3. 10: Sensitivity results for outputs – a) \$/W, b) \$/m^2, c) LCOE

The \$/W MSP values are highly sensitive to the efficiency of the module. However, the \$/m^2 values are not impacted by the module efficiency. Therefore, most studies present results per unit area, as the module efficiencies are not certain at this stage. The other common inputs affecting the module costs are the FTO cost and labour requirements. This is because the material and labour costs dominate the module cost, with FTO glass cost being a major contributor to the material costs. The LCOE costs are largely dependent on the insolation, efficiency, and degradation rate of the panels. As more of the sun's energy becomes available to generate electricity, the LCOE rates fall. Considering the wide range of available insolation in Alberta, the results show that the LCOE can change by ± 5 ¢/kWh. Further, since the degradation rate is inversely proportional to the

module lifetime, the efficiency and lifetime of the PSC modules play a pivotal role in determining the LCOE costs.

The uncertainty analysis distributions are shown in Figure 3.11. The average of the module manufacturing costs obtained from iterations is \$0.4/W and \$47.5/m^2. With all the other inputs unaltered, module efficiency alone can sway the \$/W values from \$0.28-0.5/W. A 21 MW capacity production line with 27 workers paid \$17/hour can lead to the lowest module manufacturing cost of \$40/m^2. A further increase in production capacity can bring down overall manufacturing costs.

Under this manufacturing setup, the LCOE costs, though ranging between 7 and 17 ¢/kWh, did not exceed 13¢/kWh in 90% of the cases. We found that the LCOE can reach economical values of 7 ¢/kWh when any two of the three important inputs (insolation, module efficiency, and lifetime) are at their maximum.

Replacing aluminum with nickel as the back electrode had little to no impact on the costs of the module, though nickel is 6 to 8 times more expensive than aluminum [111]. This observation can be attributed to low quantities of the metals used during magnetron sputtering for the formation of thin films on the substrate. Therefore, it is preferable to use nickel over aluminum as nickel promises higher work function and performance, while increasing the LCOE at the most by 0.2¢/kWh as per the uncertainty analysis conducted.

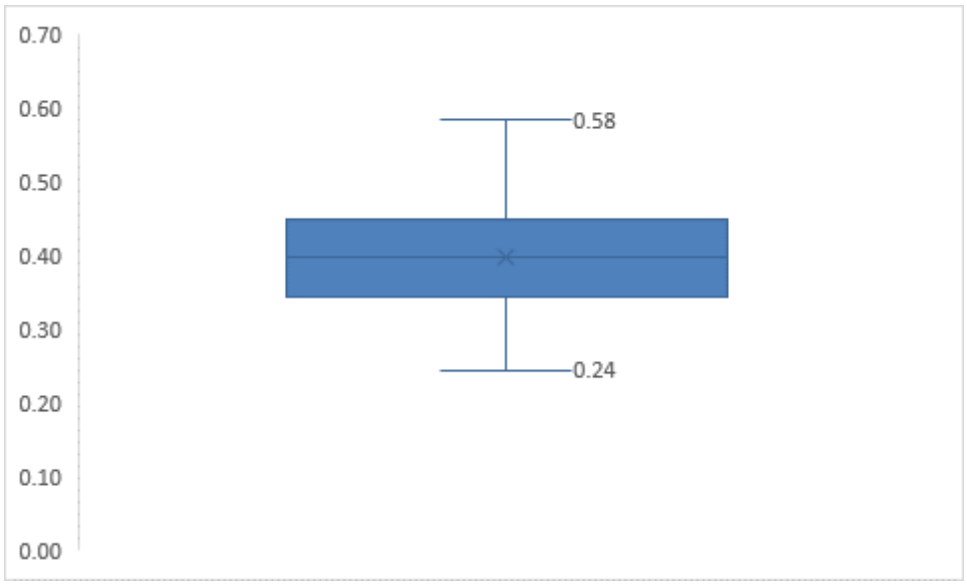
0.70
0.60
0.50
0.40
0.30
0.20
0.10
0.00
0.58
0.24

A)

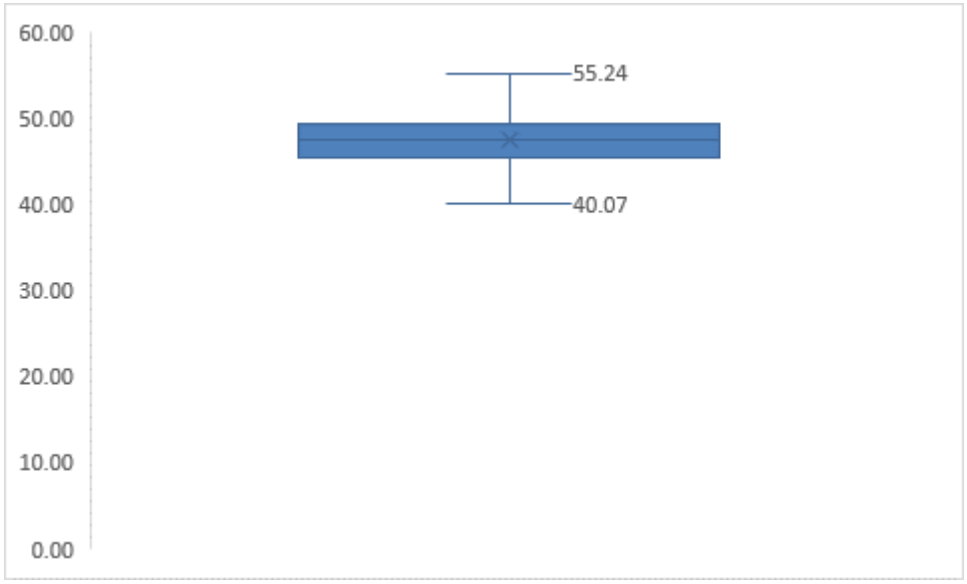
60.00
50.00
40.00
30.00
20.00
10.00
0.00
55.24
40.07

B)

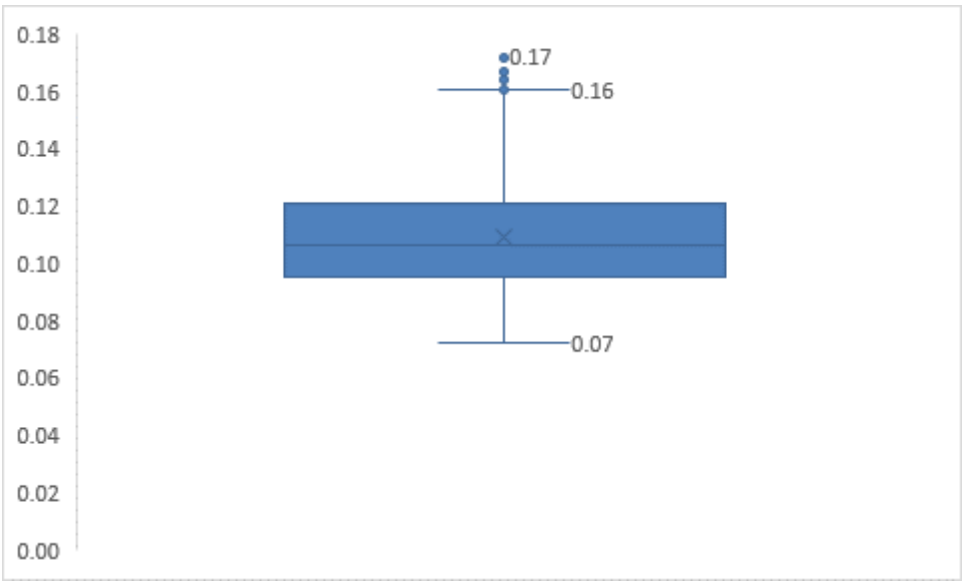

C)

Figure 3. 11: Uncertainty analysis results for outputs – A) \$/W, B) \$/m^2, C) LCOE

3.4. Conclusion

The electricity cost from PV systems has remained significantly higher than that from conventional fossil fuels, despite significant advancements in the PV industry over the past few decades. To bring down this cost, research has shifted toward new materials that are cost-effective, efficient in harnessing the sun's energy, and stable. Perovskite solar cells are among the promising future energy systems as they provide high photoconversion efficiency. Because this technology is new, many studies have examined their stability aspects and reported positive results. The primary purpose of this paper was to develop a bottom-up cost model to evaluate the economic feasibility of TiO_2 nanorod-based PSC technology, fabricated using a unique pathway with materials and fabrication processes selected to optimize cost with efficiency. This study examined the effect of varying the production capacity on the manufacturing cost and developed scale factors for the

individual cost components contributing to the overall module costs. A stand-alone electricity system with PSCs was designed to calculate the LCOE, based on the manufacturing costs estimated. The MSP values calculated were $0.53-$0.9/W, which is comparable with commercialized PV technologies. The scale factors developed for the material and capital costs (equipment and buildings) were 0.81 and 0.78, respectively. Because most of the PSC manufacturing cost is from the cost of materials, scaling up the manufacturing would bring down the fabrication costs. Meanwhile, utility costs remained linear. FTO-coated glass substrates, formamidinium iodide, and aluminum used in various phases of fabrication of the PSC panels contributed to about 70% of the overall material costs.

The LCOE for this method of electricity generation was between 11.4 and 14.8 ¢/kWh, based on the MSP of the supplier. The LCOE was found to be extremely sensitive to insolation, panel efficiency, and lifetime. Provided the efficiency and lifetime are improved in future, LCOE values will drop drastically. Furthermore, the LCOE range represents factory production capacities of 3.5 - 21 MW. With larger factory throughput, the MSP of the supplier reduces, bringing down the LCOE. Therefore, PSCs are economically feasible alternatives. The sensitivity results suggest that the LCOE depends on the insolation, module lifetime, and efficiency.

To summarize, we found that increased manufacturing plant capacity can considerably bring down production costs. Even at a capacity of 21 MW, the MSP and LCOE from PSC technology were found to be competitive with other established PV technologies, implying perovskites can be effective alternatives soon. Replacing costly materials and ineffective processes can further bring down the PSC production costs, thereby promoting their commercialization. Increasing the efficiency and the lifetime of PSC modules is necessary to realize extremely low costs.

Chapter 4: Conclusion and Recommendations

4.1. Conclusions

Past and present energy systems have presented us with a variety of challenges that need to be addressed to ease the transition to a low-carbon economy. The reliance on fossil fuels for energy must be reduced to mitigate climate change impacts. This transition can happen if the global focus on energy systems shifts towards renewable energy sources, for example, solar energy that is abundant, clean, and easily available. Numerous technologies have been developed to harness solar energy and convert it to useful forms. The primary challenge these technologies pose is high cost and low conversion efficiency. Furthermore, solar energy is intermittent in nature; therefore, energy storage systems are necessary.

The perovskite solar cell (PSC) is a technology under development and has the potential to be commercialized in the foreseeable future. Superior photoconversion efficiencies in PSCs have been recorded in laboratory conditions. The cost of PCSs is expected to be low because they are made with low-cost materials. Further, PSC architectures using titanium dioxide (TiO_2) nanorods are proven to have a high photoconversion efficiency. This thesis aims to develop information for policymakers on the environmental and techno-economic performances of TiO_2 nanorod-based PSCs. Life cycle assessment (LCA) and techno economic assessment (TEA) were used to meet the aims of this study.

The LCA study provides insights into the overall environmental performance of TiO_2 nanorod-based PSCs with an emphasis on GHG emissions and energy consumption throughout the PSC life cycle. A bottom-up LCA model was developed for this analysis considering the life cycle

inventory data associated with raw material extraction, PSC fabrication, panel production and assembly, mounting, and end-of-life phases of the PSCs.

The result indicates that more than half the GHG emissions (56%) associated with the life cycle of PSCs were related to the balance of the system (BOS) and assembly phase, as shown in Figure 4.1. The key contributors from this phase were the materials used for module assembly, mounting, and inverters. Aluminium, used for panels and mounting, was the single largest contributor, causing 24% of the GHG emissions. The perovskite production phase contributed 36% of the GHG emissions. In most of the earlier studies, only these emissions were accounted for, as BOS and end-of-life were excluded from their system boundaries.

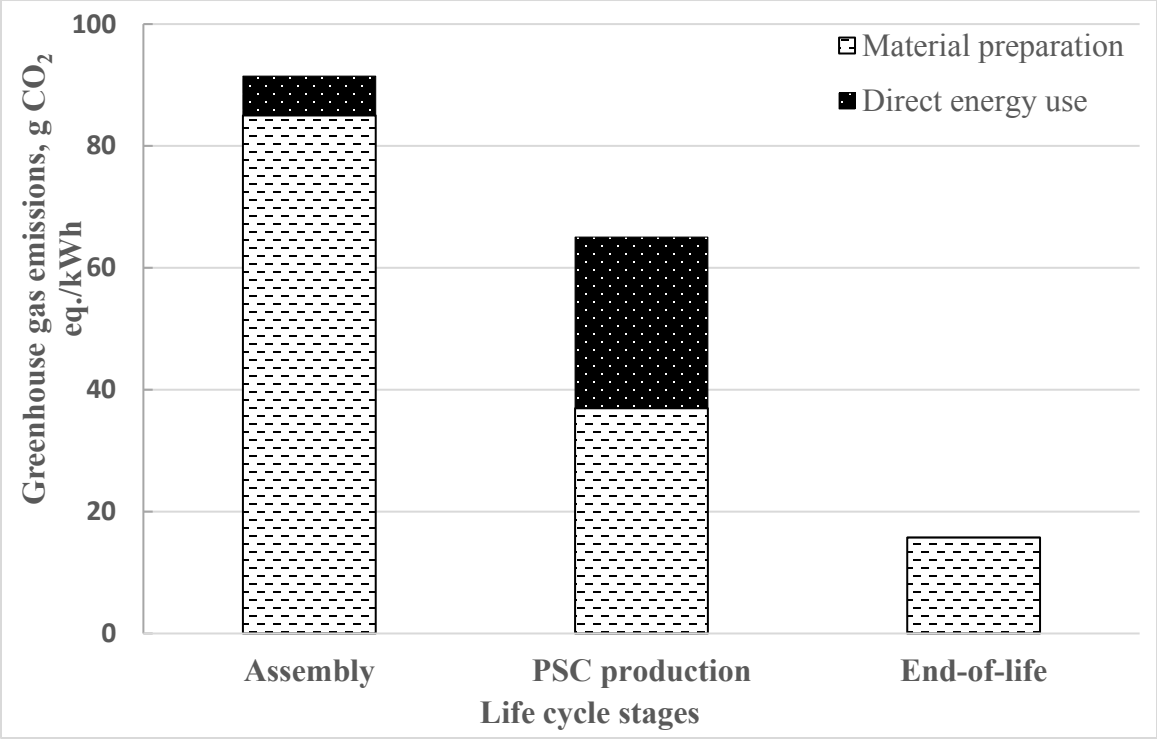

Figure 4. 1: GHG emissions distribution across the key lifecycle stages of the PSC

The scope of research was extended to understand the benefit of recycling and reusing some key components of PSC architecture that are detrimental to PSC environmental performance. A three-time reuse of FTO glass and gold together contributed to less than 4% of the total GHG emissions associated with the PSC life cycle, which is a significant reduction.

Two energy performance indicators, energy payback period (EPBT) and net energy ratio (NER), were calculated to be 0.97 years and 3.1, respectively. The shorter EPBT shows that PSCs can pay back the energy consumed during their life cycle quickly. Similarly, the NER showed that PSCs generate three times more energy than what they consume throughout their life cycle.

Sensitivity analysis results suggest that EPBT and NER are highly sensitive to solar insolation and cell efficiency. That is, if a high-efficiency PSC system is installed at locations with maximum solar insolation, the lowest EPBT and highest NER can be achieved. The NER is also sensitive to the lifetime of the PSC.

The TEA was conducted by developing a pathway to fabricate TiO_2 nanorod-based PSCs using low-cost materials and scalable processes for mass production. A bottom-up techno-economic model was developed that included all the input materials and energy used to fabricate PSC modules at a base case factory capacity of 3.5 MW_p per year. The overall manufacturing cost of the reference PSC module was estimated to be \$80.23/m^2 and \$0.73/W. The material costs contributed to about 60% of this cost, as shown in Figure 4.2. FTO glass, on top of which multiple chemical layers are deposited during the fabrication of PSC modules, was found to be the most expensive material used.

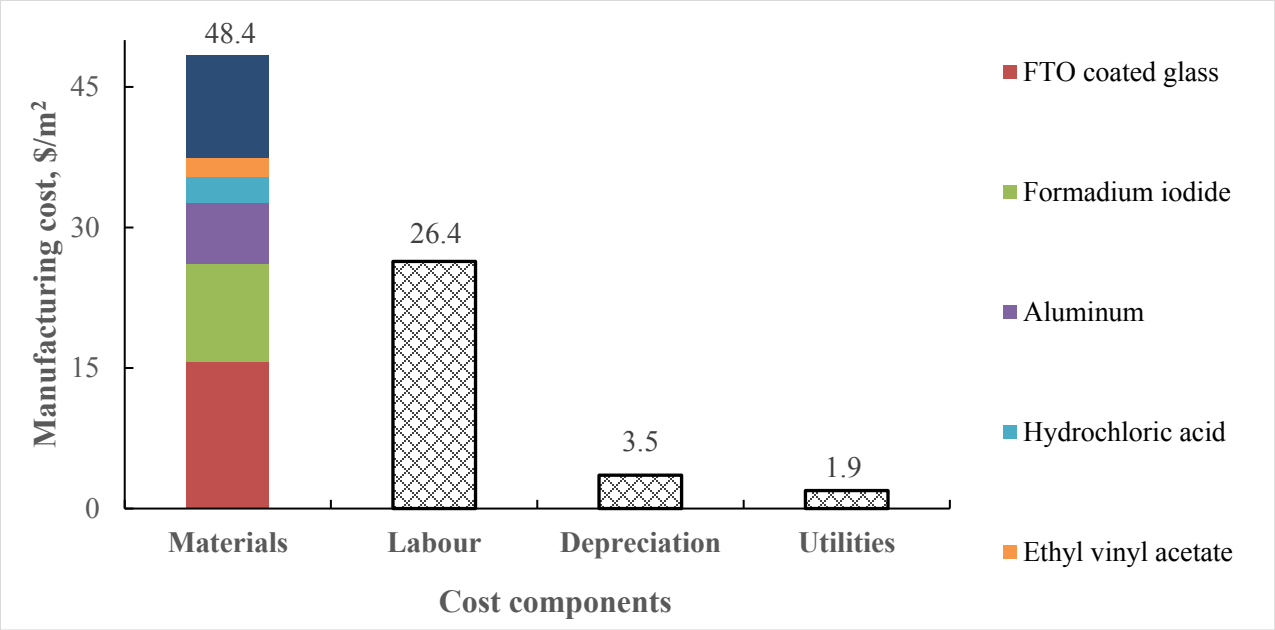

Figure 4. 2: Manufacturing cost breakup ($/m^2) – Fabrication of PSC modules

A cost-capacity relationship was derived to understand the impact of increased factory production capacity on manufacturing costs. A cost vs capacity curve was developed for capacities between 3.5 MW (base case) and 21 MW, as shown in Figure 4.3. It was seen that the manufacturing costs declined by 41%, to \$47.15/m^2 at 21 MW capacity. Material costs and capital costs (both equipment and building, together) had scale factors of 0.81, and 0.77, respectively, indicating a clear reduction in manufacturing costs with capacity.

The minimum sustainable price (MSP), also the minimum selling price for business break-even, was found to be between \$0.5/W and \$0.9/W as the plant annual output was varied from 3.5 to 21 $MW_{p.}$ A power curve was developed to predict the MSP for capacities over 21 MW. The MSP is expected to decrease further with an increase in the plant production capacity and would have an impact on the cost of electricity produced using PSC modules.

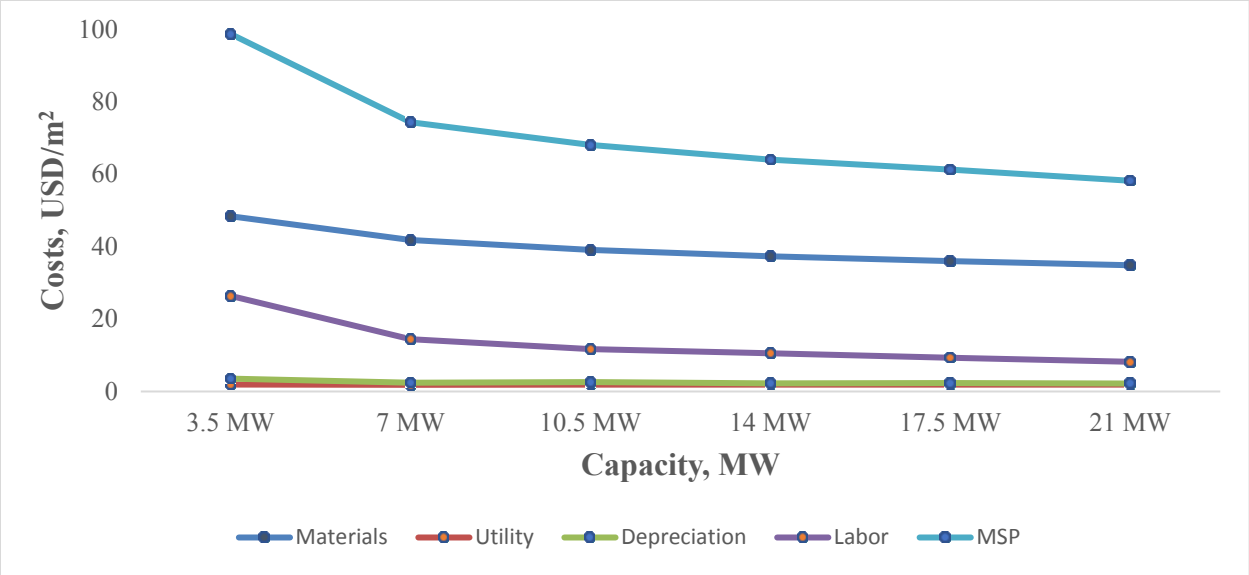

Figure 4. 3: Cost - capacity relationship ($/m^2)

The levelized cost of electricity (LCOE) was found to be in the range of 11.4 and 14.8 ¢/kWh. The Sunshot 2020 target LCOE for PV technologies is 7 to 9 ¢/kWh. With a decline in the MSP and improvement in panel efficiency and stability, achieving this target may not be difficult. Furthermore, the LCOE of utility-scale PV systems currently is 3.4 – 6 ¢/kWh. These are subsidized rates relying on government incentives and, therefore, commercializing PSC modules for installation at residential homes may be feasible if government incentives to promote green technologies is available.

Sensitivity and uncertainty analyses were performed for the TEA study, too, to identify the key input parameters that have significant impacts on the output and to obtain a range of results (through a Monte Carlo simulation), respectively. The sensitivity results suggest that the LCOE depends on the insolation, module lifetime, and efficiency. Uncertainty analysis showed that with two of these factors at their maximum (from the range chosen), the LCOE can reach as low as 6 ¢/kWh. MSP is sensitive to the cost of FTO glass, FAI, and aluminum, among the materials, apart

from the labour costs. It was seen that, at 21 MW, an optimized number of workers can be used, and their wages can lead to an MSP of $\$40/m^2$.

4.2. Recommendations for future work

Further research is recommended in the following areas:

- The PSC production pathway includes the use of several materials and processes. The LCA results obtained in this research are specific to the set of materials and processes used. However, to ensure a lower fabrication cost without compromising the efficiency of the PSCs, some of these materials and processes were replaced for the TEA based on the LCA results and published data. With this modified production path, LCA can be conducted to determine the change in the environmental performance of TiO_2 nanorod-based PSCs.
- The GHG emissions related to the transportation of raw materials to and from the production site are out of scope of this research; however, including them in the system boundary may lead to a more robust analysis. The LCA data for the BOS was taken from a study on commercialized silicon PV cells. Updating the model with PSC-specific real data, will lead to a more precise calculation of the environmental performance of this technology.
- In this research, the PSC module cost was estimated based on a plant capacity of 3.5 MW_p. The results were, however, extended to other plant capacities with a focus on every cost component up to 21 MW, and cost curves were developed for even higher capacities. The scale factors were developed for various components. More research efforts can be dedicated to extending the work done in this study to include the concept of diseconomies of scale.

- The cost estimation model developed for this thesis suggests the feasibility of using PSC-based electricity generation systems for houses in Canada. However, government incentives would make commercialization easier. Future work can be directed towards understanding government policies and providing valuable input to policymakers regarding what governments can do to promote green technologies in Canada.
- Given the current stability and lifetime issues surrounding this technology, other effective short-life applications of PSC-based power production can be explored by slightly altering the cost estimation model developed.

References

1. BP statistical review of world energy: June 2016: London: Author; 2016 [Available from: http://large.stanford.edu/courses/2016/ph240/stanchi2/docs/bp-2016.pdf].

2. Wu X, Chen G. Global primary energy use associated with production, consumption and international trade. Energy Policy. 2017;111:85-94.

3. Sartbaeva A, Kuznetsov V, Wells S, Edwards P. Hydrogen nexus in a sustainable energy future. Energy & Environmental Science. 2008;1(1):79-85.

4. Stocker TF, Qin D, Plattner G-K, Tignor M, Allen SK, Boschung J, et al. Climate change 2013: The physical science basis. Contribution of working group I to the fifth assessment report of the intergovernmental panel on climate change. 2013;1535.

5. Jones GA, Warner KJ. The 21st century population-energy-climate nexus. Energy Policy. 2016;93:206-12.

6. Shahzad U. The need for renewable energy sources. Energy. 2012;2:16-8.

7. Mohtasham J. Renewable energies. Energy Procedia. 2015;74:1289-97.

8. Trieb F, Langniβ O, Klaiβ H. Solar electricity generation—A comparative view of technologies, costs and environmental impact. Solar Energy. 1997;59(1):89-99.

9. Naumann M, Karl RC, Truong CN, Jossen A, Hesse HC. Lithium-ion battery cost analysis in PV-household application. Energy Procedia. 2015;73(C):37-47.

10. Nykvist B, Nilsson M. Rapidly falling costs of battery packs for electric vehicles. Nature Climate Change. 2015;5(4):329-32.

11. Taylor M, Ralon P, Ilas A. The power to change: Solar and wind cost reduction potential to 2025. International Renewable Energy Agency (IRENA). 2016.

12. Al-Saqlawi J, Madani K, Mac Dowell N. Techno-economic feasibility of grid-independent residential roof-top solar PV systems in Muscat, Oman. Energy Conversion and Management. 2018;178:322-34.

13. Green MA, Hishikawa Y, Warta W, Dunlop ED, Levi DH, Hohl-Ebinger J, et al. Solar cell efficiency tables (version 50). Progress in Photovoltaics: Research and Applications. 2017;25(7):668-76.

14. Wenham S, Green M. Silicon solar cells. Progress in Photovoltaics: Research and Applications. 1996;4(1):3-33.

15. Beiter P, Elchinger M, Tian T. 2016 renewable energy data book. National Renewable Energy Lab.(NREL), Golden, CO (United States); 2017.

16. Little RG, Nowlan MJ. Crystalline silicon photovoltaics: The hurdle for thin films. Progress in Photovoltaics: Research and Applications. 1997;5(5):309-15.

17. Orhan JB, Monnard R, Vallat-Sauvain E, Fesquet L, Romang D, Multone X, et al. Nano-textured superstrates for thin film silicon solar cells: Status and industrial challenges. Solar Energy Materials and Solar Cells. 2015;140:344-50.

18. Mazzio KA, Luscombe CK. The future of organic photovoltaics. Chemical Society Reviews. 2014;44(1):78-90.

19. Grätzel M. Dye-sensitized solar cells. Journal of Photochemistry and Photobiology C: Photochemistry Reviews. 2003;4(2):145-53.

20. Hagfeldt A, Boschloo G, Sun L, Kloo L, Pettersson H. Dye-sensitized solar cells. Chemical Reviews. 2010;110(11):6595-663.

21. Yin W-J, Yang J-H, Kang J, Yan Y, Wei S-H. Halide perovskite materials for solar cells: A theoretical review. Journal of Materials Chemistry. 2015;3(17):8926-42.

22. Snaith HJ. Perovskites: The emergence of a new era for low-cost, high-efficiency solar cells. The Journal of Physical Chemistry Letters. 2013;4(21):3623-30.

23. Stranks SD, Eperon GE, Grancini G, Menelaou C, Alcocer MJ, Leijtens T, et al. Electron-hole diffusion lengths exceeding 1 micrometer in an organometal trihalide perovskite absorber. Science. 2013;342(6156):341-4.

24. Celik I, Song Z, Cimaroli AJ, Yan Y, Heben MJ, Apul D. Life cycle assessment (LCA) of perovskite PV cells projected from lab to fab. Solar Energy Materials and Solar Cells; Life cycle, Environmental, Ecology and Impact Analysis of Solar Technology. 2016;156:157-69.

25. Thakur UK, Askar AM, Kisslinger R, Wiltshire BD, Kar P, Shankar K. Halide perovskite solar cells using monocrystalline TiO_2 nanorod arrays as electron transport layers: Impact of nanorod morphology. Nanotechnology. 2017;28(27):274001.

26. Polman A, Atwater HA. Photonic design principles for ultrahigh-efficiency photovoltaics. Nature Materials. 2012;11(3):174.

27. Cui Y, Van Dam D, Mann SA, Van Hoof NJJ, Van Veldhoven PJ, Garnett EC, et al. Boosting solar cell photovoltage via nanophotonic engineering. Nano Letters. 2016;16(10):6467-71.

28. Chang NL, Yi Ho-Baillie AW, Basore PA, Young TL, Evans R, Egan RJ. A manufacturing cost estimation method with uncertainty analysis and its application to perovskite on glass photovoltaic modules. Progress in Photovoltaics: Research and Applications. 2017;25(5):390-405.

29. Twidell J, Weir T. Renewable energy resources: Routledge; 2015.

30. Finnveden G, Hauschild MZ, Ekvall T, Guinée J, Heijungs R, Hellweg S, et al. Recent developments in life cycle assessment. Journal of Environmental Management. 2009;91(1):1-21.

31. Standardization IOf. Environmental Management: Life Cycle Assessment; Principles and Framework: ISO; 2006.

32. ISO E. 14044: 2006. Environmental management-Life cycle assessment-Requirements and guidelines European Committee for Standardization. 2006.

33. Buchner GA, Wulfes N, Schomäcker R. Techno-economic assessment of CO_2-containing polyurethane rubbers. Journal of CO_2 Utilization. 2020;36:153-68.

34. Gong J, Darling SB, You F. Perovskite photovoltaics: Life-cycle assessment of energy and environmental impacts. Energy & Environmental Science. 2015;8(7):1953-68.

35. Espinosa N, Serrano-Luján L, Urbina A, Krebs FC. Solution and vapour deposited lead perovskite solar cells: Ecotoxicity from a life cycle assessment perspective. Solar Energy Materials and Solar Cells. 2015;137:303-10.

36. Serrano-Lujan L, Espinosa N, Larsen-Olsen T, Abad J, Urbina A, Krebs FC. Tin- and lead-based perovskite solar cells under scrutiny: An environmental perspective. Advanced Energy Materials. 2015;5(20).

37. Zhang J, Gao X, Deng Y, Li B, Yuan C. Life cycle assessment of titania perovskite solar cell technology for sustainable design and manufacturing. ChemSusChem. 2015;8(22):3882-91.

38. Zhang J, Gao X, Deng Y, Zha Y, Yuan C. Comparison of life cycle environmental impacts of different perovskite solar cell systems. Solar Energy Materials and Solar Cells. 2017;166:9-17.

39. Monteiro Lunardi M, Wing Yi Ho-Baillie A, Alvarez-Gaitan JP, Moore S, Corkish R. A life cycle assessment of perovskite/silicon tandem solar cells. Progress in Photovoltaics: Research and Applications. 2017;25(8):679-95.

40. Tsang MP, Sonnemann GW, Bassani DM. Life-cycle assessment of cradle-to-grave opportunities and environmental impacts of organic photovoltaic solar panels compared to conventional technologies. Solar Energy Materials and Solar Cells. 2016;156:37-48.

41. Roes A, Alsema E, Blok K, Patel M. Ex-ante environmental and economic evaluation of polymer photovoltaics. Progress in Photovoltaics. 2009;17(6):372-93.

42. Song Z, McElvany CL, Phillips AB, Celik I, Krantz PW, Watthage SC, et al. A technoeconomic analysis of perovskite solar module manufacturing with low-cost materials and techniques. Energy & Environmental Science. 2017;10(6):1297-305.

43. Chang NL, Ho-Baillie AWY, Vak D, Gao M, Green MA, Egan RJ. Manufacturing cost and market potential analysis of demonstrated roll-to-roll perovskite photovoltaic cell processes. Solar Energy Materials and Solar Cells. 2018;174:314-24.

44. Cai M, Wu Y, Chen H, Yang X, Qiang Y, Han L. Cost-performance analysis of perovskite solar modules. Advanced Science. 2017;4(1):1600269.

45. Ye M, Hong X, Zhang F, Liu X. Recent advancements in perovskite solar cells: Flexibility, stability and large scale. Journal of Materials Chemistry. 2016;4(18):6755-71.

46. Mansouri Kouhestani F, Byrne J, Hazendonk P, Spencer L, Brown M. Engineering design for a large scale renewable energy network installation in an urban environment. AGUFM. 2016;2016:ED13B-0941.

47. United Nations Climate Change. What is the Paris Agreement? 2015 [cited 2020]. Available from: https://unfccc.int/process-and-meetings/the-paris-agreement/what-is-the-paris-agreement.

48. Kern F, Rogge KS. The pace of governed energy transitions: Agency, international dynamics and the global Paris Agreement accelerating decarbonisation processes? Energy Research & Social Science. 2016;22:13-7.

49. Nayak PK, Mahesh S, Snaith HJ, Cahen D. Photovoltaic solar cell technologies: Analysing the state of the art. Nature Reviews Materials. 2019;4(4):269-74.

50. Geisz JF, Steiner MA, Garcia I, Kurtz SR, Friedman DJ. Enhanced external radiative efficiency for 20.8% efficient single-junction GaInP solar cells. Applied Physics Letters. 2013;103(4):041118.

51. Yang Y, Yu A, Hsu B, Hsu W, Yang A, Lan C. Development of high-performance multicrystalline silicon for photovoltaic industry. Progress in Photovoltaics: Research and Applications. 2015;23(3):340-51.

52. Chantana J, Kato T, Sugimoto H, Minemoto T. Thin-film Cu (In, Ga)(Se, S) 2-based solar cell with (Cd, Zn) S buffer layer and Zn1− xMgxO window layer. Progress in Photovoltaics: Research and Applications. 2017;25(6):431-40.

53. Arce-Plaza A, Sánchez-Rodriguez F, Courel-Piedrahita M, Galán OV, Hernandez-Calderon V, Ramirez-Velasco S, et al. CdTe thin films: Deposition techniques and applications.: IntechOpen; 2018.

54. Elseman AM. Organometal halide perovskites thin film and their impact on the efficiency of perovskite solar cells. Coatings and Thin-Film Technologies: IntechOpen; 2018. p. 223-40.

55. Green MA, Emery K, Hishikawa Y, Warta W. Solar cell efficiency tables (version 37). Progress in Photovoltaics: Research and Applications. 2011;19(1):84-92.

56. Yang WS, Noh JH, Jeon NJ, Kim YC, Ryu S, Seo J, et al. High-performance photovoltaic perovskite layers fabricated through intramolecular exchange. Science. 2015;348(6240):1234-7.

57. Kim H-S, Lee C-R, Im J-H, Lee K-B, Moehl T, Marchioro A, et al. Lead iodide perovskite sensitized all-solid-state submicron thin film mesoscopic solar cell with efficiency exceeding 9%. Scientific Reports. 2012;2:591.

58. Nelson J. Continuous-time random-walk model of electron transport in nanocrystalline TiO_2 electrodes. Physical Review. 1999;59(23):15374.

59. Van de Lagemaat J, Frank AJ. Nonthermalized electron transport in dye-sensitized nanocrystalline TiO_2 films: Transient photocurrent and random-walk modeling studies. The Journal of Physical Chemistry. 2001;105(45):11194-205.

60. Rebitzer G, Ekvall T, Frischknecht R, Hunkeler D, Norris G, Rydberg T, et al. Life cycle assessment: Part 1: Framework, goal and scope definition, inventory analysis, and applications. Environment International. 2004;30(5):701-20.

61. Kim H-S, Lee J-W, Yantara N, Boix PP, Kulkarni SA, Mhaisalkar S, et al. High efficiency solid-state sensitized solar cell-based on submicrometer rutile TiO_2 nanorod and $CH_3NH_3PbI_3$ perovskite sensitizer. Nano Letters. 2013;13(6):2412-7.

62. Qiu J, Qiu Y, Yan K, Zhong M, Mu C, Yan H, et al. All-solid-state hybrid solar cells based on a new organometal halide perovskite sensitizer and one-dimensional TiO_2 nanowire arrays. Nanoscale. 2013;5(8):3245-8.

63. Li X, Dai S-M, Zhu P, Deng L-L, Xie S-Y, Cui Q, et al. Efficient perovskite solar cells depending on TiO_2 nanorod arrays. ACS Applied Materials & Interfaces. 2016;8(33):21358-65.

64. O'Regan BC, Durrant JR, Sommeling PM, Bakker NJ. Influence of the $TiCl_4$ treatment on nanocrystalline TiO_2 films in dye-sensitized solar cells. 2. Charge density, band edge shifts, and quantification of recombination losses at short circuit. The Journal of Physical Chemistry. 2007;111(37):14001-10.

65. Bandara J, Shankar K, Basham J, Wietasch H, Paulose M, Varghese OK, et al. Integration of TiO_2 nanotube arrays into solid-state dye-sensitized solar cells. The European Physical Journal-Applied Physics. 2011;53(2).

66. Meen T-H, Jhuo Y-T, Chao S-M, Lin N-Y, Ji L-W, Tsai J-K, et al. Effect of TiO_2 nanotubes with $TiCl_4$ treatment on the photoelectrode of dye-sensitized solar cells. Nanoscale Research Letters. 2012;7(1):579-88.

67. Yue D, Khatav P, You F, Darling SB. Deciphering the uncertainties in life cycle energy and environmental analysis of organic photovoltaics. Energy & Environmental Science. 2012;5(11):9163-72.

68. Jungbluth N, Stucki M, Flury K, Frischknecht R, Büsser S. Life cycle inventories of photovoltaics. ESU-services Ltd, Uster. 2012.

69. Kadro J, Hagfeldt A. The end-of-life of perovskite PV. Joule. 2017;1:634-50.

70. Peng J, Lu L, Yang H. Review on life cycle assessment of energy payback and greenhouse gas emission of solar photovoltaic systems. Renewable and Sustainable Energy Reviews. 2013;19:255-74.

71. Binek A, Petrus ML, Huber N, Bristow H, Hu Y, Bein T, et al. Recycling perovskite solar cells to avoid lead waste. ACS Applied Materials & Interfaces. 2016;8(20):12881-6.

72. Hsu DD, O'Donoughue P, Fthenakis V, Heath GA, Kim HC, Sawyer P, et al. Life cycle greenhouse gas emissions of crystalline silicon photovoltaic electricity generation. Journal of Industrial Ecology. 2012;16(s1):S122-S35.

73. Photovoltaic and solar resource maps - 2017 [Available from: https://www.nrcan.gc.ca/18366] . Date accessed 20-Dec-2019.

74. Davis M, Ahiduzzaman M, Kumar A. How will Canada's greenhouse gas emissions change by 2050? A disaggregated analysis of past and future greenhouse gas emissions using bottom-up energy modelling and Sankey diagrams. Applied Energy. 2018;220:754-86.

75. Grancini G, Roldán-Carmona C, Zimmermann I, Mosconi E, Lee X, Martineau D, et al. One-year stable perovskite solar cells by 2D/3D interface engineering. Nature Communications. 2017;8(1):15684-92.

76. García-Valverde R, Cherni JA, Urbina A. Life cycle analysis of organic photovoltaic technologies. Progress in Photovoltaics: Research and Applications. 2010;18(7):535-58.

77. Specification for the assessment of the life cycle greenhouse gas emissions of goods and services. PAS 2050:2011. 2011. www.bsigroup.com.

78. Pacca S, Sivaraman D, Keoleian GA. Parameters affecting the life cycle performance of PV technologies and systems. Energy Policy. 2007;35(6):3316-26.

79. Zhou P, Li W, Li T, Bu T, Liu X, Li J, et al. Ultrasonic spray-coating of large-scale TiO2 compact layer for efficient flexible perovskite solar cells. Micromachines. 2017;8(2):55.

80. Balomenos E, Panias D, Paspaliaris I. Energy and exergy analysis of the primary aluminum production processes: a review on current and future sustainability. Mineral Processing & Extractive Metallurgy Review. 2011;32(2):69-89.

81. Armstrong S, Hurley WG. A thermal model for photovoltaic panels under varying atmospheric conditions. Applied Thermal Engineering. 2010;30(11):1488-95.

82. Khoukhi M, Maruyama S. Theoretical approach of a flat plate solar collector with clear and low-iron glass covers taking into account the spectral absorption and emission within glass covers layer. Renewable Energy. 2005;30(8):1177-94.

83. Watanabe O, Kitamura K, Maenami H, Ishida H. Hydrothermal Treatment of a silica sand complex with lime. Journal of the American Ceramic Society. 2004;84:2318-22.

84. Di Lullo G, Kumar A. RUST model for uncertainty [Available from: http://www.ualbertaenergysystems.ca/]. Date accessed 06-July-2020.

85. Trancik JE. Renewable energy: Back the renewables boom. Nature News. 2014;507(7492):300.

86. Trancik JE, Cross-Call D. Energy technologies evaluated against climate targets using a cost and carbon trade-off curve. Environmental Science & Technology. 2013;47(12):6673-80.

87. McDonald A, Schrattenholzer L. Learning rates for energy technologies. Energy Policy. 2001;29(4):255-61.

88. Bettencourt LM, Trancik JE, Kaur J. Determinants of the pace of global innovation in energy technologies. PloS One. 2013;8(10):e67864.

89. Van der Zwaan B, Rabl A. The learning potential of photovoltaics: Implications for energy policy. Energy Policy. 2004;32(13):1545-54.

90. Sagar AD, Van der Zwaan B. Technological innovation in the energy sector: R&D, deployment, and learning-by-doing. Energy Policy. 2006;34(17):2601-8.

91. Haysom JE, Jafarieh O, Anis H, Hinzer K, Wright D. Learning curve analysis of concentrated photovoltaic systems. Progress in Photovoltaics: Research and Applications. 2015;23(11):1678-86.

92. Trappey AJ, Trappey CV, Tan H, Liu PH, Li S-J, Lin L-C. The determinants of photovoltaic system costs: an evaluation using a hierarchical learning curve model. Journal of Cleaner Production. 2016;112:1709-16.

93. Climate change mitigation: IPCC special report on renewable energy sources and climate change mitigation. Renewable Energy. 2011;20(11).

94. Yan J, Saunders BR. Third-generation solar cells: A review and comparison of polymer: fullerene, hybrid polymer and perovskite solar cells. RSC Advances. 2014;4(82):43286-314.

95. van der Spek M, Ramirez A, Faaij A. Challenges and uncertainties of ex ante techno-economic analysis of low TRL CO_2 capture technology: Lessons from a case study of an NGCC with exhaust gas recycle and electric swing adsorption. Applied Energy. 2017;208:920-34.

96. Extance A. The reality behind solar power's next star material. Nature. 2019;570(7762):429.

97. Matasci S. What is the average solar panel size and weight? [Available from: https://news.energysage.com/average-solar-panel-size-weight/]. Date accessed 04- April-2020.

98. Bright star solar: Common sizes of solar panels [Available from: https://brightstarsolar.net/common-sizes-of-solar-panels/] . Date accessed 15-JUNE-2020.

99. Li Z, Klein TR, Kim DH, Yang M, Berry JJ, van Hest MF, et al. Scalable fabrication of perovskite solar cells. Nature Reviews Materials. 2018;3(4):1-20.

100. Japan's NEDO and Panasonic Achieve the World's Highest Conversion Efficiency of 16.09% for Largest-area Perovskite Solar Cell Module. Business-Financial Post. 2020.

101. Yang M, Li Z, Reese MO, Reid OG, Kim DH, Siol S, et al. Perovskite ink with wide processing window for scalable high-efficiency solar cells. Nature Energy. 2017;2(5):17038.

102. Yilbas BS, Al-Sharafi A, Ali H. Chapter 3 - Surfaces for Self-Cleaning. In: Yilbas BS, Al-Sharafi A, Ali H, editors. Self-Cleaning of Surfaces and Water Droplet Mobility: Elsevier; 2019. p. 45-98.

103. Aharon S, Gamliel S, Cohen BE, Etgar L. Depletion region effect of highly efficient hole conductor free $CH_3NH_3PbI_3$ perovskite solar cells. Physical Chemistry Chemical Physics. 2014;16(22):10512-8.

104. Liu L, Mei A, Liu T, Jiang P, Sheng Y, Zhang L, et al. Fully printable mesoscopic perovskite solar cells with organic silane self-assembled monolayer. Journal of the American Chemical Society. 2015;137(5):1790-3.

105. Li GR, Gao XP. Low-cost counter-electrode materials for dye-sensitized and perovskite solar cells. Advanced Materials. 2020;32(3):1806478.

106. Gao J, Perkins CL, Luther JM, Hanna MC, Chen H-Y, Semonin OE, et al. n-Type transition metal oxide as a hole extraction layer in PbS quantum dot solar cells. Nano letters. 2011;11(8):3263-6.

107. Park SJ, Jeon S, Lee IK, Zhang J, Jeong H, Park J-Y, et al. Inverted planar perovskite solar cells with dopant free hole transporting material: Lewis base-assisted passivation and reduced charge recombination. Journal of Materials Chemistry A. 2017;5(25):13220-7.

108. Jiang Q, Sheng X, Shi B, Feng X, Xu T. Nickel-cathoded perovskite solar cells. The Journal of Physical Chemistry C. 2014;118(45):25878-83.

109. Canada fuel prices, electricity prices, natural gas prices: Global petrol prices; 2019 [Available from: https://www.globalpetrolprices.com/Canada/]. Date accessed 29-May-2020.

110. Piccinno F, Hischier R, Seeger S, Som C. From laboratory to industrial scale: A scale-up framework for chemical processes in life cycle assessment studies. Journal of Cleaner Production. 2016;135:1085-97.

111. Alibaba Marketplace [https://www.alibaba.com/]. Date accessed 01-June-2020. [

112. Walk in ovens and truck in ovens: Despatch themal processing technology; [Available from: https://www.despatch.com/walkin_truck.html]. Date accessed 01-June-2020.

113. Laser Cutters - SP Series [Available from: https://www.troteclaser.com/en/laser-machines/laser-cutters-sp-series/]. Date accessed 01-June-2020.

114. Automatic front/back windshield screen printer.: ATMA SPS printing systems; [Available from: https://www.atma.com.tw/en/product/ATMATIC_GS1220.html]. Date accessed 01-June-2020.

115. Acetone: Acs reagent grade +99.5%: Right price chemicals; [Available from: https://www.rightpricechemicals.com/buy-acetone-reagent-grade-acs.html]. Date accessed 02-June-2020.

116. Isopropanol: Sigma Aldrich; [Available from: https://www.sigmaaldrich.com/canada-english.html]. Date accessed 02-June-2020.

117. Gong C, Du J, Li X, Yu Z, Ma J, Qi W, et al. One-step acidic hydrothermal preparation of dendritic rutile TiO2 nanorods for photocatalytic performance. Nanomaterials. 2018;8(9):683.

118. Salary for Industry: Solar Photovoltaic (PV) Power Generation 2020 [19-JUNE-2020]. Available from: https://www.payscale.com/research/CA/Industry=Solar_Photovoltaic_(PV)_Power_Generation/Salary.

119. Commercial Building Costs & Estimates: Buildings Guide; [19-JUNE-2020]. Available from: https://www.buildingsguide.com/faq/what-average-commercial-building-cost-square-foot/.

120. Kavlak G, McNerney J, Trancik JE. Evaluating the causes of cost reduction in photovoltaic modules. Energy Policy. 2018;123:700-10.

121. How much electricity does a home use? : Ovo Energy; 2019 [Available from: https://www.ovoenergy.com/guides/energy-guides/how-much-electricity-does-a-home-use.html]. Date accessed 02-June-2020.

122. Verma A, Raj R, Kumar M, Ghandehariun S, Kumar A. Assessment of renewable energy technologies for charging electric vehicles in Canada. Energy. 2015;86:548-59.

123. Rahman MM, Islam AS, Salehin S, Al-Matin MA. Development of a model for techno-economic assessment of a stand-alone off-grid solar photovoltaic system in Bangladesh. International Journal of Renewable Energy Research (IJRER). 2016;6(1):140-9.

124. Solacity Inc. How to Size a Solar System That Really Works! [Available from: https://www.solacity.com/how-to-size-a-solar-system-that-really-works/ . Date accessed 03-June-2020.

125. Akbari M, Oyedun AO, Kumar A. Comparative energy and techno-economic analyses of two different configurations for hydrothermal carbonization of yard waste. Bioresource Technology Reports. 2019;7:100210.

126. Branker K, Pathak M, Pearce JM. A review of solar photovoltaic levelized cost of electricity. Renewable and sustainable energy reviews. 2011;15(9):4470-82.

127. Campolongo F, Cariboni J, Saltelli A. An effective screening design for sensitivity analysis of large models. Environmental Modelling & Software. 2007;22(10):1509-18.

128. Payscale. Production worker - solar PV [Available from: https://www.payscale.com/]. Date accessed 12-June-2020.

129. Di Lullo G, Gemechu E, Oni AO, Kumar A. Extending sensitivity analysis using regression to effectively disseminate life cycle assessment results. The International Journal of Life Cycle Assessment. 2020;25(2):222-39.

130. Hwang K, Jung YS, Heo YJ, Scholes FH, Watkins SE, Subbiah J, et al. Toward large scale roll-to-roll production of fully printed perovskite solar cells. Advanced Materials. 2015;27(7):1241-7.

131. Woodhouse M, Goodrich A, Redlinger M, Lokanc M, Eggert R. The Present, Mid-Term, and Long-Term Supply Curves for Tellurium; and Updates in the Results from NREL's CdTe PV Module Manufacturing Cost Model (Presentation). National Renewable Energy Lab.(NREL), Golden, CO (United States); 2013.

132. Haldi J, Whitcomb D. Economies of scale in industrial plants. Journal of Political Economy. 1967;75(4, Part 1):373-85.

133. Horowitz KA, Fu R, Woodhouse M. An analysis of glass–glass CIGS manufacturing costs. Solar Energy Materials and Solar Cells. 2016;154:1-10.

134. Powell DM, Fu R, Horowitz K, Basore PA, Woodhouse M, Buonassisi T. The capital intensity of photovoltaics manufacturing: barrier to scale and opportunity for innovation. Energy & Environmental Science. 2015;8(12):3395-408.

135. Powell DM, Winkler MT, Choi HJ, Simmons CB, Needleman DB, Buonassisi T. Crystalline silicon photovoltaics: a cost analysis framework for determining technology pathways to reach baseload electricity costs. Energy & Environmental Science. 2012;5(3):5874-83.

136. Jones-Albertus R, Feldman D, Fu R, Horowitz K, Woodhouse M. Technology advances needed for photovoltaics to achieve widespread grid price parity. Progress in Photovoltaics: Research and Applications. 2016;24(9):1272-83.

137. Energy hub. Electricity Prices in Canada 2020 [cited 2020. Available from: https://www.energyhub.org/]. Date accessed 27-July-2020.

138. Geisler G, B. Hofstetter T, Hungerbühler K. Production of Fine and Speciality Chemicals: Procedure for the Estimation of LCIs. International Journal of Life Cycle Assessment. 2004;9:101-13.

139. HASLAM JH. Chemistry and Uses of Titanium Organic Compounds. ACS Publications; 1959.

140. Alberola-Borràs J-A, Vidal R, Mora-Seró I. Evaluation of multiple cation/anion perovskite solar cells through life cycle assessment. Sustainable Energy & Fuels. 2018.

141. CORNER S, editor EUROPEAN CENTRE FOR ECOTOXICOLOGY AND TOXICOLOGY OF CHEMICALS. Workshop Report; 2006.

142. Roy KM. Sulfones and sulfoxides. Ullmann's Encyclopedia of Industrial Chemistry. 2000.

143. Zajáros A, Szita K, Tóth, Matolcsy K, Horváth D. Life Cycle Assessment of DMSO solvent ISAEP (2). 2016.

144. Jenkins S. Ashford's Dictionary of Industrial Chemicals. Chemical Engineering. 2011;118(5):8-9.

145. Deng Y, Li J, Li T, Gao X, Yuan C. Life cycle assessment of lithium sulfur battery for electric vehicles. Journal of Power Sources. 2017;343:284-95.

146. Shokrzadeh S, Bibeau E. Repurposing batteries of plug-in electric vehicles to support renewable energy penetration in the electric grid. SAE Technical Paper; 2012. Report No.: 0148-7191.

147. Energy Sage. What size solar inverter do I need? [Available from: https://news.energysage.com/what-size-solar-inverter-do-i-need/]. Date accessed 03-June-2020.

148. Webosolar. Charge controller sizing and selection [Available from: https://webosolar.com/charge-controller-sizing-selection-solar-panel/]. Date accessed 03-June-2020.

Appendix A

A1. **Material mass calculations:**

The material masses used in calculations were obtained from the laboratory data and other literature sources. Further details are presented in the table below. Note that, the conversions are made to account the material usage related to producing 1 kWh of electricity for an Alberta consumer in Canada. Also, 'a piece' refers to an FTO glass slide of dimensions 2.5cm X 2.5cm.

Table A1: Material mass calculations from laboratory data

Sub-step	Material	Mass (g/ kWh)	Density Of the liquid (g/ml)	Remarks
FTO Glass Preparation	FTO coated glass slides*	2.5E+0		3 pieces weigh 10.598g all together
	Acetone	2.0E+0	0.7845	10ml for 9 pieces used
	Methanol	2.0E+0	0.7914	10ml required for 9 pieces
	DI water	2.6E+0	1	10ml required for 9 pieces
TiO_2 deposition	Titanium (IV) iso propoxide	2.2E-2	0.96	10.05 µl per piece
	1 M HCl	5.3E-3	1.18	1.95 µl per piece
	iso propanol	2.5E-1	0.785	138 µl per piece
TiO_2 nanorods growth	HCl (37%)	3.4E+0	1.18	2.5ml for two pieces
	Glacial Acetic acid	3.0E+0	1.049	2.5ml for two pieces
	DI water	5.6E+0	1	5ml for two pieces
	TBO	6.8E-1	0.99	600 µl for two pieces
Drying and post treatment	DI water	5.1E-3	1	Tap water. Estimated from [34]

Sub-step	Material	Mass (g/ kWh)	Density Of the liquid (g/ml)	Remarks
	Flowing nitrogen	7.1E-2		[34]
	$TiCl_4$	3.9E-1		40mM in 200 ml for 9 pieces ¥.
Perovskite Deposition	MABr	1.0E-2		0.2 M in 1 ml solution for 5 pieces
	FAI	8.7E-2		1.1 M in 1 ml solution for 5 pieces
	$PbBr_2$	3.7E-2		0.22 M in 1 ml solution for 5 pieces
	PbI_2	2.3E-1		1.1M in 1 ml solution for 5 pieces
	DMF	3.5E-1	0.944	0.8ml for 5 pieces
	DMSO	1.0E-1	1.1	0.2ml for 5 pieces
	Chlorobenzene	2.5E-1	1.1058	0.1 ml per piece
HTL Deposition	Spiro-OMeOTAD	8.1E-3		35mg for 10 pieces
	Chlorobenzene	2.5E-1	1.1058	0.1ml per piece
	4-tert-butylpyridine	3.0E-3	0.923	14 µl for 10 pieces
	Acetonitrile	3.2E-3	0.782	17.5 µl for 10 pieces
	Lithium bis trifluoro methanesulfonyl -imide	1.0E-3		4.4mg for 10 pieces
Thermal evaporation of Gold	Gold*	7.1E-4		0.4g gold for cell dimensions of 0.5cm X 0.5cm
Manufacturing solar panels ¥	Glass-low iron	1.5E+1		10.1kg for a square meter solar panel as top cover
	Wire drawing, copper	1.6E-1		0.113 kg copper wires for a

Sub-step	Material	Mass (g/ kWh)	Density Of the liquid (g/ml)	Remarks
				square meter solar panel
	Aluminum alloy	3.8E+0		2.63 kg for a square meter solar panel for the edges
	Ethyl vinyl acetate	1.4E+0		1kg for a square meter panel for front & back of solar cells
	Polyester	5.4E-1		0.373kg for bottom cover per square meter
	Polyvinyl fluoride	1.6E-1		0.11kg for bottom cover per square meter
	Acetone	1.9E-2		0.013kg used as cleaning fluid
	Methanol	3.1E-3		2.16g used per square meter
	Propanol	1.2E-2		Soldering flux
Mounting on structures	Aluminum for mounting sys.	4.1E+0		2.84kg per square meter
	Steel	2.2E+0		1.5kg per square meter
	Corrugated board	1.9E-1		0.133kg based on a correction factor of 1.54/m^2
	Plastics(polyethylene)	2.0E-3		1.4g per m^2
	Polystyrene	1.0E-2		7.02g per square meter
Making necessary	Aluminum alloy	5.5E-1		0.682 kg for 500W inverter
	Copper	1.6E-3		2g per 500W

Sub-step	Material	Mass (g/ kWh)	Density Of the liquid (g/ml)	Remarks
connection (Inverters)				
	Low alloyed steel	1.1E-1		7.8g per 500W
	Corrugated board box	7.1E-1		1.12kg per 500W
	Capacitor, electrolytic	4.3E-2		0.054kg per 500W
	Capacitor, film	5.8E-2		0.072 kg per 500W
	Capacitor, CMC	3.9E-3		0.0048kg per 500W
	Acrylonitrile ABS polymer	1.2E-1		0.148kg for a 500W
	Transformer	2.5E-1		0.31kg for 500W
	Polycarbonate	5.5E-2		68g for a 500W inverter
	Polyethylene	1.1E-2		14g per square meter per 500W inverter
	Polyvinyl chloride	1.6E-3		2g per 500W
Disintegration	Chlorobenzene	3.5E+0	1.1059	Width of the FTO glass is 0.22cm. Mass is approximated to immerse the sample completely in chlorobenzene.
	Nitrogen stream	7.1E-2		[34]
	Deionized water	3.2E+0	1	To remove perovskites leaving behind PbI_2
Recycling the cells (Cleaning)	DMF	3.0E+0	0.944	To dissolve PbI_2
	DMF	3.5E-1	0.944	To clean the glass substrate

[¥] All molar conversions to mass: M x V x molecular weight where M is the number of moles, V is the volume of the solution in liters & molecular weight is in grams. Mass, thus obtained, is in grams.

*Further, 3-time re-use of the valuable materials considered. Mass calculations done as per [77]

[Ψ] All the information related to panel production, mounting systems and inverters from [68].

A2. **Inventory development**

The embedded energy consumption and emissions associated with materials used in manufacturing the perovskite solar cell (PSC), when unavailable, is derived based on stoichiometric relationships, solubility, output yields, mass allocations.

A2.1 **Inventory for 1kg of Titanium (IV) isopropoxide (TTIP)**

The inputs for 1 kg of TTIP are obtained partially from the supplementary information provided by [37]. The electricity, steam and other utility usages are approximated as mentioned in [138]. Mass allocation is done considering HCl to be a major by-product.

Inputs	**Mass**	**Unit**
Iso-propanol	0.9194	kg
$TiCl_4$	0.7255	kg
Electricity	2.85	MJ
Steam	4.45	kg
Nitrogen	0.23	kg
Cooling water	400	kg
Products		
TTIP	1	kg
Waste	0.65	kg
HCl	0.513	kg
Total mass	1.513	kg

A2.2 **Inventory for 1kg of Titanium (IV) n-butoxide**

The inputs for 1kg of TBO are based on the stoichiometric relationships established in [139]. Other approximations are done as per [138]. A mass yield of 0.82 was assumed, with ammonium chloride as the by-product.

Inputs	**Mass**	**Unit**
$TiCl_4$	0.670732	kg
n-butanol	1.060976	kg
Ammonia	0.199	kg
Electricity	2.85	MJ
Steam	4.45	kg
Nitrogen	0.23	kg
Cooling water	400	kg
Products		
TBO	1	kg
NH_4Cl	0.63	kg
Waste	0.300707	kg
Total mass	1.63	kg

A2.3 **Inventory for 1kg of Methylammonium Bromide (MABr)**

The embodied primary energy and emissions associated with 1 kg of MABr is obtained based on the input data available in the supplementary information document provided by [140]. The inventory table is presented below.

Inputs	**Mass**	**Unit**
Methylamine	0.277	kg
H_2	0.008936	kg
Bromine	0.714	kg
Methanol	0.4155	kg
DI water	0.7832	kg
Ethanol	0.0111	kg
Diethyl ether	0.01	kg

Inputs	Mass	Unit
Electricity	143.1	kWh
Product		
MABr	1	kg

A2.4 **Inventory for 1 kg of Formamidinium iodide (FAI)**

The inventory for 1kg of FAI is again obtained from [140]. The inventory table is presented below:

Inputs	Mass	Unit
Hydrogen cyanide (HCN)	0.1572	kg
Hydroxyl amine	0.1921	kg
Acetic anhydride	0.2968	kg
Hydrogen	0.005815	kg
Iodine	0.7379	kg
DI water	0.424	kg
Diethyl ether	0.1016	kg
Methanol	0.838	kg
Electricity	197.79	kWh
Product		
FAI	1	kg

However, since the data for HCN was unavailable, data obtained based on stoichiometric relationships as represented in [141].

Inputs	Mass	Unit
Methane	0.5919	kg
Ammonia	0.63004	kg
Oxygen/compressed air	1.776	kg
Steam	4.45	kg
Nitrogen	0.23	kg
Cooling water	400	kg
Electricity	2.85	MJ
Product		
HCN	1	kg

A2.5 **Inventory for 1 kg of Lead bromide ($PbBr_2$)**

The cradle to gate energy consumption and emissions associated with producing 1 kg of $PbBr_2$ is obtained based on the life cycle inventory available from [38]. Basically, this inventory is modelled from [138].

Inputs	**Mass**	**Unit**
Lead nitrate	0.71	kg
Potassium bromide	0.98	kg
Electricity	2.85	MJ
Steam	4.45	kg
Nitrogen	0.23	kg
Cooling water	400	kg
De-ionized water	4.5	kg
Product		
Lead bromide	1	kg

However, since the inventory related to production of potassium bromide was not available, the reaction between potassium hydroxide and bromine was considered and the inventory was developed stoichiometrically, with yields and other common data of nitrogen and cooling water use coming from [138].

Inputs	**Mass**	**Unit**
Bromine	1.46	kg
KOH	1.02	kg
Electricity	2.85	MJ
Steam	4.45	kg
Nitrogen	0.23	kg
Cooling water	400	kg
De-ionized water	4.5	kg
Product		
KOH	1	kg

A2.6 **Inventory for 1 kg of Dimethyl sulfoxide (DMSO)**

The industrial manufacturing of DMSO is by catalytic oxidization of DMS [142]. The masses of the reactants were stoichiometrically calculated with other relevant information extracted from [138]. The inputs for production of 1 kg of DMSO is presented in the table below.

Inputs	**Mass**	**Unit**
DMS	0.864	kg
Oxygen	0.111304	kg
Steam	4.45	kg
Nitrogen	0.23	kg
Cooling water	400	kg
Electricity	2.85	MJ
Product		
DMSO	1	kg

A method to recover and re-use DMSO from industrial water through distillation was elaborated by [143]. Note that the GWP is taken from the mentioned study for 1kg of DMSO while the cumulative energy demand from cradle to gate is derived based on the data presented in the table above. Additionally, since the data for production of DMS was unavailable too, the same was modelled using [138]. The reaction between methanol and hydrogen sulfide, termed as thiolation, was used to estimate the masses of the inputs to produce 1 kg DMS [144].

Inputs	**Mass**	**Unit**
Methanol	1.122	kg
Hydrogen Sulfide	0.597	kg
Electricity	2.85	MJ
Steam	4.45	kg
Nitrogen	0.23	kg
Cooling water	400	kg
Product		

Inputs	Mass	Unit
DMS	1	kg

A2.7 **Inventory for 1 kg of lithium bis(trifluoromethanesulfonyl)imide (LiTFSI)**

The inventory for producing 1kg of LiTFSI was obtained from [145]. The data utilized is presented below. Due to lack of data, few materials were replaced with equivalent materials while calculating the GWP and cumulative energy demand for 1 kg of LiTFSI.

Inputs	Mass	Unit	Remarks
SO_2	0.718	kg	
Cl_2	0.796	kg	
CH_4	0.165	kg	
Hydrogen Fluoride	1.893333	kg	Replaced with HCl
Silica	1.343	kg	
CH_3Cl	4.442	kg	Replaced with chloroform
NH_3	0.56	kg	
CH_3ONa	0.224	kg	
H_2SO_4	0.383	kg	
Li_2CO_3	0.131	kg	Obtained from the GREET model 2018
Solvent use	0.251	kg	Acetone considered
Steam	37.977	kg	
Electricity	42.331	MJ	
CH_4 Emission	5.21E-05	kg	
Product			
LiTFSI	1	kg	

Appendix B

B1. **Calculation of PSC panel area required to generate enough electricity for household needs in Alberta, Canada.**

The following equation, from Monteiro Lunardi et al. [39] was used to calculate the required panel area.

$$A = \frac{\text{Eout}}{I\ X\ PR\ X\ \eta} \qquad \text{Equation (B1)}$$

where A is the required area in square meters, I is Alberta's average solar insolation, PR is the system performance ratio, and η is the photoconversion efficiency of the PSC modules. An average insolation value of 1513.5 $kWhm^{-2}yr^{-1}$ was calculated for Alberta based on data from the literature [73]. This dataset provides monthly insolation data for every municipality across Canada. The system performance ratio is location-specific: 0.75 and 0.95 for Europe and USA, respectively, were used in an earlier study [72]. The average, 0.85, was used in this study. The geometric fill factor of the solar modules being manufactured is 70%. Therefore, the panel efficiency is 11%. An annual degradation rate of 2% per year was assumed, bringing the efficiency of each panel to 80% of its rated power in 11 years. As per industry norms [28], the system cannot be used beyond this and hence was fixed as the lifetime of the PSC system. Since the system needs to produce the average electricity requirement of 11 MWh each year throughout its lifetime, we considered the overall efficiency to be 8.8% for all the calculations throughout the analysis period. Using Equation 1, we calculated the area to be 97 m^2.

B2. **Battery, inverter and charge controller requirements for residential use in Alberta, Canada**

Batteries are used to store energy and cater to the electricity needs of the house when no solar radiation is available. Proper sizing of the batteries is of paramount importance. The battery capacity (ampere hours, or Ah) was calculated from Equation 2, from Rahman et al. [123]:

$$Ah = \frac{\mathrm{D\ X\ E}}{\mathrm{DOD\ X\ \eta c\ X\ V}} \qquad \text{Equation (B2)}$$

where D is the average daily consumption, E is location-specific days of autonomy, DOD is the depth of discharge of the battery, η_c is the efficiency of charging, and V is the nominal voltage of each battery. The average daily consumption was estimated from the annual consumption of electricity per house in Canada, the days of autonomy is 3 for Canada [124], and the depth of discharge and the efficiency of charging were assumed to be 80% and 85% [123, 146] respectively. Nominal voltage of the selected lead-acid batteries is 12V [111]. Additionally, for a 30% factor of safety, 120 small-sized batteries, each of 120Ah and 12V, are needed to meet the system requirements.

Inverters are used to convert the direct current (DC) output of a PSC system to alternating current (AC). As per a general rule of thumb, inverters must be sized to match the DC rating of the solar panel system [147]. Based on the total area occupied by the PSC panels and their power rating, the PSC system rating was calculated to be approximately 10kW. With a safety factor of 25%, the inverter capacity was designed to be 12.5 kW. Charge controllers are essential to prevent over-charging or over-discharging the batteries [148]. Thus, the choice of the charge controllers depends on the battery group voltage, short circuit current, and rated power of the PV system [148].

B3. **Input details for Nickel substitution of Aluminum as electrode**

To better the performance of the PSC panels by using nickel as the back contact, that promises higher work function close to gold, aluminum use was replaced with nickel based on the following considerations listed in table B1.

Table B1: Input considerations for Nickel as a replacement for Aluminum

Number	Parameter	Value	Comments/ Reference
1	Work function - Nickel	5.04 eV	This work function is close to that of gold [108]; therefore, nickel can be a good replacement.
2	Nickel cost ($/kg)	20	Nickel is about 6-8 times expensive than aluminum [111].
3	Nickel cost range uncertainty	15 - 25 ($/kg)	A ±25% range considered for sensitivity analysis.
4	Uncertainty distribution	Triangular	